Invited Speaker

73 Localization techniques in biomedical electron microscopy: good as gold
Wiebke Möbius[1]
[1]Max-Planck-Institute for Multidisciplinary Sciences, Göttingen, Germany

Oral Presentation

405 Whole-brain 3D quantification of alpha-synuclein spreading and toxicity in a mouse model of Parkinson's disease
Phd Student Frederikke Lynge Sørensen[1,2], Annika Højrup Runegaard Thomsen[1], Urmas Roostalu[1], Jacob Lercke Skytte[1], Evi Alexiou[1], Jacob Hecksher-Sørensen[1], Poul Henning Jensen[2], Yasir Gallero-Salas[1], Henrik Björk Hansen[1]
[1]Gubra Aps, Hørsholm, Denmark, [2]Biomedicine and DANDRITE, Aarhus University, Aarhus, Denmark
779 The effect of fixation-induced cell blebbing: how to minimize a loss of proteins from cells?
Prof. Pavel Hozak[1]
[1]Institute of Molecular Gentics ASCR, Prague, Czech Republic

Poster Presentation

27 In vitro genotoxic activity of leaf and flower extracts of four alien invasive plant species
Mirela Uzelac Bozac[1], Dr Petra Cvjetko[2], Dr Katarina Caput Mihalić[2], Miss Ela Kukac[3], Dr Slavica Dudaš[4], Dr Barbara Sladonja[1], Dr Danijela Poljuha[1]
[1]Institute of Agriculture and Tourism, Porec, Croatia, [2]Faculty of Science, University of Zagreb, Zagreb, Croatia, [3]Department of Biotechnology, University of Rijeka, Rijeka, Croatia, [4]Agricultural Department, Polytechnic of Rijeka, Rijeka, Croatia
59 Light sheet imaging across scales for preclinical drug discovery research
Yasir Gallero Salas[1], Mr. Max Hahn[1], Mr. Thomas Topilko[1], Ms. Marie Biviano Rosenkilde[1], Ms. Frederikke Lynge Sørensen[1], Ms. Lea Lydolph Larsen[1], Ms. Katrine Skovgård[1], Mr. Urmas Roostalu[1]
[1]Gubra, Hørsholm, Denmark
93 Contribution of Probiotics to the Effect of Platelet-Rich Plasma in Diabetic Rat Skin Wound Healing
Prof. Dr. Erdogan Kocamaz, Prof. Dr. Muge Karakayali, PhD Fatih Collu, Prof. Dr. Sevinc Inan, Prof. Dr. Ibrahim Tuglu
[1]Department of Histology and Embryology, Manisa Celal Bayar University, Faculty of Medicine, Manisa, Turkey, [2]Department of Microbiology, Izmir Democracy University, Faculty of Medicine, Izmir , Turkey, [3]Department of Zoology, Manisa Celal Bayar University, Faculty of Life Sciences, Manisa, Turkey, [4]Department of Histology and Embryology, Izmir University of Economics, Faculty of Medicine, Izmir, Turkey, [5]Department of Histology and Embryology, Manisa Celal Bayar University, Faculty of Medicine, Manisa, Turkey
194 Exploring cardiac innervation by 3D light sheet imaging in horses with atrial fibrillation
Mélodie Schneider[1], PhD Sarah Dalgas Nissen[1], DVM Simon Libak Haugaard[1], Prof Rikke Buhl[1], PhD Urmas Roostalu[2]
[1]University of Copenhagen, Copenhagen, Denmark, [2]Gubra, Hørsholm, Denmark
356 Evaluation of diabetes-associated testicular morphology and the effects of MSC secretome as a therapeutic intervention
PhD Serbay Özkan[1]
[1]Izmir Katip Çelebi University, Faculty of Medicine, Histology and Embryology Department, Çiğli, Türkiye
368 Generation of AFM cellular datasets and classification by ML

Ophélie THOMAS- -CHEMIN[1], Zeyd BOUMEHDI[1], Childérick SEVERAC[2], Emmanuelle TREVISIOL[3], Etienne DAGUE[1]
[1]LAAS-CNRS, Toulouse, France, [2]RESTORE Research Center, Université de Toulouse, INSERM, CNRS, EFS, ENVT, Université P. Sabatier, Toulouse, France, [3]TBI, Université de Toulouse, CNRS, INRAE, INSA, Toulouse, France

370 Chitin in the cuticular capsule of tardigrade cysts

Mr. Kamil Janelt[1,2], Filip Wieczorkiewicz[1], Izabela Poprawa[1]
[1]Institute of Biology, Biotechnology and Environmental Protection, Faculty of Natural Sciences, University of Silesia in Katowice, Bankowa 9, 40-007 Katowice, Poland, Katowice, Poland, [2]Department of Medical Genetics, Faculty of Medical Sciences in Katowice, Medical University of Silesia, Medyków 18, 40-752 Katowice, Poland, Katowice, Poland

389 Effect of electron microscopy sample preparation protocol on the preservation of liposomes in cell culture

Associate Professor Paul Kempen[1], Nikoline Lykke Faurschou[1], Jonas Rosager Henriksen[2], Andrew urquhart[2]
[1]DTU Nanolab, Technical University of Denmark, Kgs. Lyngby, Denmark, [2]DTU Health Tech, Technical University of Denmark, Kgs. Lyngby, Denmark

488 Impact of Clostridium botulinum C2 Toxin on the ultrastructure of cells

Jasmin Christine Bellemann[1], Joscha Borho[2], Dr. Clarissa Read[1], Prof. Dr. Paul Walther[1], Prof. Dr. Holger Barth[2]
[1]Central Facility for Electron Microscopy, Ulm University, Ulm, Germany, [2]Institute of Experimental and Clinical Pharmacology, Toxicology and Pharmacology of Natural Products, Ulm University Medical Center, Ulm, Germany

664 THE INVESTIGATION OF THE PRESENCE OF TELOCYTE CELLS IN THE HUMAN OVARIAN STROMA

MD. PhD. Merjem Purelku[1], Research Assistant Ceren Cebi[2], Specialist Doctor Sait Sukru Cebi[4], Prof. Dr. Ismail Cepni[2], Prof. Dr. Sennur Ilvan[3], Prof. Dr. Gamze Tanrıverdi[1]
[1]Istanbul University - Cerrahpasa, Cerrahpasa Medical Faculty, Histology and Embryology Department, Istanbul, Turkey, [2]Obstetrics and Gynecology Department, Istanbul University - Cerrahpasa, Cerrahpasa Medical Faculty, Istanbul, Turkey, [3]Pathology Department, Istanbul University - Cerrahpasa, Cerrahpasa Medical Faculty, Istanbul, Turkey, [4]Obstetrics and Gynecology Department, Samsun Training and Research Hospital, Samsun, Turkey

686 Multimodal Low Voltage Transmission Electron Microscopy Analysis of Iodine Nanoparticles for Stroke Theranostics

Ing. Ph.D. Jaromír Bačovský[1], Tomáš Vácha[2], Tereza Padrtová[3], Jan Biskupič[2], Peter Scheer[4], Jana Hložková[4], Jiří Nováček[5], Radka Holbová[5], Michaela Kuchynka[2,3]
[1]Delong Instruments, Brno, Czech Republic, [2]Department of Chemical Drugs, Masaryk University, Brno, Czech Republic, [3]Department of Chemistry, Faculty of Science, Masaryk University, Brno, Czech Republic, [4]Department of Pharmacology and Toxicology, Masaryk University, Brno, Czech Republic, [5]CEITEC Masaryk University, Brno, Czech Republic

746 New protein fluorescent labeling methods for carbonylation and S-acylation studies in plants

MSc Andrea Román[1,2], MSc Salvador Priego[1,2], Ph.D. Antonio J. Castro[1], Dr Juan De Dios Alche[1,3]
[1]Plant Reproductive Biology and Advanced Imaging Laboratory (BReMAP), Estación Experimental del Zaidín (CSIC), Granada, Spain, [2]These authors contributed equally to this work, , Spain, [3]University Institute of Research on Olive Grove and Olive Oils (INUO), Jaén, Spain

788 Cholesteatoma removal efficiency evaluated by Variable Pressure Scanning Electron Microscopy

Prof Michela Relucenti[1], Prof Edoardo Covelli[2], Prof Orlando Donfrancesco[1], Prof Giuseppe Familiari[1], Prof Maurizio Barbara[2]
[1]Department of Anatomical, Histological, Forensic and Orthopedic Sciences, Section of Human Anatomy, Sapienza University of Rome, Rome, Italy, Rome, Italy, [2]Department of Neuroscience, Mental Health and Sensory Organs (NEMOS), Sapienza University of Rome, Rome, Italy, Rome, Italy

796 Immunoexpression of estrogen receptor α in the ovary of mice after chronic exposure to arsenic(III)-oxide

Ass.prof. Marija Marin[1], Anita Birinji[1], Full prof. Anita Radovanović[2], Ass.prof. Maja Čakić-Milošević[1], Full prof. Dušan Lalošević[3]
[1]University of Belgrade, Faculty of Biology, Belgrade, Serbia, [2]University of Belgrade, Faculty of Veterinary Medicine, Belgrade, Serbia, [3]University of Novi Sad, Faculty of Medicine, Novi Sad, Serbia

846 Effects of melatonin and alpha-lipoic acid on collagen and VEGF expression in palatal wound healing

Onur Kutlu[1], Gülten Kavak[1], Aslı Erdoğan Öner[2], Selen Akyol Bahçeci[2]
[1]Department of Oral and Maxillofacial Surgery, İzmir Katip Çelebi University , İzmir, Türkiye, [2]Department of Histology and Embryology, İzmir Katip Çelebi University, İzmir, Türkiye

859 Vitamin A affects urothelial injury and regeneration in cyclophosphamide-induced cystitis

Teaching Asisstent Brina Dragar[1], Senior Research Fellow Simona Kranjc Brezar[2], Research Fellow Tadeja Kuret[1], Research Fellow Tanja Jesenko[2], Professor Maja Čemažar[2], Professor Rok Romih[1], Professor Mateja Kreft Erdani[1], Associate Professor Daša Zupančič[1]
[1]Institute of Cell Biology, Faculty of medicine, University of Ljubljana, Ljubljana, Slovenija, [2]Department of Experimental Oncology, Institute of OncologyOncology, Ljubljana, Slovenia

866 Transmission electron microscopy of dermal collagen using ethanolic phosphotungstic acid staining

Dr Astrid Obermayer[1], Dr Stefan Hainzl[2], Dr Ulrich Koller[2], Ao. Univ.-Prof. Dr. Walter Stoiber[1]
[1]Department of Environment & Biodiversity, University of Salzburg, Salzburg, Austria, [2]EB House Austria, Research Program for Molecular Therapy of Genodermatoses, Department of Dermatology and Allergology, University Hospital of the Paracelsus Medical University, Salzburg, Austria

873 Toxic buffers used in microbial sample preservation for SEM can be replaced by PBS

Indra Banas[1], Noel Kleber[1], Dr. André Soares[1], Prof. Dr. Alexander Probst[1,2,3]
[1]Environmental Metagenomics, Research Center One Health Ruhr of the University Alliance Ruhr, Faculty of Chemistry, University of Duisburg-Essen, Essen, Germany, [2]Centre of Water and Environmental Research (ZWU), University of Duisburg-Essen, Essen, Deutschland, [3]Center of Medical Biotechnology (ZMB), University of Duisburg-Essen, Essen, Deutschland

875 Exploring Role of Voltage-Gated Ion Channels in LGI1 Autoantibody-Induced Epilepsy: Insights from a Mouse Model

Dr Jacqueline Montanaro[1], Hana Stefanickova[1], Dr. Mary Muhia[1], Prof. Dr. med Christian Geis[2], Claudia Sommer[2], Josefine Sell[2], Prof. Dr. Hans-Christian Korna[3], Prof. Dr. Harald Prüß[3], Prof. Ryuichi Shigemoto[1]
[1]Institute of Science and Technology Austria (ISTA), , Klosterneuburg, Austria, [2]Department of Neurology, Section Translational Neuroimmunology, Jena University Hospital, Jena, Germany, [3]German Center for Neurodegenerative Diseases (DZNE), Berlin, Germany

877 Effect of chloroquine and naringin on the relationship between ER stress and mitochondria in trophoblasts

Research Associate Zehra Sezer[1]
[1]ISTANBUL UNIVERSITY-CERRAHPASA, Istanbul, Turkey

906 Effects of corticosterone and amyloid beta on the corticosteroid receptors in organotypic brain slice cultures

Assistant Professor Merve Alaylıoglu[2], Professor ,PhD Selma Yilmazer[1], Professor PhD Erdinc Dursun[2], Professor PhD Duygu Gezen-Ak[2]
[1]Dept. of Medical Biology, Halic University, Faculty of Medicine, Istanbul, Turkey, [2]Brain and Neurodegenerative Disorders Research Laboratories, Department of Neuroscience, Institute of Neurological Sciences, Istanbul University- Cerrahpasa, Istanbul, , Turkey

935 Is iron a hidden culprit in Alzheimer's disease?

PhD Sowmya Sunkara[1], Dr Marlene Leoni[2], Dr Johannes Haybäck[2,3], Assoc. Prof. Dr Gerd Leitinger[1]
[1]Division of Cell Biology, Histology and Embryology, Gottfried Schatz Research Center, Medical University of Graz, Graz, Austria, [2]Diagnostics & Research Institute for Pathology, Medical University of Graz, Graz, Austria, [3]Tyrolpath Obrist Brunhuber GmbH, Zams, Austria

962 Comparison of the FMT assay with the Cell Painting approach in healthy patient derived fibroblasts.

Dr Tabea Hohensee[1], Dr Fredrik Edfeldt[1]
[1]Mechanistic and Structural Biology, Discovery Sciences, R&D, AstraZeneca, Gothenburg, Sweden

967 In-vivo DAB cytochemistry and high-pressure freezing to determine the source of the human cytomegalovirus envelope

Tim Bergner[1], Laura Cortez Rayas[2], apl. Prof. Jens von Einem[2], Dr. Clarissa Read[1]
[1]Central Facility for Electron Microscopy, Ulm University, Ulm, Germany, [2]Institute of Virology, Ulm University Medical Center, Ulm, Germany

976 Evaluation of inflammation and free fatty acid metabolism as biomarkers in female patients

Assoc.prof.dr. Pınar Köroğlu[1], Sultan Üzümcüoğlu[2], Muhammed Melik Anşin[2], Prof.Dr. Ulun Uluğ[3]
[1]Halic University, Faculty of Medicine, Department of Histology and Embryology , Istanbul, Turkey, [2]Halic University, Faculty of Medicine, Istanbul,, Turkey, [3]Halic University, Faculty of Medicine, Department of Obstetrics and Gynecology, , Turkey

977 The Healing Effect Of Ferulic Acid in Monosodium Glutamate-Induced Liver Injury

Student Seda Sezer[1,2], Anıl Can[1,2], Assoc. Dr. Merve Açıkel Elmas[1], Assoc. Dr. Meltem Kolgazi[3], Prof. Dr. Serap Arbak[1]
[1]Department of Histology and Embryology, School of Medicine, Acibadem Mehmet Ali Aydinlar University, Istanbul, Turkey, [2]Department of Histology and Embryology, Institute of Health Sciences, Acibadem Mehmet Ali Aydinlar University, Istanbul, Turkey, [3]Department of Physiology, School of Medicine, Acibadem Mehmet Ali Aydinlar University , Istanbul , Turkey

982 Neuroprotective Effects of Bromelain in Peripheral Nerve Injuries: A Rat Sciatic Nerve Crush Injury Model

DR. ONUR AKSOY[3], DR. ILKER USCETIN[3], ASSOC. PROF. SAMED OZER[2], ASSOC. PROF. MERVE ACIKEL ELMAS[1], BIO. GOKCEN OZGUN[4], BIO. SEDA SEZER[5], Prof. Dr Serap Arbak[1]
[1]DEPARTMENT OF HISTOLOGY AND EMBRYOLOGY ACIBADEM MEHMET ALI AYDINLAR UNIVERSITY SCHOOL OF MEDICINE, ISTANBUL, TURKEY, [2]Animal Application and Research Center, Acibadem Mehmet Ali Aydinlar University, ISTANBUL, TURKEY, [3]Prof Dr Cemil Tascioglu City Hospital, Department of Plastic and Reconstructive Surgery, ISTANBUL, TURKEY, [4]Institute of Health Sciences, Department of Biotechnology, Acibadem Mehmet Ali Aydinlar University, ISTANBUL, TURKEY, [5]Institute of Health Sciences, Department of Histology and Embryology Acibadem Mehmet Ali Aydinlar University, ISTANBUL, TURKEY

1027 Imaging-based methods to identify prognostic and predictive biomarkers for Hereditary Spastic Paraplegia

Phd Student Gaia Fattorini[1,2], Researcher Valerio Licursi[1], Professor Filippo Maria Santorelli[3], Professor Gabriella Silvestri[4], Professor Carlo Casali[5], Researcher Cinzia Rinaldo[1], PhD Francesca Sardina[1]
[1]Institute of Molecular Biology and Pathology (IBPM), Consiglio Nazionale delle Ricerche (CNR), Rome, Italy, [2]Department of Biology and Biotechnology "Charles Darwin", Sapienza University of Rome, Rome, Italy, [3]IRCCS Stella Maris, Pisa, Italy, [4]UOC Neurologia, Fondazione Policlinico Universitario 'A. Gemelli' IRCCS, Rome, Italy, [5]Department of Medico-Surgical Sciences and Biotechnologies, University of Rome Sapienza, Latina, Italy

1052 Carbonic anhydrase immobilization for microscopic investigation of enzyme activity

Dr. Zsófia Bognár[1], Jeannette de Sparra Lundin[2], Sune Christensen[2], Joerg Jinschek[1,3], Jialong Shen[4], Sonja Salmon[4], Stig Helveg[1]
[1]Center for Visualizing Catalytic Processes (VISION), Department of Physics, Technical University of Denmark, Kgs. Lyngby, Denmark, [2]Novonesis A/S, Kgs. Lyngby, Denmark, [3]National Centre for Nano

Fabrication and Characterization (DTU Nanolab), Technical University of Denmark, Kgs. Lyngby, Denmark, [4]Textile Biocatalysis Research, Department of Textile Engineering Chemistry & Science, North Carolina State University, Raleigh, USA

1056 Histopathologic Alterations of Cerebellum in the VPA-Induced Autism Model of Rats

Dr Sila GUVENIR SEVEN[1], MSc Hakan Sahin[2], Prof. Dr. Gozde Erkanli Senturk[2], Nesibe Uysal[3], Prof. Dr. Hafize Uzun[4], Prof. Dr. Gonul Simsek[1]

[1]Department of Physiology, Cerrahpasa Faculty of Medicine, Istanbul University-Cerrahpasa, Istanbul, Turkey, [2]Department of Histology and Embryology, Cerrahpasa Faculty of Medicine, Istanbul University-Cerrahpasa, Istanbul, Turkey, [3]Cerrahpasa Faculty of Medicine, Istanbul University-Cerrahpasa, Istanbul, Turkey, [4]Department of Medical Biochemistry, Faculty of Medicine, Atlas University, Istanbul, Turkey

1068 Investigation of the Presence of Telocyte-like Cells in Human Patellar Fat Pad Tissue

Professor Doctor Gamze Tanriverdi[1], MD. PhD Merjem Purelku[1], Ph.D Zehra Sezer[1], Specialist Doctor Duygu Neccar[1], M.sC. Naziya Bagirova[1], Research Assistant Yonca Aras[1], Associate Professor Ersin Erçin[2], Specialist Doctor Alican Koluman[2], Professor Doctor Gozde Erkanli Senturk[1], Associate Professor Bulent Tanriverdi[2]

[1]Istanbul University - Cerrahpasa, Cerrahpasa Medical Faculty, Histology and Embryology Department , Istanbul , Turkey , [2]Department of Orthopedics and Traumatology, Istanbul Bakirkoy Dr. Sadi Konuk Education and Research Hospital, University of Health Sciences, Istanbul, Turkey

1116 Effects of swimming training on orexin receptor 2 distribution in brain damage of rats

Professor Dilek Akakın[1], Assoc. Prof. Merve Acikel Elmas[2], Phd Student Ayca Karagoz Koroglu[1], Assoc. Prof. Ozlem Bingol Ozakpinar[3], Prof. Filiz Onat[4], Professor Feriha Ercan[1]

[1]1, Istanbul, Turkiye, [2]2, Istanbul, Turkiye, [3]3, Istanbul, Turkiye, [4]4, Istanbul, Turkiye

1118 Microscopy to discern cells behaviour on different nano/microstructured calcium phosphates ceramics

Dr. Eva Filová[1], Dr. Carolina Oliver-Urrutia[2], Dr. Věra Hedvičáková[1], Dr. Veronika Hefka Blahnová[1], Ms. Eva Šebová[1], Ms. Radmila Žižková[1], Assoc. Prof. Karel Dvořák[2], Assoc. Prof. Ladislav Čelko[2], Dr. Edgar Montufar[2]

[1]Institute of Experimental Medicine, Czech Academy of Sciences, Prague, Czech Republic, [2]Central European Institute of Technology, Brno University of Technology, Prague, Czech Republic

1130 Development of multiciliated cells in the respiratory and esophageal epithelium of the chicken embryo

Dr. Sebastian Reinke[1], Dr. Alexander Reinke[1], Dr. Marcus Frank[1,2]

[1]Medical Biology and Electron Microscopy Centre, University Medicine Rostock, 18055 Rostock, Germany, [2]Department Life Light & Matter, University of Rostock, 18051 Rostock, Germany

1138 Nestin expression in the myocardium of normotensive and spontaneously hypertensive rats during aging

Assoc. Prof. Dana Cizkova[1], Assoc. Prof., Ph.D. Jitka M. Zurmanova[2], M.D. Lucie Gerykova[1], Ph.D. Barbara Elsnicova[2], Frantisek Galatik[2], Ph.D. Jan Silhavy[3], Ph.D. Michal Pravenec[3], Prof., M.D., Ph.D. Jaroslav Mokry[1]

[1]Charles University, Faculty of Medicine in Hradec Kralove, Department of Histology and Embryology , Hradec Kralove, Czech Republic, [2]Charles University, Faculty of Science, Department of Physiology, Prague, Czech Republic, [3]Czech Academy of Sciences, Institute of Physiology, Prague, Czech Republic

1147 Molecular insights into rapid cell death involving endoplasmic reticulum and nuclear remodeling p

Ms. Samudra Sabari, António Pedro N. B. M. Carneiro, Ines Ambite, Siddharth Chinchankar, Parisa Esmaeili, Prof. Catharina Svanborg, Dr. Arunima Chaudhuri

[1]Lund University, Lund, Sweden

1148 Effects of Myricetin on Mesenchymal Stem Cells Exposed to Oxidative Stress
Prof. Dr. Sibel Köktürk[1], Dr. Mehmet Berker[1], Aysel Bayramova[1], Sibel Doğan[1], Dr. Emel Usta[1], Feride Özdemir[1]
[1]Department of Histology and Embryology, Istanbul University, Istanbul Medical Faculty, İstanbul, İstanbul
1150 The effects of resveratrol on liver damage and ferroptosis in fructose-streptozotocin induced diabetic model
Assoc. Prof Fatma Kaya Dagistanli[1], MSc Mahsa Hoseini[1], MSc Merve Aykac[2], Prof. Dr. Turgut Ulutin[1]
[1]Department of Medical Biology, Cerrahpasa Faculty of Medicine, Istanbul University-Cerrahpasa, Istanbul, Türkiye, [2]Department of Medical Biology, Medical Faculty, Ataturk University , Erzurum, Türkiye

Late Poster Presentation

1219 An efficient method for quantifying the degree of neurodegeneration in an insect brain
Jakub Opelka[1,2], Lucie Pauchova[1], Andrea Bednarova[1], Radka Zavodska[1,3], Michal Sery[1,3], Ivo Sauman[1,2], Hana Sehadova[1,2]
[1]Faculty of Science, University of South Bohemia, Ceske Budejovice, Czech Republic, [2]Faculty of Science, University of South Bohemia, Ceske Budejovice, Czech Republic, [3]Faculty of Education, University of South Bohemia, Ceske Budejovice, Czech Republic
1249 FlexAble Labeling of Primary Antibodies with Fluorescent Dyes and Biotin for Multiplex Experiments
PhD Larisa Yurlova[1], Michael Metterlein[1], PhD Longtao Wu[2], XinXing Wang[3], Dr. Christian Linke-Winnebeck[1], Dr. Andrea Buchfellner[1], PhD Lion Lian[3], PhD Deepa Shankar[2], PhD Jason Li[2]
[1]Proteintech Group, Martinsried, Germany, [2]Proteintech Group, Rosemont, USA, [3]Proteintech Group, Wuhan, China
1305 The synthetic chaperonin Poly-CCT5 as a nanoparticle carrier
Mr. Sergio Pipaón[1], Mr. Jorge Gutiérrez[1], Mr. Jesús G. Ovejero[2], Mrs. María del Puerto Morales[2], Mr. Jorge Cuéllar[1], Mr. José María Valpuesta[1]
[1]National Center For Biotechnology (CNB-CSIC), Madrid, Spain, [2]Department of Materials for Health of the Materials Science Institute of Madrid (ICMM), Madrid, Spain
1344 Effects of Vitamin D Administration On Testicular Tissue in Metabolic Syndrome Rats
Tugce Ozbilenler[1], Betul Zorkaya[2], Sakine Rzayeva[1], Nergis Bayramova[1], Seda Akdemir[3], Cigdem Bayram Gurel[1], Evrim Bayrak Komurcu[4], Ahmet Dirican[5], Fatma Kaya Dagistanli[1], Prof Melek Ozturk Sezgin[1]
[1]Department of Medical Biology, Cerrahpasa Faculty of Medicine, Istanbul University-Cerrahpasa, Istanbul, Turkiye, [2]Department of Genetics, Aziz Sancar Institute of Experimental Medicine, Istanbul University, Istanbul, Turkiye, [3]Department of Medical Biology, Faculty of Medicine, Karabuk University, Karabük, Turkiye, [4]Department of Medical Genetics, Istanbul Faculty of Medicine, Istanbul University, Istanbul, Turkiye, [5]Department of Biostatistics, Cerrahpasa Faculty of Medicine, Istanbul University-Cerrahpasa, Istanbul, Turkiye

73

Localization techniques in biomedical electron microscopy: good as gold

Wiebke Möbius[1]
[1]Max-Planck-Institute for Multidisciplinary Sciences, Göttingen, Germany

LS-05, Lecture Theater 5, august 26, 2024, 14:00 - 15:00

Background
Combining structural information with the localization of molecules and proteins provides important information for the investigation of cellular processes especially in the context of pathology. Different strategies are available to obtain samples suitable for labeling techniques in electron microscopy.
Methods
In principle, labeling probes can be applied to a permeabilized sample before embedding and sectioning, called preembedding-labeling. Alternatively, the probes are used to localize molecules on the section by so-called post-embedding or on-section labeling. A popular example for this approach is immunolabeling of cryosections according to Tokuyasu. Apart from this, other methods are available to gain accessibility for probes to subcellular structures such as whole mount or freeze fracture replica labeling.
Results
By using mostly cryosections according to Tokuyasu we studied lipid and protein distribution in cells and tissues investigating for example the formation and composition of exosomes secreted by cultured B-cells as a mechanism of antigen presentation. Exosomes also play important roles in cell-cell communication within the nervous system. We showed that exosomes are involved in axonal support by glia cells such as oligodendrocytes which is the myelin forming cell type in the central nervous system. These properties were affected by deficiency of oligodendrocytes for specific myelin proteins. We show examples how immunoelectron microscopy provided important data complementing other investigation methods in understanding cell biology in general and axo-glia interaction in particular.
Conclusion
Different approaches for sample preparation and the different strategies in immunoelectron microscopy are available. Which of those is applied depends on the question under investigation and the properties of the sample. These techniques allow the localization of proteins or molecules in the context of the cellular or tissue environment. Localization probes require a careful validation of their specificity.

Keywords:

ImmunoEM, pre-, postembedding labeling, cryosections

Reference:

Möbius W (2023) Immunoelectron Microscopy: High Resolution Immunocytochemistry. In: Bradshaw, Hart and Stahl (eds.) Encyclopedia of Cell Biology, Second Edition, vol. 2, pp. 37–50. Oxford: Elsevier

Möbius W, Posthuma G (2018) Sugar and ice: Immunoelectron microscopy using cryosections according to the Tokuyasu method. Tissue Cell. 2019 Apr;57:90-102.

405

Whole-brain 3D quantification of alpha-synuclein spreading and toxicity in a mouse model of Parkinson's disease

Phd Student Frederikke Lynge Sørensen[1,2], Annika Højrup Runegaard Thomsen[1], Urmas Roostalu[1], Jacob Lercke Skytte[1], Evi Alexiou[1], Jacob Hecksher-Sørensen[1], Poul Henning Jensen[2], Yasir Gallero-Salas[1], Henrik Björk Hansen[1]
[1]Gubra Aps, Hørsholm, Denmark, [2]Biomedicine and DANDRITE, Aarhus University, Aarhus, Denmark
LS-05, Lecture Theater 5, august 26, 2024, 14:00 - 15:00

Background & Aim: Progressive spreading of alpha-synuclein (aSyn) aggregates in the brain plays a key role in the prodromal phase of Parkinson's disease (PD). While several preclinical models of synucleinopathies have been developed for studying the neurotoxicity of prion-like aSyn aggregate spreading, they remain to be systematically explored with regards to early pathological events that could potentially be targeted to slow down or prevent progression of PD. Using whole-brain light sheet fluorescence microscopy (LSFM), the present study aimed to provide a detailed 3D map of progressive pathological aSyn spreading and tyrosine hydroxylase (TH) expressing neurons and projections in the aSyn pre-formed fibril (PFF) mouse model of PD.

Methods: 8-weeks old C57BL/6 male mice received two unilateral, intrastriatal injections of murine aSyn PFFs (5 µg per injection). Mice were terminated at 1, 4, 8-, 12-, 16-, or 26-weeks post-injection (wpi), whole-brains were dual immunolabelled for aSyn phosphorylated at serine-129 (pS129-aSyn, marker of aSyn aggregation) and TH, optically cleared (iDISCO+) and scanned using LSFM at cellular resolution. AI-based computational analysis enabled automated whole-brain mapping and quantification of pS129-aSyn and TH fluorescence intensity across 840 individual brain regions using a custom mouse brain atlas.

Results: Distinct spatiotemporal phases of endogenous aSyn aggregate spreading observed in aSyn PFF mice over time. The phases included progressive spread of aSyn aggregates to primary seeding regions (amygdala, substantia nigra, and several cortical areas) and secondary seeding regions (entorhinal area and hippocampal formation) based on their interconnectivity to the injection site (striatum), followed by redistribution of aSyn aggregates in specific brain regions. In parallel, TH expression was progressively downregulated in the nigrostriatal pathway, suggesting axonal damage in terminal areas preceding dopaminergic neuronal loss in the aSyn PFF mouse model.

Conclusion: We here report a complete whole-brain map of aSyn aggregate spreading in an industry-standard aSyn PFF mouse model of PD. The anatomical complexity of aSyn aggregate spreading in the model underscores the unique applicability of whole-brain 3D LSFM imaging to fully capture spatiotemporal dynamics in aSyn and TH expression, making the model highly instrumental for the evaluation of therapeutic modalities that may prevent aSyn aggregate spreading and dopaminergic neuronal loss.

Keywords:

3D microscopy, tissue clearing, synucleinopathies

779

The effect of fixation-induced cell blebbing: how to minimize a loss of proteins from cells?

Prof. Pavel Hozak[1]
[1]Institute of Molecular Gentics ASCR, Prague, Czech Republic

LS-05, Lecture Theater 5, august 26, 2024, 14:00 - 15:00

In the course of the preparation of biological samples for various microscopy techniques, the first and the most essential step is a fixation. The efficiency of the fixation procedure is estimated by two main factors: the preservation of the cellular constituents and the suitability for further treatments like immunolabelling. However, till now the detailed mechanisms of the cell fixation are not fully understood and we rely mostly on empirical experiences. We concentrated on studying the fixation-induced cell blebbing, and searched for the way to minimize this deteriorating effect. By means of different microscopy methods, we quantitatively assessed the loss of cytoplasmic content during the rupture of blebs. With holography microscopy time-lapse experiments, we found that the key points are the formation and rupture of blebs, and we discuss the possible mechanism of blebs appearance. Importantly, it was shown that up to 30% of soluble proteins can be lost from cytoplasm after the blebs rupture. Based on these data, we tested a wide range of fixation mixtures applied during different time intervals to minimize the loss of cytoplasmic proteins. Taking into account different quantitative parameters, we determined the optimal procedures to fix the cells. Finally, we provide some recommendations on the fixation protocols which are suitable for future experiments.

Keywords:

formaldehyde fixation, blebbing, artefacts, microscopy

Reference:

This research and publication was supported by the Czech-BioImaging large RI project (LM2023050 funded by MEYS CR.

27

In vitro genotoxic activity of leaf and flower extracts of four alien invasive plant species

Mirela Uzelac Bozac[1], Dr Petra Cvjetko[2], Dr Katarina Caput Mihalić[2], Miss Ela Kukac[3], Dr Slavica Dudaš[4], Dr Barbara Sladonja[1], Dr Danijela Poljuha[1]
[1]Institute of Agriculture and Tourism, Porec, Croatia, [2]Faculty of Science, University of Zagreb, Zagreb, Croatia, [3]Department of Biotechnology, University of Rijeka, Rijeka, Croatia, [4]Agricultural Department, Polytechnic of Rijeka, Rijeka, Croatia

Poster Group 1

Background and aim
Alien invasive plants are rich in specialized metabolites presenting promising potential as a valuable reservoir of bioactive phytochemicals applicable to the pharmaceutical sector. A critical requirement for their practical application is their non-toxicity. This study aims to assess the genotoxic activity of leaf and flower extracts of Ailanthus altissima (Mill.) Swingle, Robinia pseudoacacia L, Helianthus tuberosus L., and Solidago canadensis L. from Istria (Croatia) by the comet (single cell gel electrophoresis) assay.
This study is performed in the framework of the project "NATURe as an ALLY: Alien Invasive Plants as Phytopharmaceuticals— NATURALLY" (IP-2020-02-6899) and "Young Researchers' Career Development Project–Training New Doctoral Students" (DOK-2021-02-3094) founded by Croatian Science Foundation. The study aims to propose a new model for exploring new invasive alien plant species in provisioning (medicinal) ecosystem services on the pilot territory of Istria (Croatia). This study represents the first of its kind in the region since it's known that the phytochemical composition and biological characteristics of plants depend on the abiotic and biotic traits of their habitat.
Methods
Plant extracts were prepared using finely minced air-dried leaves and inflorescences collected and pooled from 15 locations in Istria and solved in 2% dimethyl sulfoxide (DMSO) in Endothelial Basal Medium-2 (EBM-2, Lonza, San Diego, CA). The ability to induce in vitro genotoxic effect in human liver-derived endothelial cells (HLEC) was assessed for three extract concentrations: 1.0 mg/ml, 0.5 mg/ml, and 0.1 mg/ml. Comet assay was stained with GelRed Nucleic Acid Gel Stain, visualized with Zeiss Axioscope 5 fluorescence microscope, and analyzed using the software KOMET5 (Kinetic Imaging Ltd., Liverpool, UK). The tail DNA percentage (% tDNA) was used as the primary measure of DNA damage.
Results
The treatments with leaf and flower extracts of all four species in concentrations of 1.0 mg/ml resulted in a significant increase of % tDNA compared to the control. Additionally, the leaf and flower extracts of A. altissima and leaf extract of R. pseudoacacia in 0.5 mg/ml also increased % tDNA.
Conclusions
These findings suggest that leaf and flower extracts in concentrations below 0.1 mg/ml do not cause substantial DNA damage in human hepatocytes, indicating a promising avenue for further research regarding the potential use of these extracts in pharmaceutical applications.

Keywords:

Comet_assay, DNA_damage, plant _extracts, invasive_plants

59

Light sheet imaging across scales for preclinical drug discovery research

Yasir Gallero Salas[1], Mr. Max Hahn[1], Mr. Thomas Topilko[1], Ms. Marie Biviano Rosenkilde[1], Ms. Frederikke Lynge Sørensen[1], Ms. Lea Lydolph Larsen[1], Ms. Katrine Skovgård[1], Mr. Urmas Roostalu[1]
[1]Gubra, Hørsholm, Denmark

Poster Group 1

Whole organ 3D light sheet fluorescence microscopy (LSFM) is gaining popularity in preclinical pharmacological research to map the expression of new drug targets, characterize compound biodistribution, visualize drug induced changes in neuronal activation and to demonstrate the efficacy of pharmaceuticals to alter pathological changes in animal models of human diseases. Its broad applicability arises from the capability of imaging structures ranging from a few micrometres to centimetres, possibility of visualizing multiple fluorophores simultaneously and detecting subtle differences in their intensities. As such, LSFM bridges the gap between traditional in vivo imaging modalities and high-resolution histology and confocal microscopy of fixed tissue samples. Still, sample preparation for LSFM depends heavily on the tissue type and the desired imaging endpoints. Testing multiple parameters is often time-consuming as the protocols can take months to complete. Here we demonstrate a stepwise decision matrix to select suitable sample preparation steps for all rodent organs to characterize both compound distribution, mRNA and protein localization. We demonstrate pretreatment steps most suitable to visualize compound biodistribution, show the improved protocol to achieve uniform antibody staining in rat samples and present the workflow for 3D LSFM of hearts and other peripheral organs. Finally, we successfully expand the proposed decision matrix to include minipigs brains, a large gyrencephalic brain.

Keywords:

light-sheet microscopy
preclinical
drug discovery

93

Contribution of Probiotics to the Effect of Platelet-Rich Plasma in Diabetic Rat Skin Wound Healing

Prof. Dr. Erdogan Kocamaz, Prof. Dr. Muge Karakayali, PhD Fatih Collu, Prof. Dr. Sevinc Inan, Prof. Dr. Ibrahim Tuglu
[1]Department of Histology and Embryology, Manisa Celal Bayar University, Faculty of Medicine, Manisa, Turkey, [2]Department of Microbiology, Izmir Democracy University, Faculty of Medicine, Izmir , Turkey, [3]Department of Zoology, Manisa Celal Bayar University, Faculty of Life Sciences, Manisa, Turkey, [4]Department of Histology and Embryology, Izmir University of Economics, Faculty of Medicine, Izmir, Turkey, [5]Department of Histology and Embryology, Manisa Celal Bayar University, Faculty of Medicine, Manisa, Turkey

Poster Group 1

Background incl. aims
Diabetic (DB) wound treatment is still an important problem due to chronic non-healing ulcers that can become infected and lead to amputation. Platelet Rich Plasma (PRP) is a Cellular Therapy (CT) product that has been frequently used nowadays. Probiotics (PB) accelerate healing through the changes they make in the intestine. This study aimed to examine the contribution of PB to the effects of PRP in diabetic wound healing.
Methods
The diabetic model was created by intraperitoneal application of 45 mg/kg Streptozotocin. A 1x1 cm2 full-thickness skin wound was created in those with fasting blood sugar (FBS) above 250 mg/dl. Mature Albino rats were divided into four group (n:5, each) as DB, DB+PRP, DB+PB and DB+PRP+PB. PRP solution prepared as 100uL was used for 10 subcutaneous 10uL applications to the wound edges. PB was administered orally at a dose of approximately 200 mg/day, once a day, starting with the experiment and until euthanasia. During the seven-day experiment, the PB group was fed by gavage every day. Formalin fixed parafine embedded sections were analysis with Hematoxylin & Eosin and Masson's Trichrom histochemical staining methods. Immunohistochemical analysis was performed with eNOS, Caspase 3, IL10, VEGF and Collagen I primary antibodies.
Results
It was observed that the diabetic wound closed significantly faster with PRP. It was determined that healing speed increased significantly and there was a better recovery with PB. It was shown that increased eNOS and Caspase 3 immunoreactivities and decreased IL10, VEGF and Collagen I immunoreactivities during injury were reversed by PRP+PB. It was found that PB application made a significant contribution to the positive effects and reversed parameters realized with PRP.
Conclusion
Preventing oxidative stress and apoptosis, increasing anti-inflammation, vascularization, numerical cell support of connective tissue and signaling pathways with PRP supplemented with PB made a significant contribution to wound healing. It turns out that PB support may be important for difficult-to-heal DB wounds. It was thought that this contribution could further improve the impaired life quality of patient's.

Keywords:

Diabetes, Wound healing, Probiotic, PRP

Reference:

Qian Z, Wang H, Bai Y et al. Improving Chronic Diabetic Wound Healing through an Injectable and Self-Healing Hydrogel with Platelet-Rich Plasma Release. ACS Appl Mater Interfaces. 2020Dec16;12(50):55659-55674.
Campos LF, Tagliari E, Casagrande TAC et al. Effects of Probiotics Supplementation on Skin Wound Healing In Diabetic Rats. ArqBrasCirDig. 2020Jul8;33(1):e1498.

194

Exploring cardiac innervation by 3D light sheet imaging in horses with atrial fibrillation

Mélodie Schneider[1], PhD Sarah Dalgas Nissen[1], DVM Simon Libak Haugaard[1], Prof Rikke Buhl[1], PhD Urmas Roostalu[2]
[1]University of Copenhagen, Copenhagen, Denmark, [2]Gubra, Hørsholm, Denmark

Poster Group 1

Background incl. aims
Local hyperinnervation plays a pivotal, yet poorly understood role in the initiation and maintenance of atrial fibrillation (AF). Changes in the intricate 3-dimensional (3D) network of nerves are difficult to characterize using traditional histological methods and AF has been challenging to study in preclinical rodent models. Non-destructive imaging techniques capable of visualizing larger tissue samples from large animal models are crucial to understand innervation changes in AF. Here, we aimed to investigate the feasibility of 3D light sheet fluorescence microscopy (LSFM) in equine atrial tissue and characterize the autonomic cardiac remodeling in a horse model of experimentally induced chronic AF.
Methods
Biopsies from the anterior descending ganglionated plexus were harvested from horses after 4-months of induced AF (n = 9), from horses with naturally occurring AF (n = 3) and healthy control horses (n = 3). Immunostaining with two neuronal markers (Tyrosine hydroxylase and Neurofilament) in parallel with a vascular marker (Transgelin) was performed to determine the local density of nerves and vasculature by computational image analysis. Whole-mount immunohistochemistry and clearing was optimized for equine heart samples by testing different depigmentation, permeabilization and imaging protocols.
Results
We present a protocol for 3D imaging of nerves in large equine atrial samples, spanning several centimeters in size. Optimized sample preparation with stepwise chemical and enzymatic extracellular matrix loosening and digestion enabled uniform sample labelling with antibodies against neuronal markers. Customized autofluorescence bleaching, sample clearing and imaging parameters facilitated high resolution imaging of cardiac innervation across the entire tissue sample. Computational analysis of atrial innervation permitted quantitative analysis in the study groups to demonstrate spatial changes occurring in atrial fibrillation.
Conclusion
3D LSFM in large animal models can improve our understanding of the mechanisms of diseases. This newly developed sample preparation protocol is well suited for single-cell resolution imaging in dense cardiac biopsies. We show the applicability of the method in characterizing innervation changes in an equine model of AF.

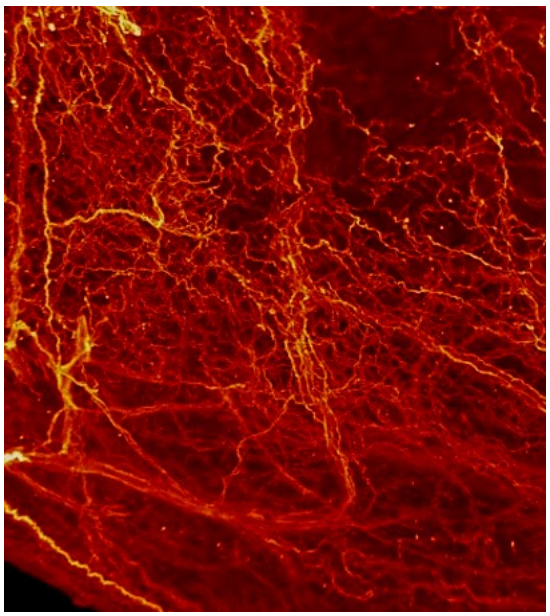

Keywords:

3D LSFM, AF, equine model

Reference:

Chang et al. Nerve sprouting and sympathetic hyperinnervation in a canine model of atrial fibrillation produced by prolonged right atrial pacing. Circ. 2001

Gussak et al. Region-specific parasympathetic nerve remodeling in the left atrium contributes to creation of a vulnerable substrate for atrial fibrillation. JCI-Insight. 2019

Susaki, et al. Advanced CUBIC protocols for whole-brain and whole-body clearing-and imaging. NatProtoc 2015

356

Evaluation of diabetes-associated testicular morphology and the effects of MSC secretome as a therapeutic intervention

PhD Serbay Özkan[1]
[1]Izmir Katip Çelebi University, Faculty of Medicine, Histology and Embryology Department, Çiğli, Türkiye

Poster Group 1

Background incl. aims
Diabetes is a metabolic disease characterized by prolonged hyperglycemia, which causes various types of complications, including impaired reproductive function. Diabetes-related microvascular damages, oxidative stress and insulin resistance could bring about a wide range of endocrine organ damages associated with the secretion of reproductive hormones and lead to hormonal imbalance, seminiferous tubule injury, including disrupted spermatogenesis and dysfunction of Sertoli cells. Ultimately, diabetes impacts male sexual function by leading to issues like erectile dysfunction, reduced libido and sperm damage. Mesenchymal stem cells (MSCs) could be a potential therapeutic intervention for the treatment of diabetes and accordingly, associated disorders like dysfunction of the male reproductive system1. Conditioned media (CM) obtained from MSCs contain soluble and non-soluble factors, all of which are collectively considered as one of the best ways of conveying MSCs' therapeutic effects, including angiogenesis, anti-inflammatory and -apoptotic effects, immunomodulation, and promotion of tissue repair and regeneration. Preconditioning of MSCs with different strategies, like incubation in hypoxic or 3-dimensional (3D) cell culture conditions, could improve their therapeutic potential2. In our previous study, the application of CM collected from MSCs cultured in 3D microfabricated scaffold to diabetic rats improved beta-cell regeneration and immunomodulation in comparison to the one obtained in conventional 2D culture conditions3. In this research, it was aimed to investigate the effects of prolonged hyperglycemia on serum reproductive hormone levels and testicular morphology of Sprague Dawley rats with diabetes, and the possible therapeutic effects of systemic application of CM derived from MSCs.
Methods
MSCs isolated from the human umbilical cord by tissue explant method were used for the collection of 2D-CM and 3D-CM. 22 rats were intraperitoneally treated with multiple low doses of streptozotocin (STZ; 5 days, 20 mg/kg) to induce diabetes. By the injection of last dose of STZ, it was confirmed that all the rats were in the range of diabetes (blood glucose level >250 mg/ml). Following the 2nd week of the first dose STZ injection, equal volumes (1 mL) of 2D-CM and 3D-CM were intraperitoneally applied to the diabetic rats (D+2D-CM, n=8; D+3D-CM, n=8) for 4 weeks as 3 doses a week. After 1 week of injection of the last dose, blood samples were collected by cardiac puncture for serum analysis of the hormones. The rats were sacrificed, and testis were obtained for light and transmission electron microscopic (TEM) evaluations. Serum concentrations of testosterone, gonadotropin-releasing hormone (GnRH), luteinizing hormone (LH), and follicle-stimulating hormone (FSH) were determined with enzyme-linked immunosorbent assay (ELISA). Light microscopic evaluation was performed with hematoxylin + eosin (H+E) staining. Semiquantitative Johnsen's tubular biopsy score (JTBS) analysis was used to histopathologically evaluate spermatogenesis out of an average 40 seminiferous tubules (STs). In this respect, STs were scored from 1 (no cell in the tubule section) to 10 (complete spermatogenesis and perfect tubules) in accordance with the level of epithelial maturation. Histomorphometric analyses were executed with the Fiji ImageJ software program by measuring the shortest diameter of ST and length of seminiferous epithelium (SE) (the distance between the basal lamina of SE and the closest spermatozoa to the lumen) out 10 STs for each specimen (n=3 for each group) at 40X magnification. Statistical analyses were performed using SPSS version 20.0 software. $P<0.05$ was accepted as statistically significant.

Results

ELISA analysis showed that serum LH and testosterone levels of experimental groups significantly decreased compared to the C group ($p < 0,05$). Serum GnRH and FSH levels were found to be significantly reduced in the D and D+2D-CM groups ($p<0,01$ and $p<0,05$ respectively), while there was no significant difference noted between the C and D+3D-CM groups. Our preliminary light microscopic analysis indicated that the JTBS values of experimental groups were significantly lower than the one of the C group while there was mild amelioration in D+3D-CM group in comparison to D group. On the other hand, our preliminary histomorphometric analysis of ST diameter and SE length did not show notable differences among the groups. TEM evaluation of SE revealed that the C group had normal ultrastructural morphology while spermatogonia with dispersed heterochromatin, primary spermatocytes having damaged mitochondria with loss of lamellar properties, cytoplasmic vacuolization in spermatogenic cell series and large intercellular spaces were noted in the D group. Additionally, assessments of spermatids at different stages of spermiogenesis demonstrated the presence of spermatids with disrupted chromatin condensation in the D group. In both treatment groups, such impairments were relatively fewer than the ones in the diabetic group and considerable restoration of ultrastructures of Sertoli and spermatogenic cells in seminiferous epithelium was observed.

Conclusion

In this diabetes model induced with multiple low doses of streptozotocin (5 days, 20 mg/kg), our preliminary light microscopic and TEM evaluations indicate that diabetes-associated damage in testis, specifically STs, was at a distinctive degree, and application of CM led to improvement in spermatogenesis and ultrastructural morphology of SE. On the other hand, when the differential changes in concentrations of serum reproductive hormones, including testosterone, GnRH, LH, and FSH, were considered, hyperglycemia seemed to affect the hypothalamic-pituitary-gonadal (HPG) axis by interrupting the feedback mechanism. The treatments with the CM, especially 3D-CM brought about considerable restoration of GnRH and FSH serum levels, but this was not enough to improve serum testosterone level, which is both a product and regulator of the HPG axis in males. The discrepancy between the morphological and hormonal analysis also suggests considering unrevealed mechanism of therapeutic action for MSCs derived CMs.

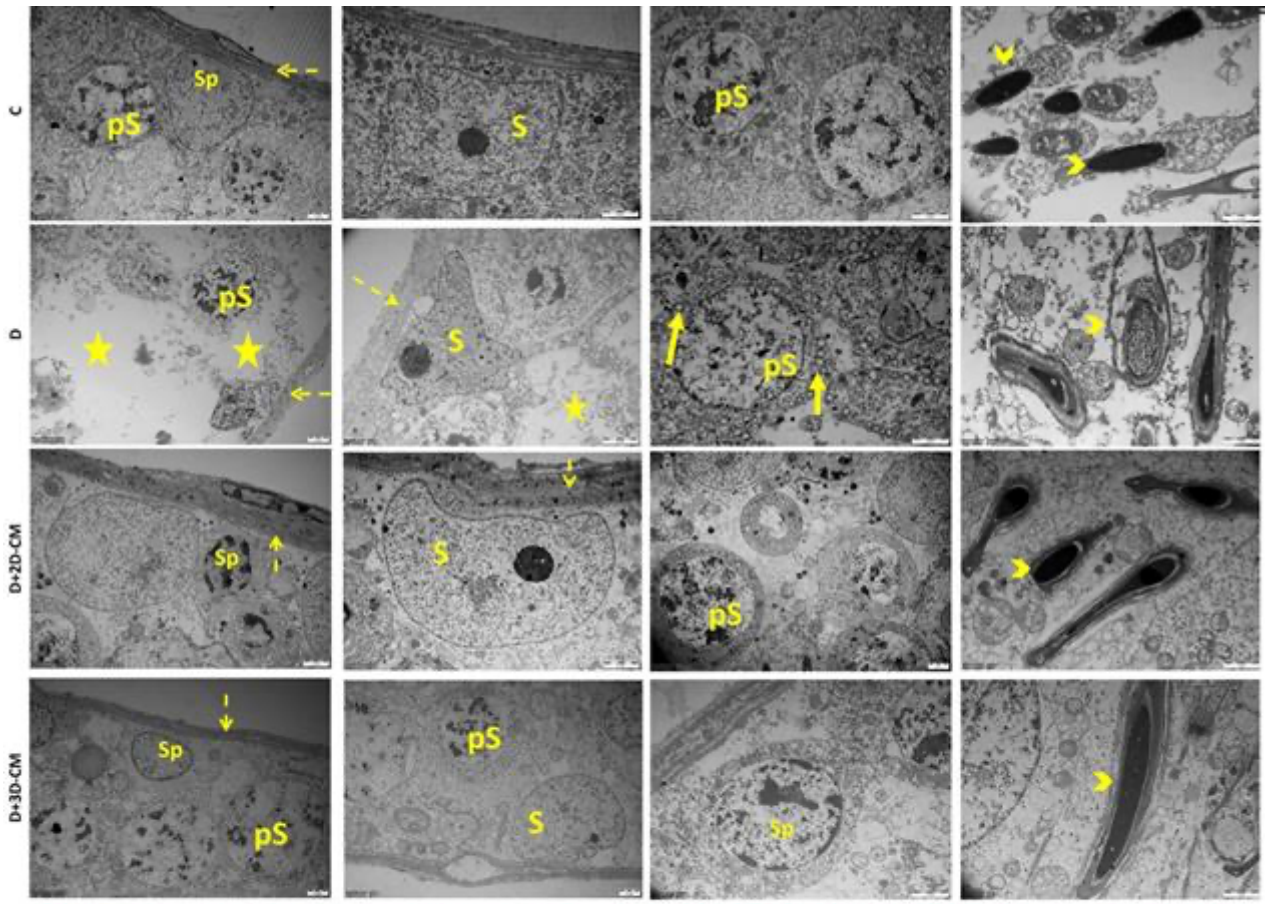

Graphic: Representative figures of TEM evaluations for C, D, D+2D-CM and D+3D-CM groups. S: Sertoli cells, Sp: spermatogonium, pS: primary spermatocyte, dashed arrow: basement membrane, arrowhead: spermatids at different stages of their development, star: intercellular space, arrow: mitochondria with loss of lamellar properties.

Keywords:

Mesenchymal-stem-cells, conditioned-medium, diabetes, testicular-damage, male-reproductive-hormones

Reference:

1. Ahi S, Ebrahimi F, Abedi HA, Kargar Jahromi H, Zarei S. The Effects of Hydroalcoholic Extract of Silk Cocoon on Hypothalamic-Pituitary -Gonadal Axis in Streptozotocin-Induced Diabetic Male Rats. Autoimmune Dis. Published online 2022. doi:10.1155/2022/7916159
2. Isildar B, Ozkan S, Koyuturk M. Therapeutic Potential of Mesenchymal Stem Cell-Derived Conditioned Medium for Diabetes Mellitus and Related Complications. Adv Ther. 2023;n/a(n/a):2300216. doi:10.1002/adtp.202300216
3. Isildar B, Ozkan S, Ercin M, Gezginci-Oktayoglu S, Oncul M, Koyuturk M. 2D and 3D cultured human umbilical cord-derived mesenchymal stem cell-conditioned medium has a dual effect in type 1 diabetes model in rats: immunomodulation and beta-cell regeneration. Inflamm Regen. 2022;42(1):55. doi:10.1186/s41232-022-00241-7

368

Generation of AFM cellular datasets and classification by ML

Ophélie THOMAS- -CHEMIN[1], Zeyd BOUMEHDI[1], Childérick SEVERAC[2], Emmanuelle TREVISIOL[3], Etienne DAGUE[1]
[1]LAAS-CNRS, Toulouse, France, [2]RESTORE Research Center, Université de Toulouse, INSERM, CNRS, EFS, ENVT, Université P. Sabatier, Toulouse, France, [3]TBI, Université de Toulouse, CNRS, INRAE, INSA, Toulouse, France

Poster Group 1

Background incl. aims
Mechano-biological measurements have the potential to distinguish healthy cells from pathological cells. Since 2007, a number of articles have shown that metastatic cancer cells have a Young's modulus (or elastic modulus) measured by atomic force microscopy (AFM) on living cells that is significantly lower than that of benign cells. However, cells are not inert and purely elastic materials, but dynamic and viscoelastic systems.
Methods
In order to measure these viscoelastic properties in living cells, we carried out dynamic mechanical analysis (DMA) measurements using AFM. After indenting a cell, we apply a strain and record the stress. The strain is proportional to the pulsation and therefore to the 6 frequencies we chose (from 1 to 200 Hz), and the stress is proportional to the phase shift of this pulsation. Knowing the strain and stress, we can then calculate G' (shear storage) in phase with the strain and G'' (shear loss) in phase with the strain rate. In our study, we sought to classify a population of cancer cells from a population of non-cancer cells. On each cell, 16 force curves (FC) and 19 characteristics/FC, corresponding to the viscoelastic properties and constituting a part of the mechanome, were calculated.
Results
All the FCs were then classified using machine learning (ML) tools with a statistical approach based on a fuzzy logic algorithm, trained to discriminate between non-malignant and cancerous cells (training basis, up to 51 cells/cell line). The proof of concept was carried out on non-malignant (RWPE-1) and cancerous (PC3-GFP) prostate cell lines.
Conclusion
After developing an algorithm to automate AFM measurements, we were able to measure 141 cells in dynamic mechanical analysis and demonstrated the ability of our method to correctly classify between 68 and 74 % of cells (31 cells in the test base/cell line).

Keywords:

AFM, DMA, viscoelasticity, ML, classification

Reference:

(Cross et al. 2007), (Wang et al. 2021), (Proa-Coronado et al. 2019), (Hedjazi et al. 2015)

370

Chitin in the cuticular capsule of tardigrade cysts

Mr. Kamil Janelt[1,2], Filip Wieczorkiewicz[1], Izabela Poprawa[1]
[1]Institute of Biology, Biotechnology and Environmental Protection, Faculty of Natural Sciences, University of Silesia in Katowice, Bankowa 9, 40-007 Katowice, Poland, Katowice, Poland,
[2]Department of Medical Genetics, Faculty of Medical Sciences in Katowice, Medical University of Silesia, Medyków 18, 40-752 Katowice, Poland, Katowice, Poland

Poster Group 1

Background incl. aims
Chitin is a biomolecule classified under carbohydrates, wherein N-acetyl-D-glucose-2-amino units are connected through β-1,4-glycosidic linkages, forming a polysaccharide biopolymer. It is a prevalent structural element in the body wall of various invertebrate groups, including nematodes, annelids, molluscs, onychophorans, and arthropods. This polysaccharide has also been observed in tardigrades, microinvertebrates commonly found in diverse habitats. Tardigrades are characterised by their ability to withstand unfavourable environmental conditions through cryptobiosis and diapause. Encystment, a form of diapause, is a natural process observed in some tardigrades, leading to the formation of a specific cyst form. Thulinius ruffoi (Tardigrada, Isohypsibioidea: Doryphoribiidae) is one of the species capable of undergoing encystment. During this process, the animal undergoes visible changes and produces a cuticular capsule composed of three layers – an outer, middle, and inner sheath. Additionally, the individual enclosed within the capsule possesses its own cuticle covering its body. This work aims to analyse the presence and localisation of chitin within the cuticular capsule of the cyst using selected methods for chitin detection on semi- and ultrathin sections.
Methods
Analyses were conducted using both light and electron microscopy. This study represents the first analysis of the composition of the cuticular capsule in tardigrade cysts. We adapted the 'chitosan-iodine' test to detect chitin indirectly on semi-thin sections. This method involved the deacetylation of chitin into chitosan, protonation of amine groups, and formation of the complex with iodine. Another method included the use of Calcofluor White, which specifically binds to β-1,4-linked polysaccharides. Control reactions in both cases involved specific enzymatic pretreatment using chitinase. Analyses were also conducted at the ultrastructural level. The first method involved a comparative analysis of material treated and untreated with chitinase. The second method utilised Wheat Germ Agglutinin (WGA) conjugated with gold particles to recognise and bind to chitin's N-acetylglucosamine (GlcNAc). The control reaction involved applying the method after prior chitinase treatment.
Results
The results revealed the presence of chitin in the cuticle of encysted animal. Also, the cuticular capsule inside which the animal was enclosed showed chitin localised within the middle and innermost sheaths of the cuticular capsule.
Conclusion
The methods used allow for an analysis of the presence and localisation of chitin on semi- and ultrathin sections, and those dedicated to transmission electron microscopy enable a more precise localisation of chitin. However, implementing the control reactions, such as treatment with chitinase, is necessary for a more specific verification of the obtained results. The analyses demonstrated the presence and precise location of chitin in the cuticle of the examined T. ruffoi. The research also allowed for the detection and analysis of the location of chitin in the cuticular capsule of tardigrade cysts on the example of the studied T. ruffoi, which is the first analysis of the chemical components of the cuticular capsule in tardigrades.

The study was supported by the Polish National Science Centre (NCN Preludium 2020/37/N/NZ8/00170).

Keywords:

chitin, cuticular capsule, encystment, tardigrades

Reference:

Greven, H., Kaya, M., Baran, T., 2016. The presence of α-chitin in Tardigrada with comments on chitin in the Ecdysozoa. Zoologischer Anzeiger-A Journal of Comparative Zoology, 264, 11-16. https://doi.org/10.1016/j.jcz.2016.06.003

Janelt K, Poprawa I., 2020. Analysis of encystment, excystment, and cyst structure in freshwater eutardigrade Thulinius ruffoi (Tardigrada, Isohypsibioidea: Doryphoribiidae). Diversity, 12:62. https://doi.org/10.3390/d12020062

389

Effect of electron microscopy sample preparation protocol on the preservation of liposomes in cell culture

Associate Professor Paul Kempen[1], Nikoline Lykke Faurschou[1], Jonas Rosager Henriksen[2], Andrew urquhart[2]
[1]DTU Nanolab, Technical University of Denmark, Kgs. Lyngby, Denmark, [2]DTU Health Tech, Technical University of Denmark, Kgs. Lyngby, Denmark

Poster Group 1

Background: Liposomes are powerful vehicles for the delivery of a broad range of drugs and other compounds to specific locations within the human body. This has made them a versatile, and often used, nanoformulation within the pharmaceutical industry. Accurately localizing these liposomes within cells and tissue is vital to understanding the uptake mechanisms and ultimately the efficacy of the liposomes. Electron microscopy is the ideal tool to localize liposomes within cells and tissue, however there are numerous challenges that must be addressed. 1st, Liposomes exhibit a pronounced sensitivity to their surroundings, and the harsh conditions often employed to prepare cells for electron microscopy may result in the dissolution of the liposome of interest. 2nd, Liposomes are composed of carbonaceous material much like the surrounding cellular matrix, making it difficult to distinguish. In this work we aimed to characterize the effect that sample preparation has on the preservation of liposomes within a cell culture sample.

Methods: 100 million CT26 colon carcinoma cells were incubated unloaded stealth liposomes for 3 hours to allow for uptake. The cells were then divided into 4 groups for further processing. Group 1 was processed using a standard chemical fixation, staining and dehydration protocol. The cells were placed in 4% paraformaldehyde, 2% glutaraldehyde in 0.1 M Na Cacodylate Buffer for 1 hour at room temperature. The cells were then pelleted, suspended in 10% gelatin, and stained with 1% osmium tetroxide in water at 4 C for 1 hour. The cells were then stained with 1% uranyl acetate in water overnight before being progressively dehydrated in ethanol and propylene oxide. After dehydration, the cells were embedded in EMBED 812 epoxy resin.

Groups 2-4 were all high pressure frozen using a Leica EM-ICE and underwent 3 different freeze substitution protocols using the Leica AFS2. Group 2 underwent a standard freeze substitution protocol in a 1% osmium tetroxide in acetone solution over the course of 3 days. This was followed by room temperature staining in 1% uranyl acetate for 1 hour before embedding in EMBED 812 Epoxy resin. Group 3 underwent a quick freeze substitution protocol over the course of 4 hours in a 1% Osmium tetroxide, 1% uranyl acetate in acetone solution before being embedded in EMBED 812 Epoxy resin. Group 4 underwent freeze substitution with a 1% uranyl acetate solution and low temperature embedding in Lowicryl HM20 at -50 C.

Ultrathin sections from each sample were prepared and imaged using a Tecnai T12 at DTU Nanolab.

Results: All 4 samples were successfully prepared into 100 nm sections for imaging. Liposomal structures were observed for all 4 samples with the samples undergoing freeze substitution exhibiting qualitatively the best-preserved liposomes. Imaging is ongoing to obtain enough data to try and definitively state which freeze substitution method will result in the best preservation.

Conclusions: Freeze substitution appears to provide better preservation of liposomes in cell culture. Additional characterization is ongoing and necessary to determine which freeze substitution method provides the best results for preserving liposomes. Even with improved preservation of the

liposomes, it is still very often difficult to ensure that the object being imaged is a liposome and not some other vesicular body within the cell.

Keywords:

sample preparation, TEM, Liposomes

488

Impact of Clostridium botulinum C2 Toxin on the ultrastructure of cells

Jasmin Christine Bellemann[1], Joscha Borho[2], Dr. Clarissa Read[1], Prof. Dr. Paul Walther[1], Prof. Dr. Holger Barth[2]
[1]Central Facility for Electron Microscopy, Ulm University, Ulm, Germany, [2]Institute of Experimental and Clinical Pharmacology, Toxicology and Pharmacology of Natural Products, Ulm University Medical Center, Ulm, Germany

Poster Group 1

Background: The C2 toxin of Clostridium botulinum is a prototypical representative of the binary actin ADP-ribosylating toxin family. It belongs to the AB toxin class, which comprises two components: the enzymatic unit A and the binding and transport unit B. In C2 toxin, C2I represents the enzymatic unit A, and C2II represents the binding component B. To gain its biological activity, C2II must be activated by proteolytic cleavage, converting it to the active component C2IIa. Upon activation, C2IIa binds to the cell surface as a homoheptameric structure and is subsequently endocytosed together with C2I into the cell. In the cytosol, the enzymatically active component, C2I, ADP-ribosylates G-actin. By this, G-actin acts as a capping protein that blocks the polymerisation of actin filaments. This alteration of the actin cytoskeleton eventually leads to cell rounding and ultimately, to cell death[1].
The effect of the C2 toxin on cells was investigated with various assays including fluorescence microscopy of labelled actin[2]. Nevertheless, to date, the effect of C2 toxin on the cellular ultrastructure was not studied. Therefore, we performed transmission electron microscopy (TEM), scanning electron microscopy (SEM) and scanning transmission electron microscopy (STEM) tomography of C2 intoxicated cells. Furthermore, to better understand the mechanism of C2 intoxication, we also investigated the effect of the individual subunits on the cell architecture.
Methods: Analysis of the ultrastructure of C2 intoxicated cells was performed using TEM and STEM tomography. For this, cells were high-pressure frozen, freeze-substituted, and embedded in Epon[3]. The impact of the C2 toxin on the cell surface was investigated using SEM of critical point-dried cells. To test whether the observed effects are mediated by actin, Cytochalasin, an actin polymerisation inhibitor, was used as a control[4].
Results: TEM analysis demonstrated that cells exposed to either C2I or C2IIa did not exhibit any ultrastructural changes compared to non-intoxicated cells. However, cells intoxicated with complete C2 toxin displayed many intracellular vesicles and a reduction in cell size. Additionally, blebs were observed along the cell membrane. Control cells, treated with Cytochalasin B, exhibited similar effects as the C2-intoxicated cells, albeit to a lesser degree.
SEM analysis revealed that C2 treated cells rounded up and confirmed plasma membrane blebbing. Furthermore, a lack of filopodia on the cell surface was observed. The combination of SEM and TEM analysis revealed that the filopodia were endocytosed by the cell. Cytochalasin B control cells seemed to be close to rounding up, with fewer filopodia on the surface compared to non-treated cells. However, the uptake of filopodia, as seen upon C2 intoxication, was not observed.
STEM tomography of C2-intoxicated cells revealed large vesicles containing cellular debris, as well as stress granules in mitochondria and swollen endoplasmic reticula. In contrast, STEM tomography of untreated cells did not exhibit any of these observations.
Conclusion: The three electron microscopic methods provided a deeper understanding of the impact of C2 toxin on cellular architecture. It was found that only the complete C2 toxin acts as a stressor and affects filopodia, causing them to be engulfed into the cell. Further examination is necessary to gain a better insight into the mechanism behind filopodia engulfment.

Keywords:

AB-Toxin, TEM, SEM, STEM tomography

Reference:

[1]Aktories, K., & Barth, H. (2004). Clostridium botulinum C2 toxin–new insights into the cellular uptake of the actin-ADP-ribosylating toxin. International Journal of Medical Microbiology, 293(7-8), 557-564.

[2]Uematsu, Y., Kogo, Y., & Ohishi, I. (2007). Disassembly of actin filaments by botulinum C2 toxin and actin-filament-disrupting agents induces assembly of microtubules in human leukaemia cell lines. Biology of the Cell, 99(3), 141-150.

[3]Bergner, T., Zech, F., Hirschenberger, M., Stenger, S., Sparrer, K. M., Kirchhoff, F., & Read, C. (2022). Near-native visualization of SARS-CoV-2 induced membrane remodeling and virion morphogenesis. Viruses, 14(12), 2786.

[4]MacLean-Fletcher, S., & Pollard, T. D. (1980). Mechanism of action of cytochalasin B on actin. Cell, 20(2), 329-341.

664

THE INVESTIGATION OF THE PRESENCE OF TELOCYTE CELLS IN THE HUMAN OVARIAN STROMA

MD. PhD. Merjem Purelku[1], Research Assistant Ceren Cebi[2], Specialist Doctor Sait Sukru Cebi[4], Prof. Dr. Ismail Cepni[2], Prof. Dr. Sennur Ilvan[3], Prof. Dr. Gamze Tanrıverdi[1]
[1]Istanbul University - Cerrahpasa, Cerrahpasa Medical Faculty, Histology and Embryology Department, Istanbul, Turkey, [2]Obstetrics and Gynecology Department, Istanbul University - Cerrahpasa, Cerrahpasa Medical Faculty, Istanbul, Turkey, [3]Pathology Department, Istanbul University - Cerrahpasa, Cerrahpasa Medical Faculty, Istanbul, Turkey, [4]Obstetrics and Gynecology Department, Samsun Training and Research Hospital, Samsun, Turkey

Poster Group 1

Background: Telocytes (TCs) have been identified as a rather new and fascinating type of interstitial cell. Previously known as interstitial Cajal-like cells (ICLCs), these cells are now distinguished in the literature by their extremely long and thin telopods (Tp) and by the various sized vesicles they secrete into their environment. To date, these cells have been detected in several organs of humans and many other species. TCs are also found in female reproductive organs, although no data on the existence or morphological characterisation of TCs in human ovaries have been identified in the literature to yet. Furthermore, studies on human ovaries have shown the existence of many stromal cell clusters. However, there is still a significant lack of detailed research describing these cell types. This emphasizes the need for more research into understanding and identifying ovarian stromal cells, including the possible discovery of telocytes (TCs) in human ovaries. The ability of TCs for cell-to-cell signaling, plays an essential role in the regulation of homeostasis, immune surveillance and tissue morphogenesis. It has also been shown that these cells play important roles in angiogenesis, embryogenesis, and various pathologies or even tumorigenesis, under the guidance of tissue-resident stem/progenitor cell self-renewal and differentiation. Expressions or co-expressions of different markers of TCs have been reported in certain organs, but in general, CD34, vimentin, PDGRF-α and PDGRF-β, c-kit and α-SMA are primarily used in TC studies and these are so far considered as reliable TC markers. A combination of double immunofluorescence and electron microscopy is the definitive approach for identifying these cells, setting the gold standard in terms of accuracy and precision.
Aims: This research aims to advance our understanding of ovarian stromal cells and detect the presence of TCs by employing techniques such as immunohistochemistry and electron microscopy. Through the investigation of their morphology and identification of telocytes in the human ovarian stroma, this study endeavors to provide novel insights into ovarian architecture and its implications for reproductive health.
Methods: Tissue samples were obtained from women aged 18 to 65 undergoing Total Hysterectomy and Bilateral Salpingo-Oophorectomy (THBSO) for uterine reasons, excluding those who had received chemotherapy. After tissue preparation procedures for light microscopy, immunohistochemical and double immunofluorescence staining used CD34/c-kit, CD34/vimentin, CD34/PDGFR-β, and CD34/α-SMA markers for telocyte identification. Transmission electron microscopy and the immunogold technique, utilizing the CD34 marker, facilitated precise telocyte identification. This comprehensive approach aimed to illuminate telocyte presence and distribution in the ovarian stroma, offering future insights into ovarian physiology and pathophysiology.
Results: Our study confirms the presence of telocyte cells within the human ovary, characterized by their distinctive morphology. We detected telocyte cells in the ovarian stroma through immunohistochemical analysis, labeling specifically with CD34 which is the most commonly used telocyte marker. Additionally, we utilized immunofluorescence analysis, employing double labeling with CD34/c-kit, CD34/vimentin, CD34/PDGFR-β, and CD34/α-SMA to further characterize these cells

and distinguish them from fibroblasts and pericytes. We found out that TCs were strongly positive for CD34, PDGFR-β, vimentin, and weakly positive for α-SMA. On the other hand fibroblasts were found to be CD34 negative, while strongly positive for vimentin and PDGFR-β. Lastly pericytes were found to be CD34 negative and strongly positive for α-SMA and PDGFR-β. Notably, our findings delineate telocyte cells from fibroblasts and pericytes, underscoring their unique cellular identity within the ovarian microenvironment. Moreover, transmission electron microscopy provided detailed insights into the ultrastructural features of these cells, enriching our understanding of their morphology. TCs were recognized for their long and thin prolongations and small cell bodies primarily situated around blood vessels and dispersed throughout the ovarian stroma. Additionally, the use of the immunogold technique in conjunction with the CD34 marker facilitated the precise identification of telocyte cells, increasing the validity of our findings.
Conclusion: Overall, our study significantly contributes to the understanding of telocyte biology within the context of the ovarian stroma, shedding light on their presence, distribution, and morphological attributes, thus paving the way for further exploration of their functional significance in ovarian physiology and pathology.

Keywords:

Human Ovary, Telocytes, Immunofluorescence, TEM.

686

Multimodal Low Voltage Transmission Electron Microscopy Analysis of Iodine Nanoparticles for Stroke Theranostics

Ing. Ph.D. Jaromír Bačovský[1], Tomáš Vácha[2], Tereza Padrtová[3], Jan Biskupič[2], Peter Scheer[4], Jana Hložková[4], Jiří Nováček[5], Radka Holbová[5], Michaela Kuchynka[2,3]
[1]Delong Instruments, Brno, Czech Republic, [2]Department of Chemical Drugs, Masaryk University, Brno, Czech Republic, [3]Department of Chemistry, Faculty of Science, Masaryk University, Brno, Czech Republic, [4]Department of Pharmacology and Toxicology, Masaryk University, Brno, Czech Republic, [5]CEITEC Masaryk University, Brno, Czech Republic

Poster Group 1

Background incl. aims
Ischemic stroke stands as the second leading cause of mortality globally, necessitating innovative approaches for its diagnosis and treatment. This project delivers a validated pipeline for assessing the kinetics and dynamics of iodine nanoparticles (IoNPs) within the organism, specifically targeting critical areas like the brain, blood-brain barrier, blood, and organs like the spleen.
Understanding thrombus characteristics, including size, composition, and origin, holds significant promise in guiding treatment strategies not only for stroke but also for related cardiovascular diseases. Current imaging modalities are limited in their ability to visualize various clot types effectively, hindering precise diagnosis and tailored treatment.
Biodegradable IoNPs have the potential to become the basis of a modern theranostics (therapy and diagnostics) approach to improve the treatment. The afore-mentioned IoNPs made of monomer MAOETIB (2-(Methacryloyloxy)ethyl-2,3,5-triiodobenzoate) have been described as desired contrasting agents. Furthermore, they can be used as drug carriers.

Methods
The essential method for the characterization of nanoparticles is undoubtedly electron microscopy, offering intricate insights into nanoparticle behavior within tissue matrices. LVEM operates at significantly lower accelerating voltages compared to conventional TEM, typically below 25 kV. This lower voltage regime offers several distinct advantages, including increased contrast and gentle electron-sample interaction.
Low voltage provides improved contrast mechanisms, which are particularly invaluable for samples composed of light elements. The reduced electron energy results in increased electron scattering, enhancing image contrast and revealing finer details within specimens. This capability is especially important in imaging biological sections and generally low-contrast materials, where conventional TEM techniques may yield limited contrast.
The application of LVEM in nanoparticle characterization involves various aspects, including morphology, size distribution, crystallinity, surface properties, and interparticle interactions. Through advanced imaging techniques such as dark-field imaging and electron diffraction, LVEM facilitates a deeper understanding of NPs structure and behavior at the nanoscale level.
The unique combination of TEM, STEM, and SEM imaging modes in LVEM instruments provides researchers with a comprehensive toolkit for investigating nanoparticles integrated into the tissue structure. Furthermore, LVEM's versatility extends beyond imaging, offering advanced analytical capabilities such as energy-dispersive X-ray Spectroscopy (EDS) and Electron Diffraction.

Results
Utilizing a multimodal approach, comprehensive insights were gathered regarding the characteristics and behavior of IoNPs, spanning from initial nanoparticle characterization and quality assessment post-fabrication to their dynamics within blood circulation and targeted organs. A rat served as the

model organism in this study, providing a relevant and translational platform for investigating IoNPs interactions in vivo. Nanoparticles were imaged throughout their entire lifecycle, starting from their presence in a native solution, followed by intravenous injection into the bloodstream, and subsequently deposited within the relevant organs. The examination of nanoparticles using low-voltage transmission electron microscopy was integrated to a comprehensive characterization utilizing various analytical methods.

Conclusion
The integration of LVEM into nanoparticle research promises to advance our understanding of nanoparticle behavior within biological systems. LVEM's unique imaging capabilities, particularly well-suited for biological sections, make it an invaluable tool for the development of theranostic strategies and personalized treatments. With its multimodal capabilities, LVEM emerges as a pivotal technology for the comprehensive analysis of biodegradable iodine nanoparticles, aiming towards improved healthcare outcomes.

Keywords:

Low-Voltage Electron Microscopy, Stroke theranostics

746

New protein fluorescent labeling methods for carbonylation and S-acylation studies in plants

MSc Andrea Román[1,2], MSc Salvador Priego[1,2], Ph.D. Antonio J. Castro[1], Dr Juan De Dios Alche[1,3]
[1]Plant Reproductive Biology and Advanced Imaging Laboratory (BReMAP), Estación Experimental del Zaidín (CSIC), Granada, Spain, [2]These authors contributed equally to this work, , Spain, [3]University Institute of Research on Olive Grove and Olive Oils (INUO), Jaén, Spain

Poster Group 1

Background
Pollen, the male gametophyte, plays a pivotal role in plant reproduction, being essential for successful fertilization and seed production in Angiosperms. Thus, understanding its biology is crucial for ensuring optimal crop yields. Carbonylation is an irreversible post-translational modification (PTM) characterized by the non-enzymatic addition of carbonyl groups to amino acid residues, leading to protein malfunction and cell death. Carbonylation leads to disruption of protein structure and function. On the other hand, S-acylation or palmitoylation is another PTM that involves the reversible attachment of palmitic acid to specific Cys residues of proteins by the action of protein S-acyltransferases (PATs). This PTM plays crucial roles response to biotic and abiotic stresses, hormonal signaling, cell polarization and expansion, and cytoskeleton organization [1].
Protein labeling techniques for in vivo studies have garnered considerable attention, with cycloaddition reactions emerging as promising methods due to their compatibility with diverse conditions. However, the cytotoxic effects of copper catalysts have limited their widespread application [2]. This study aimed to develop innovative protein labeling methods for assessing protein carbonylation and S-acylation in plant tissues.

Methods
For S-acylation studies, we developed a new method for incorporating fluorescence-labeled palmitic acid into proteins using an azide-alkyne cycloaddition reaction. This method was experimentally validated using an in vitro culture system for pollen. In a first approach, the synthetic lipid containing the azide functional group was added to the culture medium, either in the presence or not of a chemical PAT inhibitor [3], being incorporated to proteins by the enzymatic machinery of germinating pollen grains. Then, pollen was fixed and the fluorescent labeling reaction was performed and visualized by fluorescence microscopy. Alternatively, the fluorescent labeling was carried out exogenously. Then, copper was removed using size exclusion techniques, thus eliminating its cytotoxic effect. Finally, pollen was germinated in the presence of the palmitol-fluorochrome conjugate and the dynamics of the S-acylome was monitored by using time-lapse fluorescence microscopy.
For detecting carbonylated proteins, we developed two different methods. First, we carried out derivatization of carbonyl groups by DNPH (2,4-dinitrophenylhydrazine) [4] to hydrazone groups, which were further detected using an Alexa Fluor 488-conjugated antibody. Alternatively, we used the fluorescent probe BzCH (7-hydrazinyl-4-methyl-2H-1-benzopyran-2-one,), which is capable of binding specifically to carbonyl groups [5]. These two methods were further experimentally validated as above in the presence or absence of the ROS inducer Paraquat in the culture medium. Moreover, this method also allowed to quantify protein carbonylation by conducting derivatization assays followed by image processing and fluorescence quantification.

Results
Both fluorescent labeling approaches revealed the dynamics of S-acylated proteins in growing pollen tubes, showing a similar distribution pattern of S-acylated proteins. Thus, a high fluorescent signal

was observed in the cytoplasm of the vegetative cell and, to a lesser extent, in the cytoplasm of the pollen tube. Fluorescence significantly decreased in the presence of the PAT inhibitor, suggesting that was mostly due to the activity of PAT enzymes. Moreover, the exogenous labeling of the synthetic lipid allowed the real-time monitoring of the S-acylome in a single growing pollen tube by using time-lapse microscopy.
On the other hand, carbonylated proteins were found to accumulate in the cytoplasm of the vegetative cell of non-germinated pollen grains, suggesting that this PTM may be a marker of loss of pollen viability. In addition, we observed a consistent accumulation pattern of carbonylated proteins at the apical region of the pollen tube. Interestingly, protein carbonylation levels significantly increased in the presence of Paraquat in the germination medium, suggesting that ROS-mediated oxidative stress may triggers carbonylation, leading to pollen tube growth arrest.

Conclusions
In this work we have developed a novel and reliable fluorescent labeling method to study S-acylation of plant proteins, overcoming limitations associated with cytotoxic catalysts during cycloaddition reactions. Moreover, we have set up two methods to localize carbonylated proteins in plant tissues by using fluorescent probes.

This research was funded by projects PID2020-113324GB-100 and TED2021-130015B-C22 from MICIIN/AEI, both of them cofinanced by the ERDF program of the European Union. Salvador Priego and Andrea Román were granted with a PhD fellowship from Junta de Andalucía and MICINN, respectively.

Keywords:

carbonylation, cycloaddition, pollen, S-acylation, fluorescent-probes

Reference:

[1] Hemsley PA (2015) The importance of lipid modified proteins in plants. New Phytol. 205(2): 476-489.
[2] Li L, Zhang Z (2016) Development and applications of the copper-catalyzed azide-alkyne cycloaddition (CuAAC) as a cioorthogonal reaction. Molecules 21: 1393.
[3] Jennings BC, Nadolski MJ, Ling Y, Baker MB, Harrison ML, Deschenes RJ, Linder ME (2009) 2-Bromopalmitate and 2-(2-hydroxy-5-nitro-benzylidene)-benzo[b]thiophen-3-one inhibit DHHC-mediated palmitoylation in vitro. J. Lipid Res. 50(2): 233-242.
[4] Vemula V, Ni Z, Fedorova M (2015) Fluorescence labeling of carbonylated lipids and proteins in cells using coumarin-hydrazide. Redox Biol. 5: 195-204.
[5] Mukherjee K, Chio TI, Bane SL (2020) Visualization of oxidative stress-induced carbonylation in live mammalian cells. Methods Enzymol. 641: 165-181.

788

Cholesteatoma removal efficiency evaluated by Variable Pressure Scanning Electron Microscopy

Prof Michela Relucenti[1], Prof Edoardo Covelli[2], Prof Orlando Donfrancesco[1], Prof Giuseppe Familiari[1], Prof Maurizio Barbara[2]
[1]Department of Anatomical, Histological, Forensic and Orthopedic Sciences, Section of Human Anatomy, Sapienza University of Rome, Rome, Italy, Rome, Italy, [2]Department of Neuroscience, Mental Health and Sensory Organs (NEMOS), Sapienza University of Rome, Rome, Italy, Rome, Italy

Poster Group 1

Background incl. aims
Cholesteatomas are well-defined non-cancerous cystic lesion that results from the aberrant development of the keratinizing squamous epithelium within the middle ear. They can erode into the CNS and cause severe complications thus surgical removal is needed and is usually performed by manual dissection 1 however, with the possibility of recurrence. To improve the effectiveness of this technique the combined use of Mesna 5% (sodium 2-mercaptoethanesulfonate) has been introduced, this method is called Chemically Assisted Dissection (CADISS®). Our work aimed to evaluate the effectiveness of this combined surgical procedure during middle ear cholesteatoma removal, in terms of the absence of residual pathological tissue.
Methods
6 incus bones involved in cholesteatoma and removed during surgery were randomly divided into 2 groups: a) 3 subjected to CADISS-assisted dissection; b) 3 subjected to manual dissection. Samples were fixed in glutaraldehyde 2.5% in PBS (0.1M, pH 7.4) immediately upon recovery for at least 24 hours. Samples were then washed in PBS and underwent OsO4 post-fixation for 1 h. After washing samples were impregnated with tannic acid 1% for 30 min, then washed, dried on absorbent paper, and directly observed at Hitachi SU 3500 at 30 Pa and 10 kV operating conditions. Images were analyzed by the software Hitachi Map 3D advanced 8.2 (Digital Surf, France) to provide quantitative measurements of cholesteatoma tissue debris on the incus bone surface 2.
Results
Our results show that CADISS-assisted dissection provides a better outcome in terms of clean surface area concerning manual dissection. Data from software-aided BSE image analysis revealed that the clean area/ total surface area ratio is higher in the CADISS method samples (19.7±3.61) than in the manual dissection group referred to as the control group (4.57±1.66), the difference is statistically significant as revealed by t-Test results ($t= 20.91$ $P<0.001$).
The ability of Variable pressure SEM is that observation of samples in their native hydrated state is possible. The absence of dehydration steps in sample preparation allowed the observation of the samples as they came from the operatory room, without any artifact due to the preparation procedure. It is mandatory to use a procedure that does not modify sample surfaces if a comparison between two different surface cleaning procedures has to be performed.
Conclusion
The use of VP-SEM allowed sample observation without dehydration procedures, decreasing the risk of losing the pathological tissue while ossicle processing and allowing the comparison of the surgical technique's effectiveness. Our study also shows how still is important a morphological approach in establishing new surgical technique validity and how the application of innovative image analysis software can transform Scanning electron microscopy from a qualitative imaging modality into a quantitative technique.

Keywords:

Variable pressure scanning electron microscopy

Reference:

1) Barbara, M. et al. Early non-EPI DW-MRI after cholesteatoma surgery. Ear, Nose & Throat Journal. 2021;0(0).
2) Relucenti, M. et al. (2020). SEM BSE 3D Image Analysis of Human Incus Bone Affected by Cholesteatoma Ascribes to Osteoclasts the Bone Erosion and VpSEM dEDX Analysis Reveals New Bone Formation. Scanning, 2020, 9371516.

796

Immunoexpression of estrogen receptor α in the ovary of mice after chronic exposure to arsenic(III)-oxide

Ass.prof. Marija Marin[1], Anita Birinji[1], Full prof. Anita Radovanović[2], Ass.prof. Maja Čakić-Milošević[1], Full prof. Dušan Lalošević[3]
[1]University of Belgrade, Faculty of Biology, Belgrade, Serbia, [2]University of Belgrade, Faculty of Veterinary Medicine, Belgrade, Serbia, [3]University of Novi Sad, Faculty of Medicine, Novi Sad, Serbia

Poster Group 1

Background
Arsenic (As) is a naturally occurring metalloid found in soil and groundwater. As it can enter the food chain, As poses a serious environmental and health risk. In humans, the severity of symptoms of As poisoning depends on the dose and duration of exposure. Chronic exposure to low concentrations of As leads to dysfunction in virtually all body systems, including the impairment of the normal function of endocrine organs. Ovarian estrogens are the most important regulators of female fertility. Acting through specific receptors, estrogens regulate the growth and development of follicles, oocytes and granulosa cells in the ovaries as well as the function of ovulation. The aim of this study was therefore to determine the distribution of estrogen receptor α (ERα) in the ovaries of mice after administration of As(III)-oxide, which is considered to be the most toxic form of inorganic As.
Methods
Female mice from the Naval Medical Research Institute (NMRI, Bethesda, USA) aged approx. 6 months at the end of the experiment were used. Since birth, animals from the experimental group (n=6) drank water in which As(III)-oxide was dissolved at 10.6 mg/l, while the mice in the control group (n=6) drank tap water. For immunohistochemical localization of ERα in the ovaries of the mice, the sections were incubated with rabbit monoclonal anti-human ERα primary antibody (IR084, Dako, Agilent Technologies, Denmark), 1 h at room temperature and then visualized using EnVision FLEX, High pH (Link) system (K8000, Dako, Agilent Technologies, Denmark) for 30 min at room temperature. For negative control, primary anti-ERα antibody was omitted. After hematoxylin counterstaining, slides were analyzed with a Leica DMLB microscope (Leica Microsystems, Wetzlar, Germany).
Results
The control group is characterized by the preserved structure of the ovarian surface epithelium, under which there were numerous follicles in various stages of development as well as numerous corpora lutea and stromal cells. The results showed that the expression of the estrogen receptor was more pronounced in the experimental group than in the control group. A particularly positive response was observed in the corpora lutea, the secondary follicles, and the granulosa cells of the antral follicles, while immunostaining was absent in the stromal cells.
Conclusion
The present results show that chronic arsenic exposure affects the pattern and intensity of ERα-immunoexpression, suggesting involvement in the impairment of estrogen signaling with possible disruption of reproductive function.

Keywords:

Mice, arsenic(III)-oxide, ovaries, immunohistochemistry

Reference:

Garelick H, Jones H, Dybowska A, Valsami-Jones E: Arsenic pollution sources. Rev Environ ContamToxicol 2008, 197:17-60.
Palma-Lara I, Martínez-Castillo M, Quintana-Pérez JC, Arellano-Mendoza MG, Tamay-Cach F, Valenzuela-Limón OL, García-Montalvo EA, Hernández-Zavala A: Arsenic exposure: A public health problem leading to several cancers. Regul Toxicol Pharmacol, 2020, 110:104539.
Aposhian, H.V., Aposhian, M.M. (2006). Arsenic toxicology: five questions. Chemical Research in Toxicology, 19: 1-15.

846

Effects of melatonin and alpha-lipoic acid on collagen and VEGF expression in palatal wound healing

Onur Kutlu[1], Gülten Kavak[1], Aslı Erdoğan Öner[2], Selen Akyol Bahçeci[2]
[1]Department of Oral and Maxillofacial Surgery, İzmir Katip Çelebi University , İzmir, Türkiye,
[2]Department of Histology and Embryology, İzmir Katip Çelebi University, İzmir, Türkiye

Poster Group 1

Background incl. aims
Reactive oxygen species (ROS) play a crucial role in the normal physiology of wound healing. The balance between high and low levels of ROS is critical during the healing process. As regulators of oxidative stress, antioxidants are proposed as targets for new therapies to accelerate wound healing. Alpha-lipoic acid and melatonin are antioxidants that have been shown to be involved in wound healing in many different organs. In addition to protective effects against oxidative stress, they also exert anti-inflammatory effects. In this study, we aimed to evaluate the effects of alpha-lipoic acid and melatonin on rat palate wound healing and whether they have a synergistic effect when used together.
Methods
A total of 64 male and female adult Wistar rats were randomly divided into 4 main groups. All rats were anesthetized with intramuscular ketamine hydrochloride (50 mg/kg) and xylazine (10 mg/kg) injections before creating a 5 mm diameter wound using a punch biopsy in the central area of the hard palate. Experimental groups were treated with daily intraperitoneal injections of alpha-lipoic acid (60 mg/kg/day) or melatonin (30 mg/kg/day) or both of them until sacrification. Control group did not get any injection. 2 sub-groups were created for each group, according to sacrification days; 5 or 10 days after wound creation. Palatal biopsies were fixed with 10% neutral buffered formalin. After decalcification for 8 days in decalcification solution, samples were dehydrated with increasing grades of ethanol, cleared with toluene, and embedded in paraffin. 5 µm thick sections were taken with microtome. Masson trichrome stain was performed to evaluate the amount of collagen fibers in sections. VEGF expression was determined using the immunohistochemistry method. After taking photographs of the sections, Image J software was used to evaluate the results of the stainings. Statistical analyses were performed using IBM SPSS version 24.
Results
Collagen fiber density in the granulation tissue in the 5th day samples of the melatonin-treated group was significantly higher than that in the control group ($p<0.008$). On the 10th day, the collagen fiber density in the granulation tissue of the alpha-lipoic acid + melatonin group was significantly higher than that of the control group ($p<0.008$). In immunohistochemical staining using VEGF, positive immunoreactivity was detected in the epithelial areas of all group samples. Cytoplasmic and widespread VEGF expression was observed in all epithelial layers (except the stratum corneum-keratin layer), especially more prominently in the stratum granulosum. No specific and significant immunoreactivity was found in the granulation tissue or subepithelial connective tissue in the wound area. VEGF expression on the 5th day was significantly higher in the alpha-lipoic acid + melatonin group compared to the control group ($p<0.008$).
Conclusion
Growth factors and collagen production are one of the key factors that determine the wound healing. According to our results, the combinatory application of alpha-lipoic acid and melatonin might be effective in palatal wound healing via collagen synthesis in the early period and via VEGF expression in the late period.

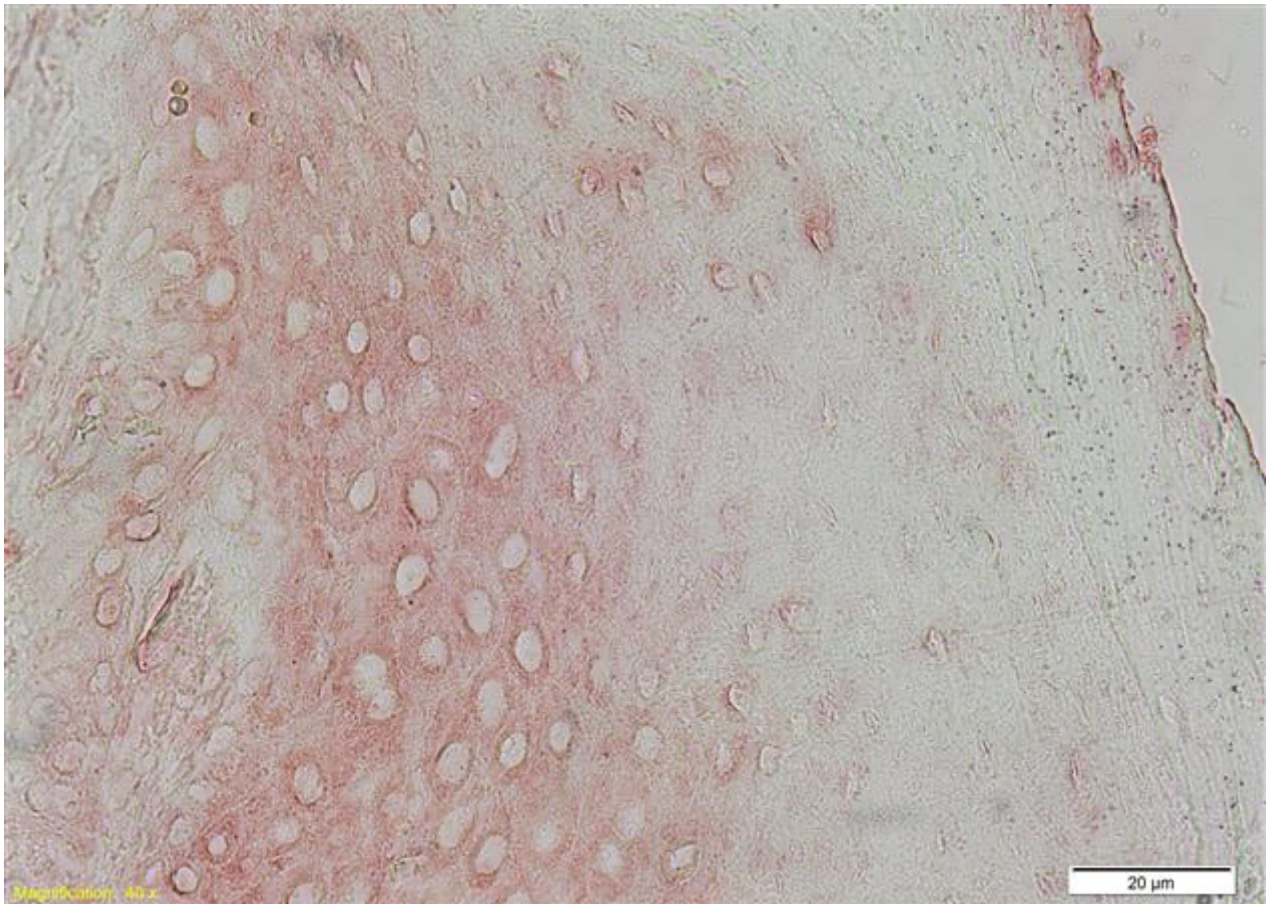

Keywords:

alpha-lipoic acid, melatonin, wound healing

Reference:

1-Comino-Sanz IM, López-Franco MD, Castro B, Pancorbo-Hidalgo PL. The Role of Antioxidants on Wound Healing: A Review of the Current Evidence. Journal of Clinical Medicine. 2021;10(16):3558.
2-Fitzmaurice SD, Sivamani RK, Isseroff RR. Antioxidant Therapies for Wound Healing: A Clinical Guide to Currently Commercially Available Products. Skin Pharmacol Physiol. 2011;24(3):113–126.
3-Şener A, Çevik Ö, Doğan Ö, Altindiş NG, Aksoy H, Okuyan B. The effects of topical melatonin on oxidative stress, apoptosis signals,and p53 protein expression during cutaneous wound healing. Turkish Journal of Biology. 2015;39(6):10.
4-Vaseenon S, Chattipakorn N, Chattipakorn SC. Effects of melatonin in wound healing of dental pulp and periodontium: Evidence from in vitro, in vivo and clinical studies. Archives of Oral Biology. 2021;123:105037.
5-Alleva R, Nasole E, Donato FD, Borghi B, Neuzil J, Tomasetti M. A-lipoic acid supplementation inhibits oxidative damage, accelerating chronic wound healing in patients undergoing hyperbaric oxygen therapy. Biochemical and Biophysical Research Communications. 2005;333(2):404–410.

859

Vitamin A affects urothelial injury and regeneration in cyclophosphamide-induced cystitis

Teaching Asisstent Brina Dragar[1], Senior Research Fellow Simona Kranjc Brezar[2], Research Fellow Tadeja Kuret[1], Research Fellow Tanja Jesenko[2], Professor Maja Čemažar[2], Professor Rok Romih[1], Professor Mateja Kreft Erdani[1], Associate Professor Daša Zupančič[1]
[1]Institute of Cell Biology, Faculty of medicine, University of Ljubljana, Ljubljana, Slovenija,
[2]Department of Experimental Oncology, Institute of OncologyOncology, Ljubljana, Slovenia

Poster Group 1

Background
Vitamin A and its derivatives, the retinoids, are involved in tissue regeneration as they can modulate cell proliferation, differentiation, apoptosis (1) and the inflammatory response (2). A single injection of cyclophosphamide (CP) in rodents disrupts the blood-urine barrier of the urinary bladder by causing injury to the urothelium, which is followed by rapid regeneration (3–5). We used a mouse model for CP-induced urothelial injury, which is also a model for the inflammation of the urinary bladder known as cystitis. The aim of our study was to investigate the effects of a vitamin A-enriched diet on CP-induced cystitis. We analysed the proliferation and differentiation of urothelial cells as well as the transcriptome of the urinary bladder.
Methods
We randomly divided 80 female BALB/c mice (8 weeks old) into 8 groups of 10 mice each (permit No. U34401-4/2022/18). 4 groups received a vitamin A-enriched diet (containing 566081UI retinyl-acetate per kilogramme; VitA groups) 1 week before intraperitoneal (i.p.) injection of CP or saline (S) and the other 4 received a normal diet (N groups). Urinary bladders were collected 1 or 3 days after i.p. injection (VitA CP1d, N CP1d, VitA S1d, N S1d, VitA CP3d, N CP3d, VitA S3d, N S3d groups) and then dissected and prepared for RNA isolation followed by RNA sequencing (RNAseq) and for scanning electron microscopy (SEM). Half of each urinary bladder was embedded in paraffin for immunolabelling. The proliferation index was determined by quantification of Ki67-positive urothelial cells, while differentiation was determined by the percentage of uroplakins' (UPs) positive apical membrane length of superficial urothelial cells. We also determined the presence of highly differentiated superficial urothelial cells by immunolabelling of keratin 20 (Krt20). SEM was used to analyse the differentiation stage of the superficial urothelial cells by assessing the percentage of microridges (terminal differentiation stage) on the entire surface examined.
Data analysis was performed with ImageJ and statistically analysed with Excel and GraphPad Prism 8.01. Results are presented as mean values and standard deviations (mean ± SD) unless specified otherwise.
Results
The RNAseq results showed higher expression of genes involved in the cell cycle and PI3k-Akt signalling in the VitA CP1d group compared to the N CP1d group, indicating higher proliferation in this group. Genes involved in cell cycle (Bub1, Bub1a, Ccna2, Cdc25b, Cdk1, Knl1) and PI3k-Akt signalling (Itga3, Epha2, Spp1, Ereg, Areg and Il6) were significantly up-regulated, as revealed by Kyoto Encyclopaedia of Genes and Genomes (KEGG) enrichment analysis. The higher proliferation indices were subsequently confirmed in the urothelial cells of the VitA CP1d group (29.5% ± 20.5%) compared to the N CP1d group (19.6% ± 16.1%). In the VitA CP3d and N CP3d groups, the proliferation indices were 42.2%±17% and 38.4%±14.3%, respectively. In comparison, all groups with S injection (VitA S1d, N S1d, VitA S3d and N S3d group) had lower proliferation index of 1 to 2%.
All groups with S injection (VitA S1d, N S1d, VitA S3d and N S3d) had terminally differentiated superficial urothelial cells with positive UPs and Krt20 immunolabelling and microridges on their apical surface. One day after CP injection (VitA CP1d, N CP1d groups), the differentiation stage of

superficial urothelial cells was significantly lower compared to the S injection groups (VitA S1d, N S1d), as indicated by the presence of microridges. The VitA CP1d group exhibited a slightly higher differentiation stage (13.9%±25.1% of microridges) than the N CP1d group (9.1%±13.6% of microridges). On the other hand, 3 days after CP injection, the VitA CP3d group showed a slightly lower UPs-positive apical surface length of superficial urothelial cells (76.6%±15.4%) than the N CP3d group (88.1%±13.5%), while no difference was observed in the presence of microridges (VitA CP3d - 6.1%±14.8% and N CP3d - 7.0%±10.3%). There was no difference in Krt20 positive superficial urothelial cells between the CP-treated groups (VitA CP1d, N CP1d, VitA CP3d and N CP3d).
Conclusion
Our results suggest that increased vitamin A intake before the onset of CP-induced cystitis influences urothelial injury and regeneration. A vitamin A-enriched diet resulted in upregulation of several genes involved in the cell cycle and PI3k-Akt signalling and increased proliferation of urothelial cells during the initial stages of regeneration (day 1). These events accelerated the formation of the initial blood-urine barrier. We were able to demonstrate that proliferation remained increased in groups with VitA-enriched diet also in the later phases of regeneration (day 3), while no difference was observed in the differentiation stage of the superficial urothelial cells. We can conclude that vitamin A influences the initial regeneration, but its effects are no longer observed in the later stages of regeneration.

Keywords:

Retinoids, cyclophosphamide, urothelium, acute cystitis

Reference:

References:
1. Carazo A, Macáková K, Matoušová K, Krčmová LK, Protti M, Mladěnka P. Vitamin A Update: Forms, Sources, Kinetics, Detection, Function, Deficiency, Therapeutic Use and Toxicity. Nutrients. 18. maj 2021;13(5):1703.
2. Huang Z, Liu Y, Qi G, Brand D, Zheng SG. Role of Vitamin A in the Immune System. Journal of Clinical Medicine. september 2018;7(9):258.
3. Gandhi D, Molotkov A, Batourina E, Schneider K, Dan H, Reiley M, idr. Retinoid signaling in progenitors controls specification and regeneration of the urothelium. Dev Cell. 16. september 2013;26(5):469–82.
4. Romih R, Koprivec D, Martincic DS, Jezernik K. Restoration of the Rat Urothelium After Cyclophosphamide Treatment. Cell Biology International. 2001;25(6):531–7.
5. Romih R, Veranic P, Jezernik K. Appraisal of differentiation markers in urothelial cells. Appl Immunohistochem Mol Morphol. december 2002;10(4):339–43.

866

Transmission electron microscopy of dermal collagen using ethanolic phosphotungstic acid staining

Dr Astrid Obermayer[1], Dr Stefan Hainzl[2], Dr Ulrich Koller[2], Ao. Univ.-Prof. Dr. Walter Stoiber[1]
[1]Department of Environment & Biodiversity, University of Salzburg, Salzburg, Austria, [2]EB House Austria, Research Program for Molecular Therapy of Genodermatoses, Department of Dermatology and Allergology, University Hospital of the Paracelsus Medical University, Salzburg, Austria

Poster Group 1

Background
For conventional transmission electron microscopy, biological samples are treated with heavy metal salt solutions to enhance contrast, either by staining ultrathin sections with lead citrate, uranyl acetate or lanthanoid salts, or by staining tissue blocks before embedding, using similar substances. However, we found that these substances are insufficient for imaging collagen fibrils and collagen VII anchoring fibrils. The latter are critical structures for a stable attachment of the epidermis to the underlying dermis, and accordingly the subject of studies concerning skin defects such as epidermolysis bullosa. Their structure and exact position can only be imaged by electron microscopy. Phosphotungstic acid (PTA) is known to interact with nucleic acids and positively charged proteins, and is widely used for light histologic staining procedures of connective tissue. It is also used in TEM, but mainly for negative staining. Only a few protocols for section or block staining are available in the recent literature. We tested PTA staining of collagen for TEM and were able to establish a block staining procedure that can be integrated in the dehydration steps.
Methods
Human and murine skin and in vitro skin equivalents were fixed in paraformaldehyde and glutaraldehyde, and postfixed in osmium tetroxide. Blocks were stained in 1% PTA in 70% ethanol, followed by further dehydration in ethanol, embedding in epoxy resin and ultrathin sectioning. Sections were analyzed in a Zeiss EM910 at 80kV.
Results
The combination of osmiumtetroxide and ethanolic PTA resulted in a versatile staining of all tissue components. We observed strong contrast of all intracellular compartments, well characterized chromatin, dark mitochondria, strong staining of ribosomes and very intensive staining of desmosomes and hemidesmosomes. Collagen fibrils, anchoring fibrils and other fibrous extracellular materials including the basal lamina were depicted in high quality.
Conclusion
Ethanolic PTA staining is a fast, easy and non-radioactive block staining method for structurally precise TEM tissue analysis. It provides good results for both, intracellular structures and extracellular fibres such as different types of collagen. This protocol may be an interesting option for various studies on cell and tissue microstructure since there is, for example, an increasing demand for reliable block staining techniques for 3D analysis of serially sectioned and scanned resin blocks.

Keywords:

TEM, staining, phosphotungstic acid, collagen,

873

Toxic buffers used in microbial sample preservation for SEM can be replaced by PBS

Indra Banas[1], Noel Kleber[1], Dr. André Soares[1], Prof. Dr. Alexander Probst[1,2,3]
[1]Environmental Metagenomics, Research Center One Health Ruhr of the University Alliance Ruhr, Faculty of Chemistry, University of Duisburg-Essen, Essen, Germany, [2]Centre of Water and Environmental Research (ZWU), University of Duisburg-Essen, Essen, Deutschland, [3]Center of Medical Biotechnology (ZMB), University of Duisburg-Essen, Essen, Deutschland

Poster Group 1

The structural preservation of uncultivated, oxygen-sensitive microorganisms for imaging via scanning electron microscopy (SEM), often relies on toxic buffers like cacodylate. As such, studies on certain archaea named Candidatus Altiarchaeum which can dominate deep biosphere ecosystems by forming biofilms using hook-shaped cell appendages (hami), currently heavily rely on cacodylate buffers. However, the twelve principles of green chemistry state that researchers should strive to minimize the use of toxic substances and ideally replace them entirely with non-toxic alternatives. Following these principles, we here tested the influence of alternative, less toxic buffers (phosphate-buffered saline (PBS) and PHEM (PIPES-HEPES-EGTA-MgCl2)) for the preservation of Ca. Altiarchaeum hamiconexum for SEM and compared them with preservation using cacodylate for subsequent imaging.

Fixation of Ca. Altiarchaeum hamiconexum was conducted immediately after the collection of the biofilm from a cold sulfidic spring located in Regensburg (Bavaria). Samples were preserved using 4% formaldehyde final concentration in cacodylate, PHEM or PBS, respectively. For SEM preparation, 2.5% glutaraldehyde in cacodylate, PHEM or PBS, were used, after which samples were rinsed four times with the corresponding buffer and post fixated with 1% osmium tetroxide in cacodylate, PHEM or PBS. A dehydration gradient was then applied with 10%, 20%, 40%, 60%, 80% and 100% acetone. Quality of preservation was examined using SEM after critical point drying and sputter coating with platinum/palladium. The so prepared archaeal cells were analyzed in comparative manner by experienced scientists used to investigate Ca. Altiarchaeum hamiconexum ultrastructure prepared with cacodylate buffer.

The preservation with cacodylate and PBS revealed no noticeable differences. The hami displayed a high degree of preservation and no visible difference in the thickness and length of those structures. However, all cells, independent of the preservation buffer used, showed deformations. The samples preserved in PHEM exhibited the least preservation of the hami, with many cells showing complete absence of appendages.

To reduce risks for researchers and the environment, the use of toxic substances in laboratory conditions should be avoided if less dangerous alternatives exist. In this study, no visible differences were observed for the quality of hami preservation between toxic buffer cacodylate and PBS. PBS can effectively replace cacodylate for preserving the ultrastructure of hami of Ca. Altiarchaeum hamiconexum for the purposes of high-resolution microscopy.

Keywords:

Sanple preparation, Microbiology, Buffer replacement

875

Exploring Role of Voltage-Gated Ion Channels in LGI1 Autoantibody-Induced Epilepsy: Insights from a Mouse Model

Dr Jacqueline Montanaro[1], Hana Stefanickova[1], Dr. Mary Muhia[1], Prof. Dr. med Christian Geis[2], Claudia Sommer[2], Josefine Sell[2], Prof. Dr. Hans-Christian Korna[3], Prof. Dr. Harald Prüß[3], Prof. Ryuichi Shigemoto[1]
[1]Institute of Science and Technology Austria (ISTA), , Klosterneuburg, Austria, [2]Department of Neurology, Section Translational Neuroimmunology, Jena University Hospital, Jena, Germany, [3]German Center for Neurodegenerative Diseases (DZNE), Berlin, Germany

Poster Group 1

Epilepsy is a debilitating condition affecting 0.5% to 1.0% of the world's population (1), but its underlying etiology often remains unknown, hence most anti-epilepsy therapies aim for reduction in seizure symptoms. Nevertheless, recent studies suggest that up to 1 to 7 out of 20 individuals with new onset seizures may have an autoimmune cause (2). Although rare, the most common epilepsy-associated autoantibodies target different proteins in the brain, such as N-methyl-d-aspartate receptor (NMDAR), leucine-rich glioma-inactivated protein 1 (LGI1), and glutamic acid decarboxylase 65 (GAD65) (3).
LGI1 is a soluble secreted protein which links Adam22/23 proteins across the synaptic cleft. LGI1 is also abundant in the axon initial segments of in the hippocampus, in particular, in the dentate gyrus (4). Anti-LGI1 autoantibodies have been found in both cerebral spinal fluid and serum of acquired epilepsy patients with symptoms of limbic encephalitis with amnesia and seizures. The specific mechanisms how any autoantibody leads to epileptic seizures is unknown. However, previous studies showed human LGI1 autoantibodies co-precipitated with voltage-gated (VG) potassium channel complexes in rodent tissue (5). Since VG-ion channels help maintain homeostasis in neuronal excitability, we hypothesize that dysregulation of these channels may be triggering LGI1 autoantibody-induced neuropathophysiology. In this study, our aim is to detect a possible mechanism for seizure onset after LGI1 autoantibody exposure. To do this, we are investigating if changes in either the distribution or numbers of VG-ion channels occur when mice are exposed to LGI1 autoantibodies.
Methods:
In mice injected with monoclonal LGI1-antibody into the hippocampus, epileptic seizures were induced, while no symptoms were observed in mice injected with control serum only. Ultrastructural observation of immunolabeled freeze-fractured replicas with colloidal gold antibodies quantified Cav2.1 calcium channels and Kv1.1 potassium channels in axon initial segments and active zones (AZ) of the dentate gyrus granule cell axons (mossy fibers).
Results:
LGI1-autoantibody-injected animals showed that Cav2.1 was slightly reduced in AZ, compared to control animals, while Kv1.1 density was low in control groups. This suggests that neither Cav2.1 and Kv1.1 could be causing mossy fiber hyperactivity at synapses. However, many other VG-ion channels remain that can be investigated using these same methods. Importantly, we observed a significant reduction in synaptic vesicle numbers in mossy fiber boutons in LGI1-autoantibody-injected mice with epilepsy symptoms compared to asymptomatic controls. The synaptic vesicle depletion has implications for presynaptic hyper-excitability and altered neurotransmitter release, and could serve as a marker for affected AZs in epilepsy.

Conclusions:
These results suggest that our mouse model will be useful in investigating if alteration of VG-ion channels trigger hyperexcitability of neurons and contribute to epilepsy in LGI1 autoimmune encephalitis. In the future, these investigations may have useful implications for helping to find triggers of epilepsy with unknown etiologies.

Keywords:

Epilepsy, LGI1, VG-ion-channels, SDS-freeze-fracture-immunolabeling

Reference:

(1) Ong M, Kohane IS, Cai T, Gorman MP, Mandl KD. Population-Level Evidence for an Autoimmune Etiology of Epilepsy. JAMA Neurol. 2014;71(5):569–574.
(2) Dubey D, Alqallaf A, Hays R, et al. Neurological autoantibody prevalence in epilepsy of unknown etiology. JAMA Neurol. 2017, Apr 1;74(4):397-402
(3) Cabezudo-García P, Mena-Vázquez N, Ciano-Petersen NL, García-Martín G, Estivill-Torrús G, Serrano-Castro PJ. Prevalence of Neural Autoantibodies in Epilepsy of Unknown Etiology: Systematic Review and Meta-Analysis. Brain Sci. 2021 Mar 19;11(3):392.
(4) Fukata Y, Adesnik H, Iwanaga T, Bredt DS, Nicoll RA, Fukata M. Epilepsy-related ligand/receptor complex LGI1 and ADAM22 regulate synaptic transmission. Science. 2006; 313 (5794): 1792–5.
(5) Irani SR, Alexander S, Waters P, et al. Antibodies to Kv1 potassium channel-complex proteins leucine-rich, glioma inactivated 1 protein and contactin-associated protein-2 in limbic encephalitis, Morvan's syndrome and acquired neuromyotonia. Brain 2010;133:2734–2748.

877

Effect of chloroquine and naringin on the relationship between ER stress and mitochondria in trophoblasts

Research Associate Zehra Sezer[1]
[1]ISTANBUL UNIVERSITY-CERRAHPASA, Istanbul, Turkey

Poster Group 1

Background incl. aims
The placenta is an interface that transports nutrients, oxygen, and waste products between the mother and the fetus. Trophoblast cells in the fetal part of the placenta differentiate for the development of a healthy placenta and the continuity of pregnancy and perform functions such as invasion and secretion. It is known that autophagy plays an essential role in these functions. Autophagy is a process responsible for degrading damaged structures to maintain cellular homeostasis. Suppression of autophagy, oxidative stress, and apoptosis in trophoblasts can lead to pathologies such as implantation failures, spontaneous miscarriages, and preeclampsia. Naringin (Nar) is a bioflavonoid with anti-apoptotic, anti-inflammatory, and antioxidant properties (Bharti ve ark., 2014). Previous studies have shown that Nar stimulates ER stress-mediated apoptosis in colon and cervical cancer cells and inhibits mitochondria and ER stress-mediated apoptotic pathways in endothelial cells. This study aims to investigate the effect of Nar on endoplasmic reticulum (ER) stress (Grp78 and PERK), mitochondria dynamics (Fis1 and MFN2), and the ER-mitochondria relationship after hydrogen peroxide (H2O2)-induced oxidative stress and the inhibition of autophagy (chloroquine; CQ) in trophoblast cells.

Methods
IC50 analysis was performed using the data obtained after the CCK8 experiment to determine the most appropriate H2O2, CQ, and Nar doses to be applied to the cells. Seven experimental groups were constructed: Control (C), H2O2, CQ, Nar, H2O2+Nar, CQ+Nar, and H2O2+CQ+Nar. To examine both ER stress and mt dynamic protein levels in cells and the relationship between ER and mitochondria, Grp78 and Fis1 and p-Perk and MFN2 proteins were double labeled by immunofluorescence (IF) method. In addition, apoptosis was evaluated by Caspase-3 protein labeling using IF, and the ER-mitochondria relationship was assessed by electron microscopy.

Results
As a result of IF, while Grp78 expression increased in CQ-treated trophoblasts, no change was observed in Fis1+ mt fission. There was a significant increase in Grp78 and Fis1 protein levels in the Nar-applied groups. Also, the p-Perk level decreased significantly in the CQ+Nar group, while MFN2+ mt fusion increased dramatically in the Nar-applied groups. Moreover, it was observed that the autophagy inhibition in trophoblasts did not show any change in the mt dynamic balance, but Nar had the opposite effect. In addition, Caspase-3 labeling showed a significant increase in apoptosis in the CQ group compared to the C and Nar groups. Nar decreased Caspase-3-mediated apoptosis combined with CQ but was ineffective when administered with H2O2.

Conclusion
ER stress (GRP78) and apoptosis increased by inhibiting autophagy (CQ), but apoptosis decreased after CQ and Nar application, although GRP78 increased. This decrease may be due to mt fission. Increased ER stress may reduce Caspase3-mediated apoptosis by triggering fission in the mitochondria, which is closely related. In addition, Nar applied to trophoblasts with inhibited autophagy caused a severe decrease in the level of p-PERK, an important protein in the ER-mitochondria relationship, and this decrease affected the level of apoptosis. Still, p-PERK did not

show any effect on mt dynamics. In conclusion, it has been observed that ER stress and mt dynamic-induced cell death may occur in pathological conditions due to autophagy in trophoblasts, and Nar may be effective in these mechanisms. The experiments regarding the study are still being conducted; ER stress mechanism and mitophagy affecting mt dynamics will be investigated by immunolabeling ATF6 and IRE1, Pink and Parkin.

Keywords:

Trophoblast, naringin, autophagy, ER, mitochondria

906

Effects of corticosterone and amyloid beta on the corticosteroid receptors in organotypic brain slice cultures

Assistant Professor Merve Alaylıoglu[2], Professor ,PhD Selma Yilmazer[1], Professor PhD Erdinc Dursun[2], Professor PhD Duygu Gezen-Ak[2]
[1]Dept. of Medical Biology, Halic University, Faculty of Medicine, Istanbul, Turkey, [2]Brain and Neurodegenerative Disorders Research Laboratories, Department of Neuroscience, Institute of Neurological Sciences, Istanbul University- Cerrahpasa, Istanbul, , Turkey

Poster Group 1

Background
Stress is accepted as an important risk factor for Alzheimer's disease (AD) (1,2).High levels of cortisol, which is the stress hormone, in the cerebrospinal fluid (CSF), plasma and serum of Alzheimer's patients and the decrease in hippocampus volume and declarative memory disorders in patients with major depression and chronic corticosteroid treatment give rise to thought for a possible relationship between AD and stress (2,3,4). This suggests that the increase in glucocorticoid levels, which occurs as a result of stress, may participate in the formation of pathological mechanisms seen in AD, and raises the question of whether stress triggers the pathways that cause neurodegeneration or not.
Methods
In the study; in organotypic brain slice cultures, which allows to obtain results closest to in vivo models by protecting tissue architecture and microenvironment, circadian rhythm and stress models with corticosterone application and Alzheimer-like model with amyloid beta 1-42 (Aβ1-42) peptide application were generated. The effects of these treatments on glucocorticoid receptor (GR) and mineralocorticoid receptor (MR) expressions, which are corticosteroid receptors, were investigated at both mRNA and protein levels. Regional localizations of these proteins in the brain were also examined by immunofluorescence method.
Results
As a result of our study, we found that GR and MR expression levels and their localizations in the hippocampus region changed both in circadian rhythm and stress models created by corticosterone applications and in AD-like models created by amyloid beta 1-42 application, and we determined that these changes differ depending on the dose. When we evaluate the findings of corticosterone and Aβ1- 42 applications we obtained in our study together, we observed that GR protein level, and GR localization in the hippocampus, especially in the stratum pyramidalis region, were similarly affected.
Conclusion:
Our findings point out that the increase in corticosterone caused by stress may be involved in the formation of pathological mechanisms seen in AD.

Keywords:

Alzheimer's disease,corticosterone,organotypic brain slice cultures

Reference:

1. de Kloet, E. R. (2000). "Stress in the brain." Eur J Pharmacol 405(1-3): 187-198.
2. Aznar, S. and G. M. Knudsen (2011). "Depression and Alzheimer's disease: is stress the initiating factor in a common neuropathological cascade?" J Alzheimers Dis 23(2): 177-193.
3. Tsigos, C. and G. P. Chrousos (2002). "Hypothalamic-pituitary-adrenal axis, neuroendocrine factors and stress." J Psychosom Res 53(4): 865-871.
4. Huang, L. T. (2014). "Early-life stress impacts the developing hippocampus and primes seizure occurrence: cellular, molecular, and epigenetic mechanisms." Front Mol Neurosci 7: 8.

935

Is iron a hidden culprit in Alzheimer's disease?

PhD Sowmya Sunkara[1], Dr Marlene Leoni[2], Dr Johannes Haybäck[2,3], Assoc. Prof. Dr Gerd Leitinger[1]
[1]Division of Cell Biology, Histology and Embryology, Gottfried Schatz Research Center, Medical University of Graz, Graz, Austria, [2]Diagnostics & Research Institute for Pathology, Medical University of Graz, Graz, Austria, [3]Tyrolpath Obrist Brunhuber GmbH, Zams, Austria

Poster Group 1

Background incl. aims
Up to 80% of dementia cases globally are down to Alzheimer's disease (AD), a major neurodegenerative disorder[1]. The disease was discovered in 1906 by Alois Alzheimer[2], and in spite of great research efforts, therapeutic progress has been slow. This is probably because AD is characterized by several factors, namely amyloid beta (Aβ) deposits, neurofibrillary tangles (NFTs), and neuronal inflammation, with an unclear connection between these factors. It has been shown previously that iron is dysregulated in AD pathology [3]. Here we used an organotypic tissue culture model for studying the contribution of iron overload to the disease.
Methods
We established an organotypic tissue culture model of AD, for which we cultivate either human or porcine brain tissue and inject Aβ monomers into the tissue, which triggers aggregation of Aβ and the deposition of the aggregates in the tissue. In order to study the contribution of excess iron in this model we injected ferric citrate into the tissue.
Results
A careful analysis of the shape of the deposits in vitro showed that iron changes the shape of the deposits. Furthermore, we reveal that combined iron overload and Aβ injection exacerbated neuronal loss, enhancing the toxicity of Aβ on its own.
Conclusion
The advantage of our organotypic brain tissue culture model is that the natural organization of the cells within the tissue is preserved. This technique will eventually also open the possibility of reducing animal experiments. This integrated approach will elucidate the complex mechanisms underlying neuronal degeneration in AD, paving the way for targeted therapeutic interventions.
Grant sponsors : Austrian Science Fund FWF, grants P29370, P32058; MEFO Graz.

Keywords:

Azheimer's disease, Amyloid beta, iron

Reference:

[1] Alzheimers & Dementia in Austria. https://www.worldlifeexpectancy.com/austria-alzheimers-dementia.
[2] Stelzmann, R. A., Norman Schnitzlein, H. & Reed Murtagh, F. An english translation of alzheimer's 1907 paper, "über eine eigenartige erkankung der hirnrinde". Clinical Anatomy 8, 429–431 (1995).
[3] Peng, Y., Chang, X. & Lang, M. Iron Homeostasis Disorder and Alzheimer's Disease. International Journal of Molecular Sciences 2021, Vol. 22, Page 12442 22, 12442 (2021).

962

Comparison of the FMT assay with the Cell Painting approach in healthy patient derived fibroblasts.

Dr Tabea Hohensee[1], Dr Fredrik Edfeldt[1]
[1]Mechanistic and Structural Biology, Discovery Sciences, R&D, AstraZeneca, Gothenburg, Sweden

Poster Group 1

IPF, a fatal chronic disease of the lung, is caused by an inflammatory response that results in aberrant fibroblast activation, the deposition of excessive extracellular matrix, and progressive fibrotic remodelling of the lungs1. Though the exact pathophysiological mechanisms of IPF remain unknown, myofibroblasts are considered to play a major role in the pathology of IPF. Transforming growth factor β (TGF-β1), a well-established fibrogenic mediator, induces FMT. In cells undergoing FMT, increased expression of α-smooth muscle actin (αSMA) is observed. In vitro, increased αSMA expression positively correlates with contraction of myofibroblast populated collagen gels, indicating that αSMA is a strong marker of myofibroblast differentiation, and thus a relevant readout for lung fibrosis.

A validated, robust TGF-β1-induced FMT cell-based imaging assay in normal human lung fibroblasts (NHLF) with αSMA expression as a readout exists in-house to support multiple R&I IPF projects. As an inhibitor control, the highly specific Alk5 inhibitor SB-525334 is used to block TGF-β1 signalling2.

Cell Painting is a non-target hight content imaging assay to identify morphological profiles of different cell types with diverse compound treatments3. In this study the compounds used for the FMT assay have been simultaneously analysed via cell painting and the data has been compared. The Cell Painting results correlate well with the FMT data and could potentially be used as an alternative to the FMT assay. Especially while the assay is one day shorter.

Additionally, three patient-derived IPF cell lines have been tested with 27 compounds to see if it is possible to reverse the diseased phenotype to the healthy one, with or without TGF-β1 treatment. All three donors showed a different response profile when compared to each other, which made it difficult to distinguish if there are compounds being especially responsive to TGF-β1 treatment or to diseased cells, but not healthy ones. This needs further investigation.

Keywords:

alphaSMA, FMT, Cell Painting, HTS

Reference:

1 Control of lung myofibroblast transformation by monovalent ion transporters, Elsevier, Nickolai O Dulin, Sergei N Orlov et al., PMID: 31196603 DOI: 10.1016/bs.ctm.2019.01.002

2 Disease modelling of pulmonary fibrosis using human pluripotent stem cell-derived alveolar organoids, CellPress, Takahiro Suezawa, Shimpei Gotoh et al., PMID: 34798066 PMCID: PMC8693665 DOI: 10.1016/j.stemcr.2021.10.015

3 Cell Painting, a high-content image-based assay for morphological profiling using multiplexed fluorescent dyes, Nature Portfolio, Mark-Anthony Bray, Anne E Carpenter et al., PMID: 27560178 PMCID: PMC5223290 DOI: 10.1038/nprot.2016.105

967

In-vivo DAB cytochemistry and high-pressure freezing to determine the source of the human cytomegalovirus envelope

Tim Bergner[1], Laura Cortez Rayas[2], apl. Prof. Jens von Einem[2], Dr. Clarissa Read[1]
[1]Central Facility for Electron Microscopy, Ulm University, Ulm, Germany, [2]Institute of Virology, Ulm University Medical Center, Ulm, Germany

Poster Group 1

Background/aims:
The human cytomegalovirus (HCMV), an enveloped DNA virus, significantly alters host cell morphology during infection. Formation of infectious virus progeny requires two critical envelopment processes: primary and secondary envelopment. Secondary envelopment occurs in a specialized juxtanuclear region known as the cytoplasmic viral assembly complex (cVAC), where capsids bud into the lumen of cellular vesicles and by this acquire the final virion envelope. The identity of these vesicles is debated, with both trans-Golgi and endosomal vesicles proposed as potential sources (1-3, and see abstract by T. Bergner, L. Cortez Rayas, J. von Einem, C. Read).

To address this, we adapted the protocol by Ellinger et al. 2010 (4) for cytochemical labelling of endocytic membranes for visualization by electron microscopy (EM). The protocol uses wheat germ agglutinin (WGA) conjugated to horseradish peroxidase (HRP) for labelling and diaminobenzidine (DAB) cytochemistry that is performed in living cells. WGA specifically binds to N-acetyl-glucosamine and sialic acid, abundant in the plasma membrane, whereby it is endocytosed in large quantities. The peroxidase-catalyzed DAB reaction results in a specific labelling of the endocytic compartment. Performing this reaction in vivo allows cryo-immobilization through high-pressure freezing. The combination with freezing within milliseconds allows capturing snapshot of the dynamic membrane system, making this approach suitable for pseudo-dynamic EM studies. Moreover, high-pressure freezing provides excellent structural preservation, allowing differentiated visualization of the endocytic compartment, HCMV capsids in different maturation stages, and their interaction during the secondary envelopment process in EM. This is a prerequisite for detailed 3D EM analysis.

Methods:
The study was performed with human foreskin fibroblasts infected with HCMV for 5 days, following the adapted protocol of Ellinger et al. 2010 (4). For pulse-chase experiments, WGA-HRP was added to the living cells and incubated for specific pulse times (e.g., 60 or 10 minutes). After the pulse, WGA-HRP was removed, and the samples were incubated for an additional chase period of 30 minutes. In vivo DAB cytochemistry was then performed by applying DAB to induce the formation of an insoluble reaction product at intracellular membranes, visible as a dark precipitate in EM. Samples were immediately cryo-immobilized through high-pressure freezing, freeze-substituted, and embedded in epoxy resin. Transmission electron microscopy (TEM) was used for quantitative analysis of 10 infected cells. Capsids were categorized as budding or enveloped and further categorized as either WGA-labelled or not labelled. 3D visualization of the endocytic compartment was achieved using STEM tomography.

Results:
TEM analysis revealed that the WGA-HRP precipitate is clearly visible and located along the intraluminal face of various intracellular membrane compartments, including vesicles, endosomes, multivesicular bodies, and the trans-side of the Golgi apparatus. Examination of the cVAC showed numerous capsids associated with WGA-labelled membranes. Notably, within 90 minutes of WGA-HRP pulse-chase, about 90% of budding capsids and 50% of enveloped capsids were WGA-labelled.

This indicates rapid plasma membrane endocytosis, translocation to the cVAC and completion of the secondary envelopment process. Reducing the pulse-chase time to 30 minutes still resulted in WGA-labelled membranes that were used for secondary envelopment, suggesting that this process is even faster. STEM tomography further unambiguously identified capsid budding at the trans-side of Golgi cisternae.

Conclusion:
This study demonstrated that combining peroxidase-catalyzed cytochemistry with high-pressure freezing and freeze substitution ensures optimal structural preservation and specific labelling of the endocytic compartment suitable for EM studies. With this approach, we showed that endocytosed membranes are the primary source of the HCMV envelope. Additionally, the findings highlight the rapidity of secondary envelopment.

Keywords:

herpesvirus, cytochemistry, dynamics, TEM, STEM

Reference:

1 Cepeda et al. (2010). doi: 10.1111/j.1462-5822.2009.01405.x
2 Homman-Loudiyi et al. (2003). doi: 10.1128/JVI.77.5.3191-3203.2003
3 Tooze et al. (1993). Progeny Vaccinia and Human Cytomegalovirus Particles Utilize Early Endosomal Cisternae for Their Envelopes
4 Ellinger et al. (2010). doi: 10.1016/j.jsb.2009.10.011

976

Evaluation of inflammation and free fatty acid metabolism as biomarkers in female patients

Assoc.prof.dr. Pınar Köroğlu[1], Sultan Üzümcüoğlu[2], Muhammed Melik Anşin[2], Prof.Dr. Ulun Uluğ[3]
[1]Halic University, Faculty of Medicine, Department of Histology and Embryology , Istanbul, Turkey, [2]Halic University, Faculty of Medicine, Istanbul,, Turkey, [3]Halic University, Faculty of Medicine, Department of Obstetrics and Gynecology, , Turkey

Poster Group 1

Background incl.aims: Ovulatory and tubaperitoneal factors constitute an important part of the female infertility factor. At the beginning of the reproductive period, there are approximately 400 thousand primordial follicles in the human ovary. Follicular fluid is the environment in which the oocyte resides throughout oogenesis and is important in oocyte development (1). Follicular fluid is aspirated with the oocyte during oocyte retrieval. By analyzing the follicular fluid, the relationship between the oocyte and surrounding cells can also be evaluated. The most common risk factors for infertility are smoking, body mass index being less than 18.5 kg/m2 or more than 25 kg/m2, excessive exercise or no exercise, alcohol consumption, caffeine consumption, and stress. IL-8 is known as a cytokine growth factor that contributes to the pathogenesis of endometriosis by promoting endometrial cell attachment, invasion, cell growth, proliferation, and immune protection in the endometrium (2). Although IL-8 has been shown to have an effect on many areas such as female infertility, endometriosis and Polycystic Ovary Syndrome, no study has been found showing its relationship with different parameters on oocyte quality. The aim of this study was to investigate the relationship between free fatty acids in follicular fluid, body mass index and oocyte reserve quality. It was aimed to evaluate the effects of data on the relationship between free fatty acid level in follicular fluid, IL-8, lipid droplet count, body mass index and peripheral blood smear in female infertility samples.

Methods: A total of 60 people who applied to the in vitro fertilization clinic for various reasons (male factor, female factor, unexplained infertility) were included in the study. In our study, a sample of 60 patients diagnosed with infertility was created. These patients will be evaluated in two groups according to body mass index. Body mass index of less than or more than 25 kg/m2 was evaluated as group 1 and group 2. Various exclusion criteria were applied to determine the patient groups in order not to affect the study design. In our study, free fatty acid (FABP) and IL-8 parameters in follicular fluid taken for routine treatment from women applying assisted reproductive techniques were evaluated by ELISA (Enzyme-Linked ImmunoSorbent Assay) method. In blood samples, peripheral smears were used to determine the distribution of shaped elements of blood and also to examine whether there was a correlation between them and body mass index. At the same time, Oil red staining of neutral lipids and lipid droplet morphology were identified by light microscopy. All data were analyzed by statistically.

Results: When the differences between the groups were examined, it was determined that FABP and IL-8 levels were higher in the group with high body mass index (group 2). The concentrations of follicular IL-8 and FABP were significantly higher in the group 2 and were positively correlated with the levels of fatty acids. At the same time, when blood smear samples were examined in this group, it was determined that the number of leukocytes and the number of lipid droplets was higher. Accordingly, a semiquantitative histopathological damage score was made and lipid droplet distribution and blood smear between groups was determined. It was observed that over body mass index and cellular degeneration caused infertility, inflammation and increased oxidative damage.

Conclusions: Follicular fluid and blood smear samples taken from women who have used assisted reproductive techniques will become more important in the diagnosis and course of the disease. By evaluating several parameters together, it is aimed to obtain faster and more reliable results in assisted reproductive techniques. IL8 and FABP affects female fertility at both serum level and light microscopic levels.

Keywords:

Follicular, fatty acid, Infertility, Microscopy.

Reference:

Reference:
1. Yao X, Liu W, Xie Y, Xi M, Xiao L. Fertility loss: negative effects of environmental toxicants on oogenesis. Front Physiol. 2023 Aug 4;14:1219045. doi: 10.3389/fphys.2023.1219045. PMID: 37601637; PMCID: PMC10436557.
2. Lai Y, Ye Z, Mu L, Zhang Y, Long X, Zhang C, Li R, Zhao Y, Qiao J. Elevated Levels of Follicular Fatty Acids Induce Ovarian Inflammation via ERK1/2 and Inflammasome Activation in PCOS. J Clin Endocrinol Metab. 2022 Jul 14;107(8):2307-2317. doi: 10.1210/clinem/dgac281. PMID: 35521772.

977

The Healing Effect Of Ferulic Acid in Monosodium Glutamate-Induced Liver Injury

Student Seda Sezer[1,2], Anıl Can[1,2], Assoc. Dr. Merve Açıkel Elmas[1], Assoc. Dr. Meltem Kolgazi[3], Prof. Dr. Serap Arbak[1]
[1]Department of Histology and Embryology, School of Medicine, Acibadem Mehmet Ali Aydinlar University, Istanbul, Turkey, [2]Department of Histology and Embryology, Institute of Health Sciences, Acibadem Mehmet Ali Aydinlar University, Istanbul, Turkey, [3]Department of Physiology, School of Medicine, Acibadem Mehmet Ali Aydinlar University , Istanbul , Turkey

Poster Group 1

Background incl. aims
Monosodium glutamate (MSG), a flavor enhancer in prepared foods, can lead to harmful effects in different organs and systems. Based on the literature data, monosodium glutamate is known to cause liver injury by generation of reactive oxygen species leading to damage of lipids, proteins, and DNA by the formation of free radicals (1). Ferulic acid, as a potent antioxidant, is mentioned to ameliorate the harmful effect of biomolecules by suppressing the production of reactive species and the oxidative stress. In this experimental study, MSG-induced liver injury putative healing effect of ferulic acid were assessed at histochemical, transmission electron microscopical and biochemical levels.

Methods
In this study, male Wistar albino rats (7 weeks old, 160-200g) were used and kept in a laboratory environment (Acıbadem University Experimental Animal Laboratory) with a temperature of 22±2°C and a standard light/dark (12/12 hours) cycle throughout the experimental period. Rats were randomly divided into 5 groups (n:8/group). Experimental groups were fed by a standard rat chow and tap water. Control group (Gr 1) was treated with 1 ml of distilled water by gavage every day during the experiment for 38 days. Rats in the DMSO+FA group (Gr 2) were given 1 ml of dimethyl sulfoxide (DMSO) for 28 days and FA solution (25mg/kg, dissolved in DMSO) by gavage in the last 10 days of the experiment. To create an MSG-induced liver injury model, MSG solution (600 mg/kg, dissolved in DMSO) was orally administered to the rats (MSG group-Gr 3) for 28 days (2). MSG+DMSO group (Gr 4) was treated by MSG solution (600 mg/kg, dissolved in DMSO) by gavage for 28 days and 1 ml of DMSO was given by gavage on the last 10 days of the experiment. MSG solution (600 mg/kg) for 28 days and then FA solution (25 mg/kg) on the last 10 days of the experiment were administered by gavage to the rats in the treatment group (MSG+FA-Gr 5) (3). At the end of the experiment the rats were sacrificed under anesthesia. Liver tissues samples were processed for light and transmission electron microscopical evaluations. Paraffin sections were stained with Hematoxylin-eosin (H&E), Masson's trichrome stains and Periodic acid-Schiff reaction (PAS). Histopathological scoring of the liver tissue was performed according to; vacuolization in hepatocyte cytoplasm, sinusoidal dilatation, leukocyte cell infiltration and distribution and amount of connective tissue in the parenchyme, as well as glycogen content within the hepatocytes. Oxidative stress markers, as malondialdehyde (MDA), glutathione (GSH), superoxide dismutase (SOD), total antioxidant capacity (TAS), total oxidant capacity (TOS) and oxidative stress index (OSI) values were measured for biochemical assesments (4).

Results
The light microscopical examinations revealed normal morphology of liver parenchyme in control and DMSO+FA groups. Steatosis and vacuolization in hepatocytes, sinusoidal dilatation, leukocyte infiltration, increased connective tissue in the parenchyme and decreased amount of glycogen in

hepatocyte cytoplasm were detected in MSG and MSG+DMSO groups. Based on histopathological scoring, liver tissue injury was significantly reduced in MSG+FA group, compared to MSG and MSG+DMSO groups. Transmission electron microscopy revealed the similar ultrastructural data as in light microscopy to point out a prominent recovery in MSG+FA group. In MSG and MSG+DMSO groups, an increase in MDA, TOS and OSI levels were detected whilst GSH, TAS and SOD were decreased. Deteriorated biochemical data has been reversed and ameliorated in MSG+FA group, as the treatment group.

Conclusion

Based on the current biochemical and histopathological data, we could suggest that administration of ferulic acid to rats in this experimental model of MSG-induced liver injury contribute significantly to ameliorate/heal the hepatic damage by regulating the formation of reactive oxygen species.

Keywords:

MSG, Ferulic Acid,Liver, Microscopy.

Reference:

1. A Sharma, Monosodium glutamate-induced oxidative kidney damage and possible mechanisms: a mini-review. A Journal of Biomedical Science 2015; 22:93.
2. Banerjee A, Das D, Paul R, Roy S, Das U, Saha S, Dey S, Adhikary A, Mukherjee S, Maji BK. Mechanistic study of attenuation of monosodium glutamate mixed high lipid diet induced systemic damage in rats by Coccinia Grandis. Scientific Reports 2020;10(1):15443.
3. Eman G. Kelainy1 &Ibrahim M. Ibrahim Laila &Shaimaa R. Ibrahim. The effect of ferulic acid against lead-induced oxidative stress and DNA damage in kidney and testes of rats, Environmental Science and Pollution Research 2019;26:31675–31684.
4. Allameh A, Niayesh-Mehr R, Aliarab A, Sebastiani G, Pantopoulos K. Oxidative Stress in Liver Pathophysiology and Disease. Antioxidants (Basel). 2023; Aug 22;12(9):1653.

982

Neuroprotective Effects of Bromelain in Peripheral Nerve Injuries: A Rat Sciatic Nerve Crush Injury Model

DR. ONUR AKSOY[3], DR. ILKER USCETIN[3], ASSOC. PROF. SAMED OZER[2], ASSOC. PROF. MERVE ACIKEL ELMAS[1], BIO. GOKCEN OZGUN[4], BIO. SEDA SEZER[5], Prof. Dr Serap Arbak[1]
[1]DEPARTMENT OF HISTOLOGY AND EMBRYOLOGY ACIBADEM MEHMET ALI AYDINLAR UNIVERSITY SCHOOL OF MEDICINE, ISTANBUL, TURKEY, [2]Animal Application and Research Center, Acibadem Mehmet Ali Aydinlar University, ISTANBUL, TURKEY, [3]Prof Dr Cemil Tascioglu City Hospital, Department of Plastic and Reconstructive Surgery, ISTANBUL, TURKEY, [4]Institute of Health Sciences, Department of Biotechnology, Acibadem Mehmet Ali Aydinlar University, ISTANBUL, TURKEY, [5]Institute of Health Sciences, Department of Histology and Embryology Acibadem Mehmet Ali Aydinlar University, ISTANBUL, TURKEY

Poster Group 1

Background: An aqueous, coarse extract called bromelain is obtained from the fruit and stems of the pineapple. Bromelain is a substance that can be easily absorbed into the body without losing its proteolytic activity and without showing any significant side effects. In vitro and in vivo studies have demonstrated various fibrinolytic, antiedema, antithrombotic, and anti-inflammatory activities of bromelain. Experimental studies have demonstrated the properties of bromelain, such as accelerating healing effect in tendon and muscle injuries, faster healing rate in burn wounds, and reducing post-surgical edema. This present study aims to investigate the neuroprotective effects of bromelain on peripheral nerve injuries, specifically through a rat sciatic nerve crush injury model.The study focused on the ability of bromelain to improve nerve regeneration and functional recovery after injury through histological and electron microscopic evaluations.

Materials and Methods: A controlled experimental study was conducted on 36 adult male Sprague-Dawley rats, divided into four groups: Sham, Control (Nerve injury), and two Treatment groups receiving oral bromelain at doses of 25 mg/kg and 50 mg/kg respectively. The sciatic nerve crush injury was induced using a standardized protocol. The intervention groups received their respective doses of bromelain daily for six weeks post-injury. Evaluation of neuroprotective effects was assessed through walking track analysis for functional recovery, hot plate tests for nociception, nerve conduction studies and histological examinations including light and transmission electron microscopy. Sciatic nerve samples taken from all the experiemental groups were fixed in 10% buffered formalin solution. Masson's trichrome stain was applied to paraffin section to reveal myelinated axon morphology. Tisue samples from sciatic nerve, fixed in 2.5% glutaraldehyde solution were processsed for transmission electron microscopy.

Results: The bromelain-treated groups exhibited significant improvements in functional recovery assessed by the Sciatic Functional Index (SFI) compared to the control group. The 50 mg/kg bromelain group showed the most pronounced improvement ($p<0.05$). Nociceptive testing indicated a reduction in pain sensitivity in bromelain-treated groups. Electrophysiological studies revealed enhanced nerve conduction velocities in treatment groups ($p<0.05$) with histochemical and ultrastructural analysis confirming accelerated nerve regeneration and reduced scar tissue formation. Statistically significant differences were observed between treatment groups and the control group with the higher bromelain dose demonstrating superior outcomes.

Conclusion: Bromelain administration in post-sciatic nerve crush injury in rats significantly enhances nerve regeneration, functional recovery, and reduces pain sensitivity. The study highlights bromelain's potential as a beneficial therapeutic agent in the management of peripheral nerve

injuries with dose-dependent effectiveness. Further research is warranted to elucidate the underlying mechanisms and explore the clinical applicability of bromelain in peripheral nerve injury treatment.

Keywords:

Bromelain, nerve injury, histopathology

Reference:

1. Pavan R, et al. “Properties and therapeutic application of bromelain: a review.” Biotechnol Res Int. (2012): 976203.
2. Tuncer, Kutsi, et al. "The effects of Tendoflex® (polytendon complex) and Hypericum perforatum (St. John’s wort oil) on repaired Achilles tendon healing in rats." Joint Diseases and Related Surgery 32.3 (2021): 676.
3. Rosenberg, L., et al. "Minimally invasive burn care: a review of seven clinical studies of rapid and selective debridement using a bromelain-based debriding enzyme (Nexobrid®)." Annals of burns and fire disasters 28.4 (2015): 264.

1027

Imaging-based methods to identify prognostic and predictive biomarkers for Hereditary Spastic Paraplegia

Phd Student Gaia Fattorini[1,2], Researcher Valerio Licursi[1], Professor Filippo Maria Santorelli[3], Professor Gabriella Silvestri[4], Professor Carlo Casali[5], Researcher Cinzia Rinaldo[1], PhD Francesca Sardina[1]
[1]Institute of Molecular Biology and Pathology (IBPM), Consiglio Nazionale delle Ricerche (CNR), Rome, Italy, [2]Department of Biology and Biotechnology "Charles Darwin", Sapienza University of Rome, Rome, Italy, [3]IRCCS Stella Maris, Pisa, Italy, [4]UOC Neurologia, Fondazione Policlinico Universitario 'A. Gemelli' IRCCS, Rome, Italy, [5]Department of Medico-Surgical Sciences and Biotechnologies, University of Rome Sapienza, Latina, Italy

Poster Group 1

Background
Hereditary spastic paraplegias (HSPs) are rare motor neuron diseases characterized by axonal degeneration involving the lateral corticospinal tracts. The most common is caused by haploinsufficient mutations in the SPG4 gene, which encodes spastin, a microtubule (MT) severing ATPase, that controls cytokinesis, endosomal traffic, lipid droplets (LDs) homeostasis, and axonal transport. Clinically, HSP-SPG4 age of onset and the severity of symptoms are strongly variable even among individuals belonging to the same family. Given this heterogeneity, it is important to identify prognostic biomarkers. To date, no effective disease-modifying therapies are currently available, but approaches based on drugs counteracting dysfunctional mechanisms or spastin-elevating treatments are emerging, so it will be crucial to identify biomarkers that can help to monitor the effects of spastin recovery treatments.
We have developed an automated, simple, rapid, and non-invasive cell imaging-based method to quantify the organization of the MT-cytoskeleton. By using this method, we demonstrated that the dcnc-parameter, measuring the distance between cell and nucleus centroids, is able to distinguish HSP-SPG4 from healthy donor (HD) lymphoblastoid cell lines (LCLs) and peripheral blood mononuclear cells (PBMCs).
We are now extending the dcnc-based method to a larger cohort of SPG4 patient cells to evaluate its sensitivity and specificity in relation with molecular and clinical patient features and to detect the effects of different spastin-elevating drugs. Additionally, we are also focusing on other subcellular components affected by spastin mutations, such as LDs.

Methods
The study included 13 HDs and 18 SPG4 patients with different types of mutations (12 truncating mutations and 6 missense mutations). Cell image analysis was performed using PBMCs or LCLs stained with specific antibodies (anti-β-tubulin-cy3 for MT-cytoskeleton) and dyes (Bodipy™ 493/503 for LD and Hoechst for Nucleus). Automated image acquisition was achieved by using the inverted Nikon Eclipse-Ti microscope and the JOBS module of NisElements 5.11 software to obtain a file containing more than 50 images and 500 cells related to each single sample. The acquired images were then analyzed using Cell Profiler 4.3 software, with an ad hoc designed pipeline that recognizes cellular compartments using thresholding segmentation and measures several parameters, including “dcnc” and “number of LD in each cell (nLD)”.

Results
We performed correlation analysis between the “dcnc” parameter and molecular patient features, showing that SPG4 cells from patients with missense mutations have higher “dcnc” than those with

truncating mutations. Correlations with clinical features, such as the age at onset of the disease or the Spastic Paraplegia Rating Scale (SPRS) score, are ongoing.
By assessing the effect of three different spastin-elevating drugs, we observed that dcnc-based method is able to detect the reduction of MT defects induced by spastin recovery in cells from SPG4 patients carrying truncating mutations. Similar analyses on cells carrying missense mutations are ongoing.
We have implemented our pipeline to evaluate other cellular components, such as LD, so it automatically recognises the staining of the nucleus, cytoskeleton and LD, in our cells. By using this tool, we have analysed the parameter “nLD”. Correlation analysis between dcnc and “nLD” was performed, showing a positive correlation in SPG4 patients.

Conclusions and future perspectives
Our analyses revealed that the dcnc-based method is able to sense the effects of spastin elevating drugs in cells from SPG4 patients carrying truncating mutations, suggesting a predictive role. Now, we are performing correlation analyses among molecular and clinical patients features and the “dcnc” and “nLD” parameters to evaluate whether our method might have prognostic value. These results will open the possibility to identify new prognostic and predictive tools for HSP-SPG4.

Keywords:

HSP-SPG4
biomarker
neurodegenerative disease

Reference:

- Sardina F, Valente D, Fattorini G, Cioffi E, Zanna GD, Tessa A, Trisciuoglio D, Soddu S, Santorelli FM, Casali C, Rinaldo C. New cellular imaging-based method to distinguish the SPG4 subtype of hereditary spastic paraplegia. Eur J Neurol. 2023 Jun;30(6):1734-1744. doi: 10.1111/ene.15756. Epub 2023 Mar 26. PMID: 36815539.
- Francesca Sardina, Claudia Carsetti, Ludovica Giorgini, Gaia Fattorini, Gianluca Cestra, Cinzia Rinaldo, Cul-4 inhibition rescues spastin levels and reduces defects in hereditary spastic paraplegia models, Brain, 2024;, awae095, https://doi.org/10.1093/brain/awae095

1052

Carbonic anhydrase immobilization for microscopic investigation of enzyme activity

Dr. Zsófia Bognár[1], Jeannette de Sparra Lundin[2], Sune Christensen[2], Joerg Jinschek[1,3], Jialong Shen[4], Sonja Salmon[4], Stig Helveg[1]
[1]Center for Visualizing Catalytic Processes (VISION), Department of Physics, Technical University of Denmark, Kgs. Lyngby, Denmark, [2]Novonesis A/S, Kgs. Lyngby, Denmark, [3]National Centre for Nano Fabrication and Characterization (DTU Nanolab), Technical University of Denmark, Kgs. Lyngby, Denmark, [4]Textile Biocatalysis Research, Department of Textile Engineering Chemistry & Science, North Carolina State University, Raleigh, USA

Poster Group 1

Background incl. aims
Carbonic anhydrase (CA) is an efficient catalyst for CO2 absorption in solvent-based carbon capture. 1 However, replenishment of CA could be required, because the solvent regeneration temperature is often higher than the enzyme's thermal tolerance, leading to CA deactivation. Alternatively, immobilizing the enzyme on solid carriers can improve its stability and longevity, allowing for catalyst recovery and reuse, and reducing overall costs. 2,3 We are developing immobilization techniques to address this challenge, which calls for high-resolution visualization techniques to design the distribution of enzymes immobilized at condensed matter interfaces and optimize their accessibility with gases and liquids. 4

Methods
We use transmission electron microscopy (TEM) and fluorescent microscopy (FM) to investigate the interaction of the immobilized enzyme with the support nanostructure and substrate, with the aim of uncovering attributes that maximize the biocatalytic interaction.

Results
Various immobilization techniques were employed to achieve the desired surface coverage of the CA enzyme on carbon nanotubes. Two different methods were used - secondary π-π interaction and EDC/NHS covalent coupling. After fluorescent labeling and immobilization, the enzymes were found to be active. High-resolution TEM and fluorescent microscopy were used to further characterize the immobilization process, which showed a high enzyme coverage and activity on the surface.

Conclusion
With the systematic development of immobilization chemistry and imaging techniques, we would unlock new insights into the dispersion and structural aspects of immobilized enzymes.

Keywords:

carbonic anhydrase,TEM, fluorescent microscopy

Reference:

1 Kim, S.; Sung, J.; Yeon, J.; Choi, S. H.; Jin, M. S. Crystal Structure of a Highly Thermostable α-Carbonic Anhydrase from Persephonella marina EX-H1. Mol. Cells 2019, 42 (6), 460-469.
2 Sheldon, R. A.; van Pelt, S. Enzyme Immobilization in Biocatalysis: Why, What and How. Chem. Soc. Rev. 2013, 42 (15), 6223–6235.
3 Shen, J., Yuan, Y., Salmon, S. Carbonic Anhydrase Immobilized on Textile Structured Packing Using Chitosan Entrapment for CO2 Capture. ACS Sustainable Chem. Eng. 2022, 10 (23), 7772–7785.

4 The project was funded by the Novo Nordisk Foundation (Grant no. NNF22SA0078767) and DTU VISION was supported by the Danish National Research Foundation (DNRF146).

1056

Histopathologic Alterations of Cerebellum in the VPA-Induced Autism Model of Rats

Dr Sila GUVENIR SEVEN[1], MSc Hakan Sahin[2], Prof. Dr. Gozde Erkanli Senturk[2], Nesibe Uysal[3], Prof. Dr. Hafize Uzun[4], Prof. Dr. Gonul Simsek[1]
[1]Department of Physiology, Cerrahpasa Faculty of Medicine, Istanbul University-Cerrahpasa, Istanbul, Turkey, [2]Department of Histology and Embryology, Cerrahpasa Faculty of Medicine, Istanbul University-Cerrahpasa, Istanbul, Turkey, [3]Cerrahpasa Faculty of Medicine, Istanbul University-Cerrahpasa, Istanbul, Turkey, [4]Department of Medical Biochemistry, Faculty of Medicine, Atlas University, Istanbul, Turkey

Poster Group 1

Background
Autism Spectrum Disorder (ASD), classified under neurodevelopmental disorders, is characterized by persistent deficits in social communication and interaction, along with repetitive behavioral patterns. Histomorphological changes occur in various brain regions in ASD. This study aims to investigate pathophysiological alterations in the cerebellum of rats with valproic acid (VPA)-induced autism model.
Methods
Adult female and male Sprague-Dawley rats were allowed to mate overnight. Rats with confirmed vaginal plugs the following day were considered pregnant, and embryonic day 0 (E0) was recorded. VPA (500 mg/kg) was injected intraperitoneally (i.p.) on embryonic day 12 (E12). On postnatal day 21 (P21) the genders of the offspring were determined and weaned. Rats were sacrificed at P46, and cerebellar tissues were collected. The sections were firstly stained with cresyl violet, and then random micrographs of the cerebellar cortex were captured from three serial sections at three different areas for each section. Afterward, the number of Purkinje cells was divided by the line measurement expressed as µm between the molecular and granular layers.
Results
In light microscopic examination, the number of Purkinje cells per unit length was significantly lower in the VPA-treated groups compared to the control groups in both sexes ($p<0.001$) (Female-control:0,0296±0,00263, male-control:0,0286±0,00365, Female-VPA:0,0224±0,00280, Male-VPA:0,0216±0,00254). There was no statistically significant difference between genders.
Conclusion
The number of Purkinje cells in cerebellum decreased in VPA-induced autism model. Additionally, there was no difference between genders. These results may consider that autism is also related with Purkinje cells.

Keywords:

Autism Model, cerebellum, Purkinje cell

1068

Investigation of the Presence of Telocyte-like Cells in Human Patellar Fat Pad Tissue

Professor Doctor Gamze Tanriverdi[1], MD. PhD Merjem Purelku[1], Ph.D Zehra Sezer[1], Specialist Doctor Duygu Neccar[1], M.sC. Naziya Bagirova[1], Research Assistant Yonca Aras[1], Associate Professor Ersin Erçin[2], Specialist Doctor Alican Koluman[2], Professor Doctor Gozde Erkanli Senturk[1], Associate Professor Bulent Tanriverdi[2]
[1]Istanbul University - Cerrahpasa, Cerrahpasa Medical Faculty, Histology and Embryology Department , Istanbul , Turkey , [2]Department of Orthopedics and Traumatology, Istanbul Bakirkoy Dr. Sadi Konuk Education and Research Hospital, University of Health Sciences, Istanbul, Turkey

Poster Group 1

Stromal cells remain the focus of research in tissue biology from past to present. It is known that the stroma hosts mainly fibroblasts, pericytes, neurons, endothelial cells and immune cells. These cell types also have various distinctive features due to their different morphologies and functional properties. In addition, other different cell types have also been described in the stroma, including the interstitial cells of Cajal and telocytes. Telocytes (TC), which are characterized with small cell bodies and long telopods, have been identified in the connective tissue of many organs and are strategically positioned between target cells, near nerve endings and capillaries. Telocytes coordinate tissue homeostasis by integrating information from multiple sources and their extracellular vesicles provide bidirectional communication between them and the other stromal cells. They are able to regulate stem cell proliferation and differentiation through their secretome and play crucial roles in embryogenesis, angiogenesis, and various diseases, including cancer. Human telocytes have so far beenidentified in the heart, lung, brain, eye, thyroid, skeletal muscles, skin, gastrointestinal tract and accessory glands, urinary system, and male and female reproductive systems. But there is no information about the relationship between the telocyte cells and the Infrapatellar Fat Pad (IPFP). The approach to serious joint diseases such as osteoarthritis (OA), which is highly prevalent in our society and causes significant morbidity in the population and treatment is currently limited to microfracture treatments, autologous chondrocyte transplantations and prosthetic surgery. The incidence of symptomatic OA in the obese and elderly population and the high costs of joint replacement surgeries are increasing every year. Therefore, in addition to current treatments, the search for tissue engineering and stem cell-based research continues to meet the needs for alternative treatment methods. In recent years, tissue engineering studies have emerged as promising methods in orthopedic treatment approaches. Difficulties that may be experienced in obtaining mesenchymal stem cells (MSCs) obtained from various sources may also lead to undesirable pathological conditions such as heterogeneity in the obtained stem cell populations and teratoma formation in new cartilage cell differentiation. For this reason, researchers are now focusing on different cellular sources. Infrapatellar fat pad (IPFP), also known as Hoffa; fat pad due to its proximity to articular cartilage, in recent years has been the focus of researchers working on the relationship between cartilage regeneration and the surrounding stem cells. Studies have shown that IPFP has a good stem cell reserve and is very suitable for studies based on cartilage retrieval. On the other hand, there are also studies showing that the use of IPFP-derived stem cells in repairing joint cartilage damage may be limited due to their heterogenity. In recent years, the presence of a unique cell group called telocytes, which is in close relationships with the stem cell niche, has been described in the stroma of many organs. These cells can stimulate stem cells with the microstructures they secrete called exosomes and induce tissue regeneration by creating cellular differentiation. The existence of infrapatellar fat pad cells with surface markers same as telocytes have been reported in only one article in the literature. TC markers including CD34, vimentin, PDGRF-α and PDGRF-β, c-kit,

and α-SMA are frequently used in telocyte studies and are regarded trustworthy. Double immunofluorescence is the most accurate and precise method for identifying these cells.

Aims: This research aims to advance our understanding of the heterogenity of IPFP cells and detect the presence of TCs by employing techniques such as immunohistochemistry and immunofluorescence. Through the investigation of their morphology and identification of telocytes in the IPFP stroma, this study endeavors to provide novel insights into IPFP architecture and its implications for regenerative medicine.

Methods: In this study, IPFP tissues were obtained from 5-10 patients preparing for knee replacement surgery at Sadi Konuk Training and Research Hospital, Orthopedics and Traumatology Clinic. After obtainiing the specimen one small piece of it underwent tissue preparation procedures for light microscopy and immunohistochemical staining was performed using CD34 which is the most common marker for telocyte identification. The rest of the specimen was used for cell culture from which these cells were isolated using tissue digestion agent such as collagenase II and cell strainers of different diameters in order to separate them from other stromal cells with the cell adhesion method and subculturing the media in which the telocytes were present during 96 hours. The cells were photographed at different incubation times such as at 24h, 48, and 96h and were examined under the inverted microscope. Finally the cells resembling to telocytes with their long projections were analyzed by double immunofluorescence staining used CD34/c- kit, CD34/vimentin, CD34/PDGFR- α and β, and CD34/ α-SMA markers for telocyte identification. This comprehensive approach aimed to illuminate telocyte presence and distribution in the IPFP stroma, offering future insights into IPFP physiology and pathophysiology.

Results: In this study, the existence of telocytes within the IPFP was identified by their different shape and immunophenotypes. We identified telocytes by immunohistochemical analysis, labeling with CD34, the most extensively utilized telocyte marker. We used immunofluorescence analysis with double labeling of CD34/c-kit, CD34/vimentin, and CD34/PDGFR α and β, CD34/α-SMA in order to distinguish these cells from fibroblasts and pericytes in cell culture.
We found out that TCs were strongly positive for CD34, PDGFR α and β, and vimentin and weakly positive for α-SMA. On the other hand fibroblasts and were found to be CD34 negative, while strongly positive for vimentin and PDGFR α and β. Notably, our findings delineate telocyte cells from fibroblasts and pericytes, underscoring their unique cellular identity within the IPFP microenvironment. TCs were recognized for their long and thin prolongations and small cell bodies primarily situated around blood vessels and dispersed throughout the IPFP stroma.

Conclusion: Our study adds greatly to our understanding of IPFP telocyte biology by shedding light on their presence, distribution, and morphological properties. As a result, these cells have the potential to be a unique progenitor cell source for cartilage regeneration, and they need full attention from researchers in the tissue engineering field.

Keywords:

Infrapatellar Fat Pad, Telocytes

1116

Effects of swimming training on orexin receptor 2 distribution in brain damage of rats

Professor Dilek Akakın[1], Assoc. Prof. Merve Acikel Elmas[2], Phd Student Ayca Karagoz Koroglu[1], Assoc. Prof. Ozlem Bingol Ozakpinar[3], Prof. Filiz Onat[4], Professor Feriha Ercan[1]
[1]1, Istanbul, Turkiye, [2]2, Istanbul, Turkiye, [3]3, Istanbul, Turkiye, [4]4, Istanbul, Turkiye

Poster Group 1

Background incl. Aims
The World Health Organization defines obesity as hyperplasia and hypertrophy of adipose tissue that poses a health risk. Obesity is increasing in Western countries and is one of the major epidemic problems. In particular, the high-fat diet (HFD) is one of the most important factors in the spread of obesity in these countries. It is also known that HFD causes cognitive dysfunction and impaired memory, and exercise can improve cognitive function in animals. It is known that neuroinflammation, which is associated with progressive neuronal loss, is exacerbated by cognitive decline and obesity. Orexin neurons are projected throughout the central nervous system, including the hippocampus. Orexin neurons are also involved in operant activities, and cognitive functions. In addition, the loss of orexin also impairs memory. Experimental studies have shown that mice lacking orexin neurons exhibit increased cognitive deficits, and the brain also becomes more susceptible to neuronal insults and increased levels of neuroinflammation. HFD induces impairment of long-term memory, and HFD exposure and orexin loss in mice lead to increased inflammatory markers. In this study, we focused on the possible neuronal degenerative effects of HFD on brain tissue and the protective effect of swimming training. The aim of this study is to investigate HFD-induced brain damage and the putative healing effect of exercise on orexin expression on cortical neuroinflammation and cognitive decline.
Methods
Male Sprague-Dawley rats were fed either standard chow (Control group, 6% fat) or a HFD (HFD group, 45% fat) for 18 weeks. Half of the animals fed with each diet were trained by swimming exercise (1 h/day, 5 days/week) for the last 6 weeks of the experimental period (Ex and HFD-Ex groups). At the end of the study, an object recognition test was applied to evaluate cognitive function, and brains were collected for routine light and transmission electron microscopy (TEM) and biochemical analysis. Histopathological evaluation was performed in hematoxylin-eosin (H&E)-stained paraffin sections and Orexin-2 (OX-2) and Glial fibrillary acidic protein (GFAP) immunohistochemistry were performed. Malondialdehyde (MDA) and glutathione (GSH) levels were measured in the brain homogenates. The histological and biochemical data were evaluated statistically and a p-value <0.05 was accepted as significant.
Results
Deteriorated object recognition test was observed in the HFD group compared to the rats in the control group, which was ameliorated with exercise. Morphological evaluation revealed increased neuronal degeneration compared to that of the control groups in the HFD group ($p<0.05$). The HFD+Ex group showed decreased neuronal degeneration relative to the HFD group ($p<0.05$). Altered GFAP immunohistochemistry and OX-2 immunofluorescence observed in the HFD group were similar to controls in the HFD+Ex groups. Increased MDA and decreased GSH levels of the HFD group compared to control and Ex groups ($p<0.001$) were observed. However, decreased MDA levels ($p<0.001$) and increased GSH levels ($p<0.01$) in the HFD-Ex group relative to the HFD group.
Conclusions
Our study revealed HFD-induced neuronal damage and increased oxidative stress in the brain tissue. Swimming exercise protects the high fat diet-induced brain damage including the alteration of GFAP and OX-2 immunoreactivity in the cortex of rats by modulating oxidant/antioxidant balance. It is also

thought that the regulation and neuronal development of the rodent cerebral cortex is influenced by HFD and that Ox-2 expression may contribute to this cortical development.

“This study was supported by European Commission Horizon Europe Programme under the call HORIZON-WIDERA-2021-ACCESS-03 (grant number 101078981 – GEMSTONE).”

Keywords:

HFD, Exercise, Brain, Orexin-2, GFAP

Reference:

1. C.M. Duffy, J.J. Hofmeister, J.P. Nixon, T.A. Butterick, High fat diet increases cognitive decline and neuroinflammation in a model of orexin loss,
Neurobiology of Learning and Memory, Volume 157, 2019, 41-47.
2. Funato H, Tsai AL, Willie JT, Kisanuki Y, Williams SC, Sakurai T, Yanagisawa M. Enhanced orexin receptor-2 signaling prevents diet-induced obesity and improves leptin sensitivity. Cell Metab. 2009 Jan 7;9(1):64-76.
3. Spencer, S. J., D'Angelo, H., Soch, A., Watkins, L. R., Maier, S. F., & Barrientos, R. M. High-fat diet and aging interact to produce neuroinflammation and impair hippocampal- and amygdalar-dependent memory. Neurobiology of aging, 2017, 58, 88–101.

1118

Microscopy to discern cells behaviour on different nano/microstructured calcium phosphates ceramics

Dr. Eva Filová[1], Dr. Carolina Oliver-Urrutia[2], Dr. Věra Hedvičáková[1], Dr. Veronika Hefka Blahnová[1], Ms. Eva Šebová[1], Ms. Radmila Žižková[1], Assoc. Prof. Karel Dvořák[2], Assoc. Prof. Ladislav Čelko[2], Dr. Edgar Montufar[2]
[1]Institute of Experimental Medicine, Czech Academy of Sciences, Prague, Czech Republic, [2]Central European Institute of Technology, Brno University of Technology, Prague, Czech Republic

Poster Group 1

Background incl. aims
The formation bone tissue and the mineralization are positively influenced by the nanostructure or microstructure of calcium phosphate ceramics and by pore architecture of implants (1). Moreover, the release of Ca2+ was shown to induce cell growth, and PO43- released into medium induced osteogenic genes expression (2). The nano- or microstructure may significantly influence cell adhesion, proliferation and differentiation. The aim of this work was to study the effect of hydroxyapatite (HA) and beta tricalcium phosphate (β-TCP) of different structure on osteosarcoma cells adhesion, proliferation and osteogenic differentiation using microscopy techniques.
Methods
Porous ceramics from hydroxyapatite (HA), nanostructured HA (N-HA), calcium-depleted HA (CDHA), β-tricalcium phosphate (β-TCP), and nanostructured β-TCP (N-β-TCP) were prepared by 3D printing and sintering, and were characterized with SEM, XRD and tested in vitro with osteosarcoma SaOS-2 cells, seeded at a density of 368 x 103 cells/cm2 cultured in McCoy's 5A, 15% foetal bovine serum, 1 % of antibiotics (Penicilin/Streptomycin), and 40 µg/mL ascorbic acid. Cell proliferation was evaluated by dsDNA assay, and the metabolic activity was tested using MTS assay on days 7, 14, and 21. Focal adhesions were visualized using mouse monoclonal antibody Anti-Talin (T3287, Sigma Aldrich, 1:200), secondary Anti-mouse IgG Fab2-AlexaFluor488 (1:400, Molecular probes) and beta-actin was stained with Phalloidon-ATTO633 (1:1000, Sigma Aldrich) on day 1. Moreover, gene expressions of alkaline phosphatase (ALP) activity, Runx2, osteocalcin, collagen type I were tested. RNA was isolated from discs using RNeasy Mini Kit (74104, Qiagen, Hilden, Germany). The isolated mRNA was reverse transcribed to cDNA using qScript cDNA Synthesis Kit (QuantaBio, USA), following the manufacturer's protocol. Polymerase chain reaction was performed on Light Cycler 480 (Roche, Basel, Switzerlands), primers and probe were obtained from ThermoFisher Scientific. Data were evaluated using the $2^{-\Delta Cp}$ method, for each gene relative to the housekeeping gene GAPDH.
Collagen type I, a midterm marker, was visualized using monoclonal antibody anti collagen I M-38c (1:50, DSHB, Iowa City, USA) and Anti-mouse IgG Fab2-AlexaFluor488 (1:400, Molecular probes) and propidium iodide (cell nuclei) on day 7 and 14. Osteocalcin, a late marker of osteogenic differentiation, was stained with Rabbit Anti-Osteocalcin (1:20, T4744, BMA Biomedicals) and Alexa Fluor 633 goat anti-Rabbit IgG (H+L) (1:200, Invitrogen) and Hoechst 34580 (2 µg/mL, H21486, Invitrogen) on day 21. All proteins were visualized using confocal microscopy and quantified using ImageJ. Statistical analysis was performed using GraphPad Prism 8.1.2. software, using One-way analysis of variance (ANOVA), according to normality test. The significance was set at $p < 0.05$.
Results
CDHA, N-HA and N-β-TCP had a nanostructure made of plate-like crystals. In contrast, HA and β-TCP had a microstructure of polyhedral grains. All nanostructured samples showed dot-like talin shape with low density of focal adhesions. Oppositely, both microstructured HA and β-TCP ceramics showed well visible and fibrous-like talin structures.
β-TCP showed significantly higher proliferation of Saos-2 cells compared to all groups on day 7. CDHA showed lower proliferation than HA, and β-TCP on day 7, and 14, respectively.

Gene expression of collagen I, Runx2 were highest in HA and N-HA samples on day 1, and 7, Runx2 was lowest in β-TCP on day 14. ALP expression of HA and N-HA was higher than on CDHA on day 7 and higher than N-β-TCP on day 1. Osteocalcin showed significantly increased expression on β-TCP compared to HA, N-HA and N- β-TCP on day 14. CDHA showed higher osteocalcin expression on HA on day 7. Interestingly, both collagen I and osteocalcin synthesis were positive in high amounts in all scaffolds without significant differences.

Conclusions

Nanostructured calcium phosphate ceramics significantly influenced the localization of focal adhesions. HA scaffolds supports early and midterm marker expression, while β-TCP supported osteocalcin gene expression. Collagen I and osteocalcin synthesis were highly produced in all scaffolds but were not influenced by different ceramics structures or chemical composition.

Project was supported by MEYS of the Czech Republic, the program IMPROVE V (CZ.02.01.01/00/22_010/0002552), from European Regional Development Fund – Project Excellence in Regenerative Medicine" CZ.02.01.01/00/22_008/0004562, and MSCA RISE project iP-OSTEO (824007).

Keywords:

microscopy, nanostructures, osteoconductivity, adhesion, differentiation

Reference:

Barba A. et al. ACS Appl Mater Interfaces. 2017, 9(48):41722-41736.
Wang, H. et al. Biomaterials 2007, 28(22):3338–3348.

1130

Development of multiciliated cells in the respiratory and esophageal epithelium of the chicken embryo

Dr. Sebastian Reinke[1], Dr. Alexander Reinke[1], Dr. Marcus Frank[1,2]
[1]Medical Biology and Electron Microscopy Centre, University Medicine Rostock, 18055 Rostock, Germany, [2]Department Life Light & Matter, University of Rostock, 18051 Rostock, Germany

Poster Group 1

Background and Aims
Cilia are highly conserved cell organells which emerge from the cell surface. They are frequently involved in signaling functions as well as in the coordinated motion of extracellular fluids and particles along epithelial surfaces. While monocilia are present in many cell types, the generation of multiple elongated cilia in multiciliated cells is restricted to specialized epithelia, e.g. the respiratory epithelium covering the trachea and the nasal conchae.
Until now there is still limited knowledge on the development of multiciliated cells, specifically regarding the details of their cell surface morphology during the ciliogenesis process. Using scanning electron microscopy (SEM) we have investigated the appearance and spatial extension of multiciliary cells in the trachea, in the concha nasalis media and adjacent regions of the embryonic chicken addressing developmental days E12 to E18. In addition, the esophageal epithelium bearing a more restricted lining of multiciliated cells was analyzed from E10 onwards.

Methods
Embryonic tissues were collected from fertilized chicken eggs (var. white leghorn) at the indicated days of incubation (E) and, after fixation, were processed for critical point drying for SEM using pieces with longitudinal cuts from trachea or oesophagus and coronal slices for evaluation of the nasal conchae. Additional processing for histology included resin embedding for transmission electron microscopy (TEM), or paraffin embedding for immunohistochemistry. Here, antibodies to acetylated tubulin have been used as a ciliary marker.

Results
At E12 to E14 short monocilia are detected with SEM on the surface of epithelial cells of the trachea and concha nasalis media. Following E14 the formation of much more elongated monocilia is observed and at E14,5 first multiciliated cells are found next to many cells with elongated monocila. At E15 an increased number of multiciliated cells is present showing multiple growing cilia with different length profiles whereas fewer cells with extended monocilia remain next to the clustered multiciliated cells until E16. At E17 monociliated cells are largely absent and most of the multiciliated cells have grown a large number of individual cilia to their final length of 5-6 µm. Here and in the following stages, the epithelial surface of the trachea and concha nasalis media is almost completely covered by cilia, whereas epithelial grooves that have emerged during development and have gradually increased in depth show a strongly reduced number of multiciliary cells, e.g. at E18 in the conchae nasalis media.
Interestingly, a distinct earlier onset of this ciliogenesis process was noted in the nasal septum adjacent to the former conchae, where cells with elongated monocilia and multiciliated cells are detected starting at E13. Accordingly the full coverage of the epithelium with cilia does occur earlier in the nasal septum i.e. at E16. Again, a much earlier onset of ciliogenesis is observed in the developing epithelium of the esophagus where at places we have detected nascent multiciliary cells at E10 onwards which are located next to cells with short monocilia and some cells with extended monocilia. While much less multiciliated cells are formed during development in the esophageal epithelium compared to the respiratory epithelia examined above these findings suggest a similar

sequence of ciliogenesis in multiciliated cells of the esophagus epithelium that involves transitory monocilia and a specific temporal development.

Conclusions
Our findings indicate that the appearance of cells with extended monocilia is a morphological marker for cells that are likely to further develop as multiciliated cells in an epithelium and will emerge with multiple cilia in the following. The observed developmental sequence of multicilated cells is completed in a relatively short period of time comprising approximately 3 days after onset in the chicken embryo.

Keywords:

multiciliated cells, chicken, electron microscopy

1138

Nestin expression in the myocardium of normotensive and spontaneously hypertensive rats during aging

Assoc. Prof. Dana Cizkova[1], Assoc. Prof., Ph.D. Jitka M. Zurmanova[2], M.D. Lucie Gerykova[1], Ph.D. Barbara Elsnicova[2], Frantisek Galatik[2], Ph.D. Jan Silhavy[3], Ph.D. Michal Pravenec[3], Prof., M.D., Ph.D. Jaroslav Mokry[1]
[1]Charles University, Faculty of Medicine in Hradec Kralove, Department of Histology and Embryology , Hradec Kralove, Czech Republic, [2]Charles University, Faculty of Science, Department of Physiology, Prague, Czech Republic, [3]Czech Academy of Sciences, Institute of Physiology, Prague, Czech Republic

Poster Group 1

Background incl. aims
Nestin, an interesting intermediate filament protein, is expressed in several tissues in the stem cells or within a certain period of development and reoccurs in the newly formed cells in adulthood. It is a proven marker of skeletal muscle regeneration and angiogenesis. Nestin is shortly expressed during the development of the heart and in some cell types in the adult myocardium, particularly in pathological conditions such as myocardial infarction or fibrosis. In this work we described expression and distribution pattern of nestin and its copolymerizing tissue-specific proteins desmin and vimentin in the intact and hypertrophic, adult and aged rat myocardium with the aim to contribute to understanding the reappearance of nestin in the diseased heart.
Methods
Nestin was detected by enzyme indirect two-step immunohistochemical method in the left ventricle myocardium of normotensive Wistar Kyoto (WKY) rats and in the hypertrophic left ventricle myocardium of spontaneously hypertensive (SHR) rats, both at the age of 1 and 1.5 year. Nestin expression in all samples of the myocardium was quantified by image analysis and statistically evaluated. For double immunofluorescent detections a novel method was introduced to enhance intensity of nestin signal based on application of Dako EnVision+ System-HRP Labelled Polymer.
Results
In the intact myocardium of normotensive rats nestin was expressed only in the endothelial cells of some blood vessels in 1.5-year-old animals, whereas in the 1-year-old WKY rats no nestin immunoreactivity was noticed. In the hypertrophic myocardium of SHR rats of both ages nestin was rarely detected in desmin+ vimentin- cardiomyocytes and in some vimentin+ interstitial cells that were usually accumulated forming the clusters and differing in intensity of desmin immunoreactivity. In addition, nestin was sparsely expressed in myocardial capillaries and in the endothelium of larger blood vessels in one-year-old SHR rats.
Quantitative image analysis of nestin expression in the myocardial samples confirmed significant increase in 1.5-year-old WKY rats and in SHR rats of both ages compared to the intact 1-year-old WKY rats.
Conclusion
This work firstly describes re-occurrence of intermediate filament nestin in some cardiomyocytes and in certain interstitial cells in the hypertrophic myocardium of adult and aged spontaneously hypertensive rats. Nestin re-appearance in the endothelial cells of the blood vessels documents important role of angiogenesis during aging in the intact and early hypertrophic myocardium. Nestin re-expression during cytoskeletal remodelling in the different cell types accompanies complex changes in the chronically pressure over-loaded heart and is related not only to myocardial hypertrophy and aging, but also likely to cardiac regeneration.

Keywords:

nestin, hypertension, myocardial hypertrophy, rat

1147

Molecular insights into rapid cell death involving endoplasmic reticulum and nuclear remodeling p

Ms. Samudra Sabari, António Pedro N. B. M. Carneiro, Ines Ambite, Siddharth Chinchankar, Parisa Esmaeili, Prof. Catharina Svanborg, Dr. Arunima Chaudhuri
[1]Lund University, Lund, Sweden

Poster Group 1

Conformationally fluid peptide-lipid complexes have been identified as potent tumoricidal agents in cellular models and clinical trials (1, 2). Here, we identify the mechanistic details of how the peptide-lipid complex, alpha1-oleate, achieves this outcome by rapidly engaging with the largest membranous organelle in the cell, the endoplasmic reticulum (ER). We identify a previously unknown mechanism of tumor cell death, involving ER and nuclear remodeling and the creation of a joint ER and nuclear compartment for the scavenging of cellular contents. Induced by the membrane-active alpha1-oleate complex. This response also affected molecular mechanisms of cancer and cell adhesion gene networks. Cell death was not affected by inhibitors of apoptosis, necrosis or autophagy but was sensitive to ion channel inhibitors. In addition, the novel cellular changes triggered by alpha1-oleate, included massive detachment of dying cells loaded with alpha1-oleate was also observed.

The results identify a new, ER-driven mechanism for capturing constituents of dying cells for final processing and shedding from treated tumors, to avoid tissue toxicity.

Keywords:

Endoplasmic reticulum, nuclear remodeling, cancer

Reference:

1. A. Brisuda et al., Bladder cancer therapy using a conformationally fluid tumoricidal peptide complex. Nat Commun 12, 3427 (2021).
2. T. T. Hien et al., Bladder cancer therapy without toxicity-A dose-escalation study of alpha1-oleate. Int J Cancer 147, 2479-2492 (2020).

1148

Effects of Myricetin on Mesenchymal Stem Cells Exposed to Oxidative Stress

Prof. Dr. Sibel Köktürk[1], Dr. Mehmet Berker[1], Aysel Bayramova[1], Sibel Doğan[1], Dr. Emel Usta[1], Feride Özdemir[1]
[1]Department of Histology and Embryology, Istanbul University, Istanbul Medical Faculty, İstanbul, İstanbul

Poster Group 1

Background: The mesenchymal stem cells (MSCs) have been widely used both in cell therapies. Myricetin is a flavonoid which suppresses oxidative stress and inflammation, reduces bioactivation of carcinogens, and affects cell signaling.
Aims: The aim was to evaluate the effects of myricetin in the hydrogen peroxide (H2O2) oxidative stress model in MSCs by immunocytochemical staining and electron microscopy.
Methods: The groups were determined by control, H2O2, myricetin and myricetin + H2O2 groups. The MSCs were treated with concentrations of 500 µM H2O2 and 5 µM myricetin for 24 hours. The MSCs ultrastructure and caspase-3, TIMP17 and TNF-α expressions were analyzed using transmission electron microscope and immunocytochemistry.
Results: The effects of myricetin against H2O2 oxidative stress damage in the MSCs, an increase in cell count, decrease in caspase-3 and TNF-α immunocytochemistry staining, increase in Tim17 immunocytochemistry staining and decrease in degenerative cell morphology in electron microscopic were observed.
Conclusion: Flavonoid myricetin may be a promising target for an alternative treatment option for increased cell viability, anti-apoptotic and anti-inflammatory effects in the MSCs.

Keywords:

Mesenchymal stem cell, myricetin

Reference:

1. Li M, Qian M, Jiang Q, Tan B, Yin Y, Han X. Evidence of Flavonoids on Disease Prevention. Antioxidants (Basel). 2023 Feb 20;12(2). PubMed PMID: 36830086. Pubmed Central PMCID: PMC9952065. Epub 20230220. eng.
2. Agraharam G, Girigoswami A, Girigoswami K. Myricetin: a Multifunctional Flavonol in Biomedicine. Curr Pharmacol Rep. 2022;8(1):48-61. PubMed PMID: 35036292. Pubmed Central PMCID: PMC8743163. Epub 20220110. eng.
3. Nammian P, Asadi-Yousefabad SL, Daneshi S, Sheikhha MH, Tabei SMB, Razban V. Comparative analysis of mouse bone marrow and adipose tissue mesenchymal stem cells for critical limb ischemia cell therapy. Stem Cell Res Ther. 2021 Jan 13;12(1):58. PubMed PMID: 33436054. Pubmed Central PMCID: PMC7805174. Epub 20210113. eng.
4. Jerkic M, Rabani R. Special Issue "Mesenchymal Stromal Cells' Involvement in Human Diseases and Their Treatment". Int J Mol Sci. 2024 Jan 20;25(2). PubMed PMID: 38279269. Pubmed Central PMCID: PMC10816837. Epub 20240120. eng.

1150

The effects of resveratrol on liver damage and ferroptosis in fructose-streptozotocin induced diabetic model

Assoc. Prof Fatma Kaya Dagistanli[1], MSc Mahsa Hoseini[1], MSc Merve Aykac[2], Prof. Dr. Turgut Ulutin[1]
[1]Department of Medical Biology, Cerrahpasa Faculty of Medicine, Istanbul University-Cerrahpasa, Istanbul, Türkiye, [2]Department of Medical Biology, Medical Faculty, Ataturk University , Erzurum, Türkiye

Poster Group 1

Background
The liver is the main detoxification organ in the body and regulates normal glucose homeostasis. There is a relationship between diabetes and liver disease. Pathological changes such as hepatic steatosis, accumulation of fatty acids, and fibrosis have been demonstrated in the livers of diabetic patients. Due to the connection between Type 2 Diabetes Mellitus (T2DM) and progressive liver disease, further research is needed to understand the pathogenesis of diabetic liver disease (1). Studies on liver damage in diabetes have focused on inflammatory and insulin signaling pathways, as well as oxidative stress. Recent studies have found that ferroptosis plays a significant role in acute or chronic liver damage (2).
Ferroptosis is a form of non-apoptotic cell death characterized by excessive lipid peroxidation, iron dependence, and is associated with various pathological conditions in the liver. Increased interest has been shown in the role of ferroptosis in liver diseases because excessive iron overload and oxidative stress are major triggers for liver damage and disease progression in many liver diseases. Therefore, targeting ferroptosis could provide a promising new therapeutic strategy for the treatment of liver disease in affected patients (2,3).
A fructose-rich diet impairs aerobic capacity and leads to diabetes and fatty liver disease. It triggers various metabolic disorders, including hypertriglyceridemia, hyperglycemia, insulin resistance, and glucose intolerance. Fructose reduces antioxidant activity and harms the livers of animals (4).
Resveratrol (RSV) is a compound belonging to the stilbenes group, found in grape skins and leaves. It exhibits properties of phytoalexins, which are produced by plants in response to fungal or bacterial infections, and it prevents cellular damage caused by free radicals. In addition to its antioxidant and anti-inflammatory effects, resveratrol has protective effects against cancer, aging, obesity, diabetes, cardiovascular, and nervous system diseases. Resveratrol has various beneficial effects, such as normalizing the activities of antioxidant enzymes like catalase, superoxide dismutase, and glutathione S-transferase, as well as lowering blood sugar levels. Low doses of resveratrol can reduce blood sugar levels and improve insulin sensitivity in diabetic patients (4,5).
The aim of this study is to demonstrate the role of ferroptosis in the formation of liver damage in a diabetic model created with a high fructose diet and streptozotocin (STZ) and to investigate the potential effects of resveratrol treatment on this process.
Methods
In the study, 8-week-old Sprague-Dawley rats were divided into four groups: 1) Diabetic group (D), fed with a 10% fructose solution for two weeks, injected with STZ (40mg/kg) at the end of the second week, and then fed with a 10% fructose solution for three more weeks. 2) Diabetic + resveratrol group (D+RSV), treated with 1mg/kg/day resveratrol for four weeks. 3) Non-diabetic rats treated with resveratrol (C+RSV) (1mg/kg/day) for four weeks. 4) Control group (C). At the end of the experiment (9th week), all rats were sacrificed, and liver tissues were collected. Throughout the experiment, calorie intake, body weight, and blood sugar levels were measured. The liver tissue sections were immunostained with GPX-4, COX-2, and H2AX antibodies. All values were analyzed using statistical methods.
Results

In the fasting blood glucose measurements of the rats that were administered STZ (40 mg/kg, i.p.) after 10% fructose for 2 weeks ($p < 0.001$), a highly significant difference was detected between the diabetic groups and the control groups. At the end of the experiment, there was a significant difference between the diabetic group and the control groups ($p < 0.001$). Additionally, a significant difference in blood glucose levels was detected between the control and D+RSV groups ($p < 0.05$). The calorie intake in the second and fifth weeks was significantly different in the D and D+RSV groups compared to the control groups ($p < 0.001$). However, at the end of the study, there were no differences between all groups.

H&E, Van Gieson, and Prussian blue staining of liver tissue sections revealed vacuolization of hepatocytes, an increase in collagen fibers in the portal areas and around the central vein, which is an indicator of fibrosis, and iron accumulation in the tissue in the diabetic group. In the D+RSV group, it was found that the damage caused by diabetes was recovered and iron accumulation in liver tissue was inhibited. Decreased GPX-4 protein expression and increased COX-2 expression were detected by immunohistochemistry staining in the diabetic group. Additionally, GPX-4 immune positive cell numbers were significantly higher in the D+RSV group. H2AX is used by many researchers as a tool to measure induced DNA damage. In the D group, an increase in the number of cells marked with phosphorylated H2AX antibody was observed, while there was a decrease in the D+RSV groups.

Conclusion

We suggest that the high-fructose diet and low-dose STZ administration increased blood glucose levels, caused liver fibrosis, and led to iron accumulation. Additionally, resveratrol treatment decreased blood glucose levels in diabetic rats, positively affected oxidative stress by increasing GPX-4 expression, the main purifier of lipid peroxides in cells, and prevented iron accumulation in hepatocytes, thereby protecting liver tissue from ferroptosis.

Keywords:

Ferroptosis, Streptozotocin, Fructose, Resveratrol, Liver

Reference:

1- Rafaqat et al. (2023).Role of liver parameters in diabetes mellitus -a narrative review. Endocrine regulations, 57(1), 200–220. https://doi.org/10.2478/enr-2023-0024

2- Chen, et al. (2021).Characteristics and Biomarkers of Ferroptosis. Frontiers in cell and developmental biology, 9, 637162. https://doi.org/10.3389/fcell.2021.637162

3- Chen et al. (2022).The multifaceted role of ferroptosis in liver disease. Cell death and differentiation, 29(3), 467–480. https://doi.org/10.1038/s41418-022-00941-0

4- Anapali et al. (2022). Combined resveratrol and vitamin D treatment ameliorate inflammation-related liver fibrosis, ER stress, and apoptosis in a high-fructose diet/streptozotocin-induced T2DM model. Histochemistry and cell biology, 158(3), 279–296. https://doi.org/10.1007/s00418-022-02131-y

5- Öztürk et al. (2017).Resveratrol and diabetes:A critical review of clinical studies. Biomedicine&pharmacotherapy = Biomedecine & pharmacotherapie, 95, 230-234.

1219

An efficient method for quantifying the degree of neurodegeneration in an insect brain

Jakub Opelka[1,2], Lucie Pauchova[1], Andrea Bednarova[1], Radka Zavodska[1,3], Michal Sery[1,3], Ivo Sauman[1,2], Hana Sehadova[1,2]
[1]Faculty of Science, University of South Bohemia, Ceske Budejovice, Czech Republic, [2]Faculty of Science, University of South Bohemia, Ceske Budejovice, Czech Republic, [3]Faculty of Education, University of South Bohemia, Ceske Budejovice, Czech Republic

Poster Group 1

Background
For decades, the fruit fly Drosophila melanogaster has served as a model organism for studying the molecular and genetic basis of many human diseases, including neurodegeneration. In this study the comparative analysis was performed using the Drosophila model that mimics the human pathological condition associated with spinocerebellar ataxia type 1 (SCA1), which is characterized by progressive problems in movement (3). In Drosophila, such anatomical evidence can be obtained by viewing serial paraffin sections of the mutant brain under a light or fluorescence microscope. This method was originally developed by Heisenberg and Böhl (2). The extent of brain damage was determined subjectively based on the frequency of brain neuropathology on the 6-point scale from "none" to the highest level of neurodegeneration (1). Our study aimed to address this limitation by developing a novel method for accurate quantifying of brain damage in Drosophila models of SCA1, using Fiji (ImageJ) and Imaris 3D modeling software on Z-stacks of whole adult Drosophila brain.
Methods
Flies were anesthetized under CO2 and prefixed in 4% paraformaldehyde (PFA) in phosphate buffer (PB). The prefixed flies were then washed in PB and the brains were dissected in PB. The dissected brains were fixed in 4% PFA. After fixation, brains were rinsed in PB-Tween and were blocked with 5% normal goat serum in PB-Tween for 2 hours as blocking solution. After thorough rinsing with PB-Tween (four times for 15 min at room temperature), the preparations were transferred to the goat anti-mouse IgG secondary antibody conjugated with Alexa Fluor 448 diluted 1:200 in the blocking solution and incubated overnight at 4 ºC. Preparations were rinsed with PB-Tween and mounted on microscopic slides (Figure 1). The confocal laser scanning microscope (FV 3000 Olympus) was used to acquire images of the Drosophila brain using a high sensitivity detector with a resolution of 1024x1024 pixels and a pixel acquisition time of 8 µs. To match the size of the Drosophila brain, the UPLANSApo 20XO objective was used. Serial Z-stack images were acquired with the optimal thickness. The data in oir format obtained with the confocal microscope were uploaded to the Fiji software and subjected to analysis by Threshold and Analyse particles modules. The obtained data were summed and multiplied by the layer thickness to obtain the exact volume of neurodegeneration in µm3.Three-dimensional models of areas of neurodegeneration were reconstructed in Imaris software (Bitplane) using the Surpass module - > Contour Surface. We correlated the obtained values to the volume of the whole brain thus determined the percentage loss of the brain volume caused by the neurodegeneration.
Results
In this study, two analytical approaches are presented to determine the degree of brain tissue damage in the Drosophila adult brain, and they are compared in terms of the time required and the accuracy of the measurements. The first method of raw data analysis was primarily based on the use of the publicly available software Fiji. The second method of brain damage extent analysis uses the commercial image software Imaris. In both types of analyses (Fiji and Imaris), statistical analyses using Student t-test confirmed a significant difference in the degree of neurodegeneration between mutant and control brains, p-value was $P < 0.001$. To compare results obtained by these two

analytical methods, the extent of neurodegeneration in mutants measured by Fiji and Imaris software was subjected to statistical analysis using Student t-test and linear regression. The results showed no significant differences.

Conclusion

In Fiji software, the Analyze Particles function enables automatic selection of neurodegenerative holes. However, subjective adjustment of the Threshold level may introduce measurement error. Conversely, Imaris software requires manual selection of each hole across all optical sections of the Z-stack using the Contour Surface module, which is time-consuming. Thus, the choice between the two methods depends on the degree of neurodegeneration. For low levels, Imaris is recommended for its 3D visualization capabilities, albeit at the expense of time and effort. Conversely, for high levels of neurodegeneration, Fiji is more efficient.

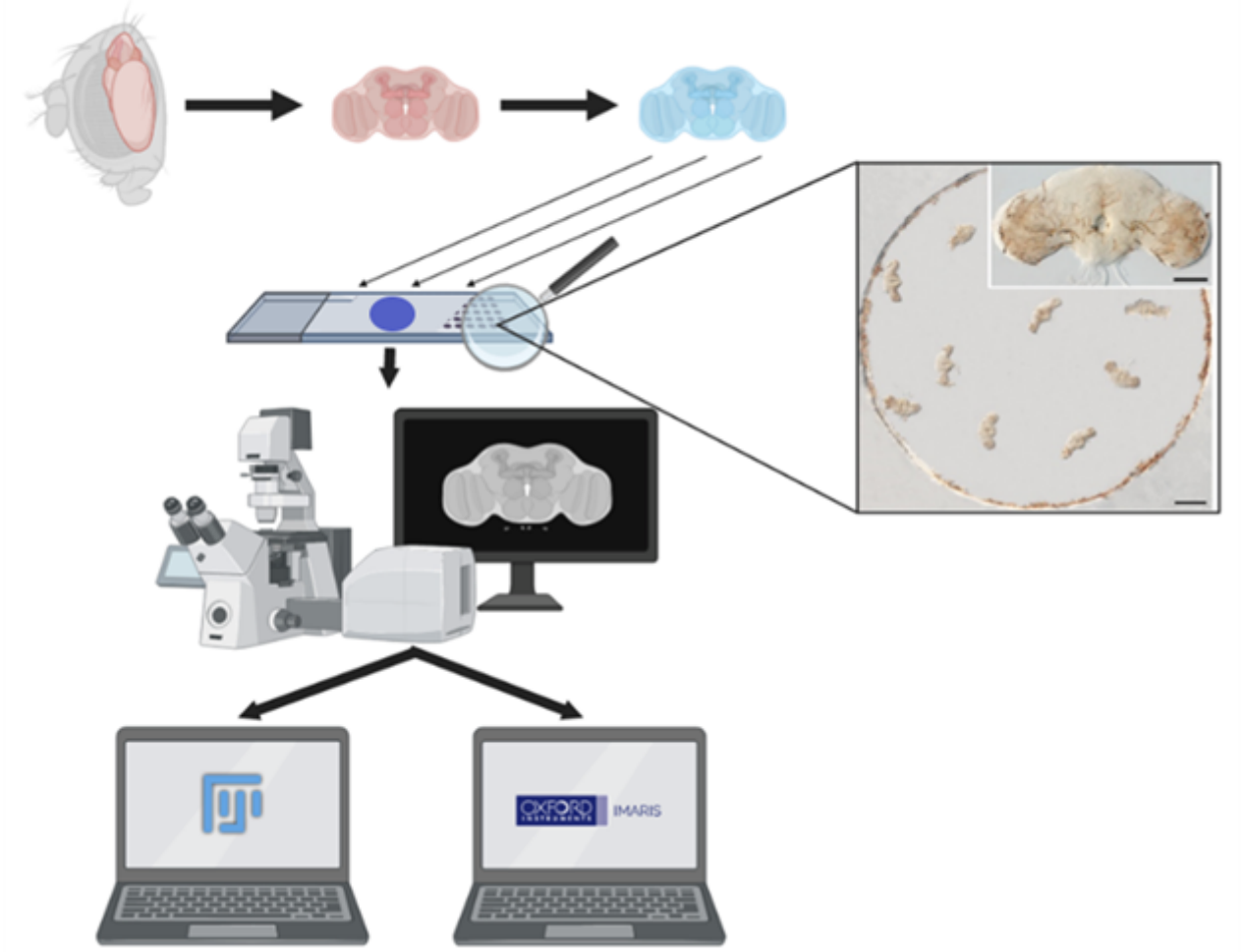

Keywords:

neurodegeneration, insect, Fiji, Imaris, confocal-microscopy

Reference:

1. Fergestad, T., Ganetzky, B., and Palladino, M.J. (2006). Neuropathology in Drosophila membrane excitability mutants. Genetics 172, 1031-1042.
2. Heisenberg, M., and Bohl, K. (1979). Isolation of Anatomical Brain Mutants of Drosophila by Histological Means. Zeitschrift Fur Naturforschung C-a Journal of Biosciences 34, 143-147.
3. Klockgether, T., Mariotti, C., and Paulson, H.L. (2019). Spinocerebellar ataxia. Nature Reviews Disease Primers 5

1249

FlexAble Labeling of Primary Antibodies with Fluorescent Dyes and Biotin for Multiplex Experiments

PhD Larisa Yurlova[1], Michael Metterlein[1], PhD Longtao Wu[2], XinXing Wang[3], Dr. Christian Linke-Winnebeck[1], Dr. Andrea Buchfellner[1], PhD Lion Lian[3], PhD Deepa Shankar[2], PhD Jason Li[2]
[1]Proteintech Group, Martinsried, Germany, [2]Proteintech Group, Rosemont, USA, [3]Proteintech Group, Wuhan, China

Poster Group 1

Background incl. aims:
Multiplex immunostaining has become an increasingly important approach in current biomedical research. However, the availability of directly labeled primary antibodies often poses a bottleneck for multiplex methods. Here we aimed to develop an antibody-labeling process that enables fast and easy conjugation of primary antibodies to fluorophores at a microgram to milligram scale, e.g. for the amount needed for one immunostaining experiment.
Methods:
For the development of this labeling procedure, we employed a broad range of methods including in silico protein design, molecular cloning, protein expression, protein purification, site-directed conjugation, BLI, DLS, cell culture, IF, IHC, flow cytometry and X-ray crystallography. Successful application of the developed labeling technique takes around 10 minutes and does not require any special equipment or proficiency in chemical conjugation or antibody purification.
Results:
We designed peptide-based multivalent linkers that bind to primary IgGs from rabbit, mouse, rat or human species with an apparent dissociation rate koff (1/s) below 0.0001 and covalently conjugated them to different fluorophores (CL+405/488/555/647/750). We validated the specificity of the binding between the linkers and their target IgGs and confirmed the proposed molecular arrangement with X-ray crystallography. Since these linkers are fluorescent, they offer a simple and convenient tool to functionalize primary IgGs from the aforementioned species with the desired fluorophores. We called this labeling approach FlexAble labeling because it embodies the simple steps of mixing and briefly incubating linkers and primaries. This procedure can be performed virtually in any laboratory for any amount of primaries right before applying the antibodies in the desired assay. Moreover, primary antibodies can be in any buffer, since glycerol or other additives do not interfere with FlexAble labeling.
Here, we show that FlexAble-labeled antibodies are suitable for immunofluorescence stainings, especially when multiplexing of primaries from the same species is required. Also, we present examples of FlexAble applied to flow cytometry, WB, tissue IF, live time-lapse imaging, cyclic IF, and other more advanced experiments employing immunofluorescence detection of the target molecules.
Conclusion:
We have established FlexAble, a novel antibody labeling process that enables rapid conjugation of primary antibodies to fluorophores and facilitates multiplex immunofluorescence experiments. We are expanding this method further to expedite labeling of primary antibodies with reporter proteins (HRP, PE, APC), biotin, DNA oligonucleotides, rare-earth metals etc. to support multiplex flow cytometry, nucleotide barcoding (e.g. 10x Genomics) and IMC (e.g. CyTOF).

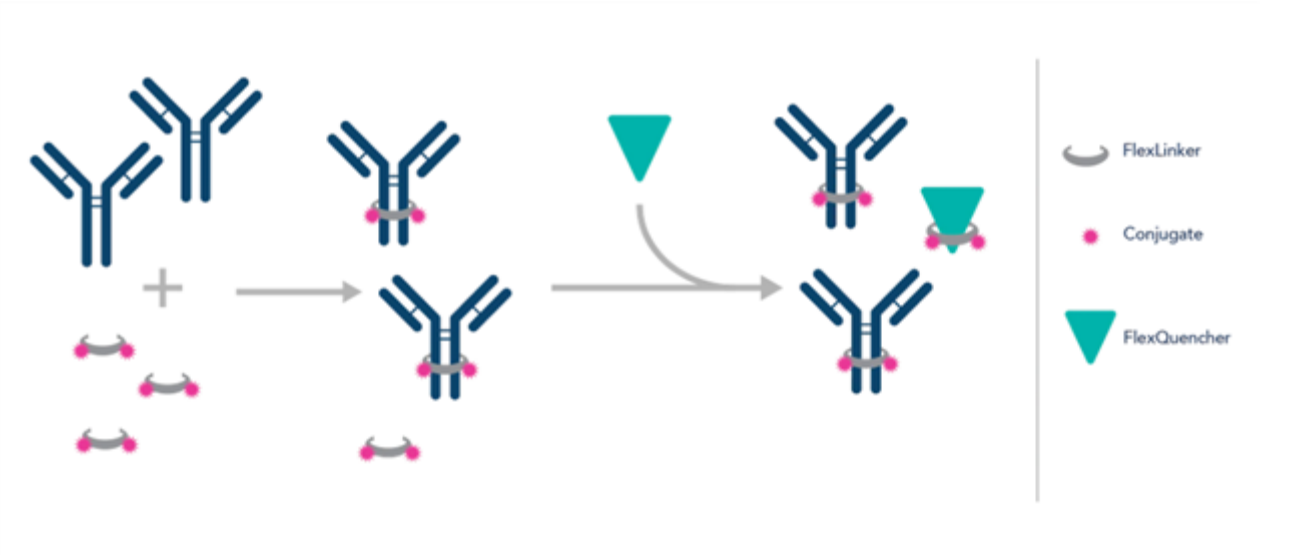

Keywords:

Multiplex, immunofluorescence, antibody conjugation, FlexAble

Reference:

www.nature.com/articles/d42473-023-00120-w

1305

The synthetic chaperonin Poly-CCT5 as a nanoparticle carrier

Mr. Sergio Pipaón[1], Mr. Jorge Gutiérrez[1], Mr. Jesús G. Ovejero[2], Mrs. María del Puerto Morales[2], Mr. Jorge Cuéllar[1], Mr. José María Valpuesta[1]
[1]National Center For Biotechnology (CNB-CSIC), Madrid, Spain, [2]Department of Materials for Health of the Materials Science Institute of Madrid (ICMM), Madrid, Spain

Poster Group 1

Chaperones assist in the de novo protein folding and prevent protein aggregation. One of the most important chaperone families are the chaperonins (Hsp60s), which are organized as two oligomeric back-two-back rings generating a cavity in each ring where the substrate is placed for its folding. The most complex and important of all chaperonins is the eukaryotic CCT (Chaperonin Containing TCP-1) whose structure and the folding mechanism are key for nanotechnological applications.

The main aim of this project is to build a stable synthetic cylindrical structure capable of encapsulating chemical reagents or small proteins. It has been shown that CCT5 is able to self-oligomerize. When compared to the eukaryotic CCT, poly-CCT5 is easier to purify, can be genetically modified in all subunits and allows a more manageable image processing. These capabilities could enable poly-CCT5 to act as a nanocontainer delivering molecules to specific targets.

Our group used negative staining EM to assess the encapsulation of various nanoparticles inside synthetic poly-CCT5. VENOFER, an iron-sucrose coating NP, produced the best results overall and was chosen for Cryoelectron microscopy (CryoEM) analysis. We generated a 3.3 Å 3D reconstruction of the NP-bound poly- CCT5, with the NP presumably held by CCT5 apical domains. As part of this project, we are now focusing our efforts on the design and the structural characterization of three poly-CCT5 mutants, which rearrange the charge distribution on the cavity, to improve nanoparticle internalization and to prevent undesired interactions.

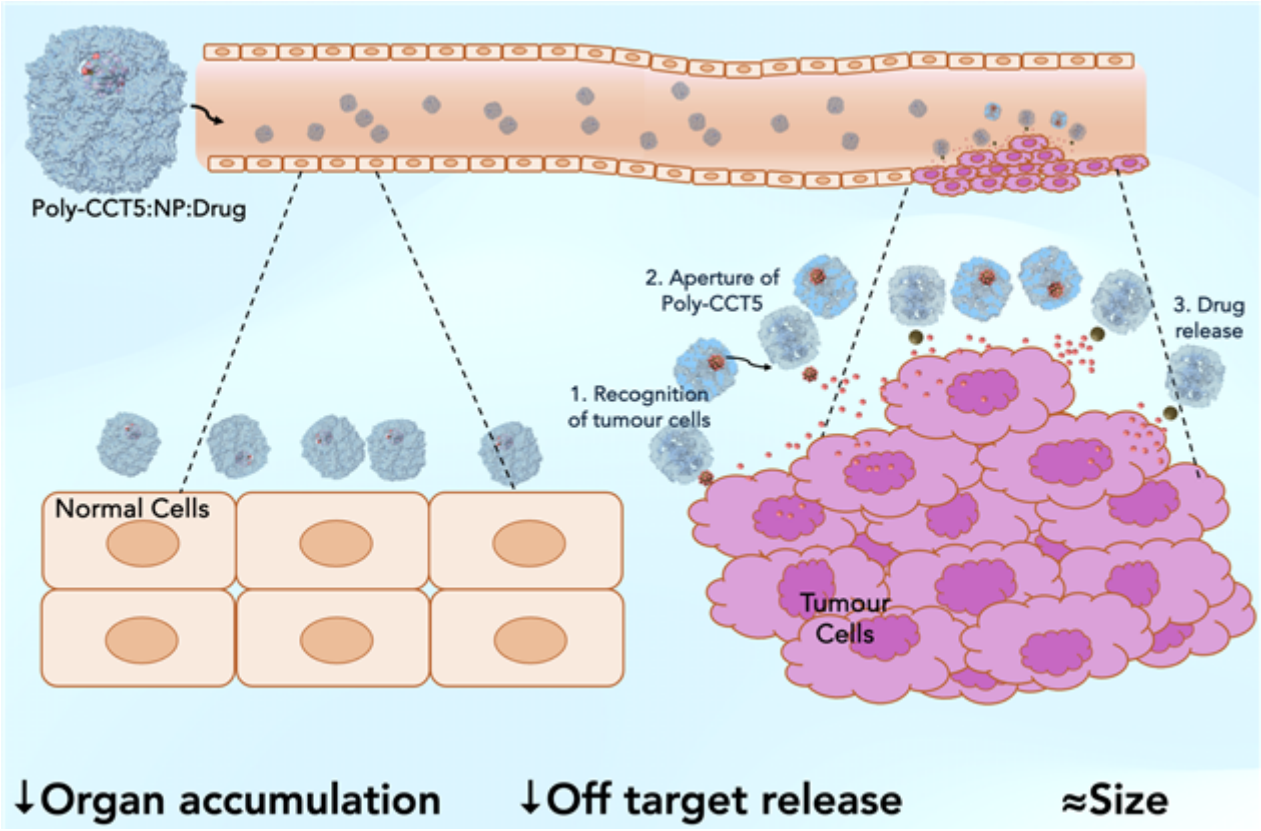

Keywords:

Poly-CCT5, nanocarrier, nanoparticles, CryoEM

Reference:

1. Sergeeva OA, Tran MT, Haase-Pettingell C, King JA. Biochemical characterization of mutants in chaperonin proteins CCT4 and CCT5 associated with hereditary sensory neuropathy. J Biol Chem. 2014;289(40):27470–80.

2. Ishii D, Kinbara K, Ishida Y, Ishii N, Okochi M, Yohda M, et al. Chaperonin-mediated stabilization and ATP- triggered release of semiconductor nanoparticles. Nature. 2003;423(6940):628–32.

3. YuanY,DuC,SunC,ZhuJ,WuS,ZhangY,etal. Chaperonin-GroEL as a Smart Hydrophobic Drug Delivery and Tumor Targeting Molecular Machine for Tumor Therapy. Nano Lett. 2018;18(2):921–8.

1344

Effects of Vitamin D Administration On Testicular Tissue in Metabolic Syndrome Rats

Tugce Ozbilenler[1], Betul Zorkaya[2], Sakine Rzayeva[1], Nergis Bayramova[1], Seda Akdemir[3], Cigdem Bayram Gurel[1], Evrim Bayrak Komurcu[4], Ahmet Dirican[5], Fatma Kaya Dagistanli[1], Prof Melek Ozturk Sezgin[1]
[1]Department of Medical Biology, Cerrahpasa Faculty of Medicine, Istanbul University-Cerrahpasa, Istanbul, Turkiye, [2]Department of Genetics, Aziz Sancar Institute of Experimental Medicine, Istanbul University, Istanbul, Turkiye, [3]Department of Medical Biology, Faculty of Medicine, Karabuk University, Karabük, Turkiye, [4]Department of Medical Genetics, Istanbul Faculty of Medicine, Istanbul University, Istanbul, Turkiye, [5]Department of Biostatistics, Cerrahpasa Faculty of Medicine, Istanbul University-Cerrahpasa, Istanbul, Turkiye

Poster Group 1

Background: Metabolic Syndrome (MS) includes a series of metabolic disorders such as abdominal obesity, insulin resistance, impaired fasting glucose, hypertension, and dyslipidemia, with insulin resistance being a dominant factor in these conditions (1. MS is associated with obesity resulting from a high-fat and high-sugar diet combined with a sedentary lifestyle and is increasing as a global public health issue. Infertility affects 15% of couples worldwide, with male factors playing a role in 50% of cases (2). Paternal obesity leads to reduced sperm count, increased sperm DNA damage, and long-term epigenetic changes (3). Vitamin D3 plays a role in the regulation of reproductive processes in addition to maintaining calcium and phosphorus homeostasis. Vitamin D deficiency can impair testicular development and spermatogenesis by inhibiting testicular germ cell proliferation (4). We aimed to explore the impact of metabolic syndrome on male infertility and analyze the influence of vitamin D supplementation on testicular damage, cell proliferation, and apoptosis induced by a high-fat and high-fructose diet.
Methods: To create a metabolic syndrome model, we utilized a specialized diet comprising 17% fat and 17% fructose, along with another diet consisting of 20% fructose water over a period of 15 weeks. The study involved twenty-four male Sprague-Dawley rats. Based on dietary variations and vitamin D administration, we established four groups: Healthy Control (SC), Metabolic Syndrome (MS), MS+Vitamin D (MSD), and Healthy Control+Vitamin D (HCV) groups. The Vitamin D-treated groups received oral vitamin D supplementation at a rate of 170 IU/week for 12 weeks. At the end of the 15-week period, the animals were euthanized. Testicular tissue samples were fixed in 10% buffered neutral formalin and embedded in paraffin for further analysis. Throughout the experiment, daily food intake, water consumption, weight changes, as well as fasting blood glucose levels were monitored. Immunohistochemistry techniques involving primary antibodies against aromatase, StAR, 8-OHdG, Vitamin D receptor (VDR), PCNA, and activated caspase-3 proteins were performed. Serum testosterone levels were measured using ELISA method, and TUNEL method was used to determine apoptotic cells.
Results: Statistical analysis revealed that animals in the MS group exhibited significantly higher daily caloric intake, were heavier, and had elevated fasting blood glucose levels compared to other groups. VitaminD administration led to decreased blood glucose levels inthe MSD group compared tothe MS group possibly due to its metabolic regulatory effect. Morphological examination indicated irregular seminiferous tubules with reduced diameters in the MS group compared to other groups, resulting from germ cell loss and a thickening of the basement membrane. Moreover, the number of spermatid cells within these tubules as well as the number of spermatozoa within the lumen were significantly diminished when contrasted with other groups. Testicular morphology showed improvement in the MSD group compared to the MS group. Expressions of aromatase, 8-OHdG,

activated caspase-3, and TUNEL positivity were markedly increased with in the MS group; conversely StAR, VDR, and PCNA expressions along with serum testosterone levels was substantially decreased. Conclusion: It is suggested that high fat and fructose-induced metabolic syndrome contributes to male infertility by disrupting testicular structure however, vitamin D administration can ameliorate this damage.

Keywords:

Metabolic syndrome, VitaminD, Testis, Rat

Reference:

(1) Goel, P., Popa, A. R. (2018). The relation between metabolic syndrome and testosterone level. Romanian Journal of Diabetes Nutrition and Metabolic Diseases, 25(1), 109-114.
(2) Lanktree, M. B., Hegele, R. A. (2017). Metabolic syndrome. In Genomic and precision medicine (pp. 283-299). Academic Press.
(3) Pépin, A. S., et al. (2022). Paternal obesity alters the sperm epigenome and is associated with changes in the placental transcriptome and cellular composition. bioRxiv, 2022-08.
(4) Jeremy, M., et al. (2019). Vitamin D3 regulates apoptosis and proliferation in the testis of D-galactose-induced aged rat model. Scientific Reports, 9(1), 14103.